Making the Most out of Distributed Generation without Endangering Normal Operation:

A Model-Based Technical-Policy Approach

Masoud Honarvar Nazari

Engineering and Public Policy
Carnegie Mellon University
and

Electrical and Computer Engineering
Faculty of Engineering of the University of Porto

A thesis submitted for the degree of

Doctor of Philosophy (Ph.D.)

2012 September

1. Reviewer: Professor Marija Ilic

2. Reviewer: Professor Joao Pecas Lopes

3. Reviewer: Professor Granger Morgan

4. Reviewer: Professor Manuel Matos

Day of the defense: 28, September, 2012

Signature from head of PhD committee:

Abstract

In this dissertation we introduce a model-based approach for efficiently locating and operating distributed generation (DG) without endangering stable system operation. The proposed approach supports quantifiable policy making based on technical design. The model used is structural and it comprises local models of DGs and loads interconnected via distribution grid system. While similar model structure can be used to represent meshed transmission grids, identifying model properties unique to distribution systems sets the basis for interpreting power delivery losses as the key measure of the overall system efficiency. It furthermore sets the basis for designing decentralized control specifications necessary to ensure system-wide stability. Once the underpinnings of the technical design are understood, the findings are used to propose a model-based quantifiable policy design to support process of integrating and operating DGs in distribution systems.

We first investigate efficient integration of distributed generation on the distribution side of electric energy systems. We introduce a notion of efficiency in distribution systems which is uniquely determined by the fact that DG units are clean and inexpensive; because of this DGs are always scheduled and there is no need for economic dispatch. This points to the fact that the main measure of efficiency is loss minimization. This notion helps us in streamlining specific methods for optimizing losses both in planning and operation. At the planning stage the best location is found, and in operation optimal voltage dispatch is done to reduce losses. We show that a 10% penetration of DG units can reduce up to 50% of distribution losses, if DG units are strategically located and optimally operated in distribution systems.

One possible problem with optimal placement of DG units may be an overly high sensitivity of their response to even small perturbations from normal conditions. Therefore, a very efficient distribution system with optimally-placed DG units may not be robust in operations. In order to assess robustness of distribution energy systems with respect to small disturbances, we model distribution systems as dynamical systems. We show that because of the strongly coupled voltage/real-power interdependencies in power flows of distribution systems, it is no longer possible to use a decoupled real-power dynamic model which neglects the effects of voltage dynamics. This conclusion is a direct consequence of a non-negligible resistance-reactance ratio in distribution systems which differentiates them from the typical transmission systems. Therefore, only coupled models should be used for stability analysis and for control tuning of DGs in distribution systems.

Using such a dynamic model we show that distribution systems with high penetration of DG units can exhibit frequency- and/or voltage-instabilities when power plants have conventionally tuned control. Such instabilities are particularly pronounced when the DG units are electrically close. Gerschgorin circle theorem and participation factor-based methods are used to identify the main cause of instabilities as being the interactions of the local DG dynamics through the distribution power grid. Since the proposed dynamical model structure allows us to represent any type of DG plant and its local control, stability analysis can be performed for a general type of a DG using these methods to determine bounds on interactions between each specific DG and the rest of the system so that no interactions occur. These bounds are dependent on the machine type and parameters, the local control and the grid parameters. Some DGs may not have sufficient control as measured in terms of these bounds, and, these are the ones which require enhanced control to ensure system-level stability without unstable interactions, as discussed next.

The severity of dynamical problems in specific distribution systems with DGs depends on the technology and control of DGs and on the electrical distances between the DGs. Typical DGs are either synchronous ma-

chines or induction machines whose inertia may be much smaller than the inertia of large generators. Their local control may range from no control, through well-understood governor-excitation control of synchronous machines, through power electronically controlled inverters of synchronous and/or induction machine type DGs (power system stabilizers (PSS) and/or doubly fed induction machines (DFIG)).

In this dissertation we have studied stability problems in systems with DGs being small and/or medium size synchronous machines controlled by governor-excitation systems and/or by pitch control combined with PSS control. We assess possible instabilities in such systems when controllers are tuned on a stand-alone machine connected to the impedance representing the rest of the system (today's practice). We show that a more systematic fully decentralized, and, therefore, simple, control design proposed, in this dissertation, could stabilize synchronous machine-type DGs, such as diesel and hydro plants, without inverter control. Moreover, synchronous machine-type wind power plants can be stabilized in a decentralized way by combining advanced pitch control and/or PSS control.

Based on the above technical findings we propose a policy-making process for giving guidelines: (1) to best locate candidate DG units; (2) to dispatch set points on the voltage controllers of DGs in coordination with dispatching set points of other voltage-controllable equipment for ensuring minimal losses in operations; and, (3) to enhance the existing control of the DGs and/or deploy new enhanced decentralized control. Because the solutions are system-dependent, simple one-size-fits-all policies are no longer viable; Instead, policy decisions must be supported by software for placing the DGs and for designing their voltage dispatch and control. This approach leads to systematic institutional agreements and policies needed to support large penetration of DG units while ensuring both efficiency and robustness of distribution energy systems.

To My Family: My Lovely Wife Roheila, My Mother, My Father, My Brothers, and My Sister. Thank you for all the Love. Masoud

Acknowledgements

I would like to acknowledge my great advisers Professor Marija Ilic and Professor Pecas Lopes. I also acknowledge my incredible committee members Professor Granger Morgan and Professor Manuel Matos.

I also appreciate the help of the EDA in providing technical data for the Azores Islands. Financial support for this dissertation was provided by the Portugal-Carnegie Mellon joint program under CMU—Portugal Fellowship and under Grant 18396.6.5004458. I truly appreciate this support.

Contents

List of Figures

LIST OF FIGURES

List of Tables

1

Introduction

1.1 The Challenge of Making the Most out of Distributed Generation

In the past electric power systems have had hierarchical structures in which electricity is produced by large central power plants and delivered to the end users by means of transmission and distribution networks. This structure has several drawbacks. For instance, waste heat is typically not used. Transmission is expensive, difficult to expand and lossy. Large power plants and transmission systems cause a host of environmental and land-use problems.

New pressures for cleaner and more efficient use of energy have led to active efforts toward deploying smaller-scale power plants close to the end users. These plants are broadly referred to as distributed generation (DG). DG units offer potential advantages. For example, natural gas fired distributed generation which is combined with local heating and cooling holds the potential to almost double the efficiency with which primary energy is converted into useful services (40). Gas-fired and PV-based DG could improve dramatically the electric power delivery in the event of disruption of supply from the bulk power system, when they are combined with distribution automation and smart meters (1). Furthermore, DG units hold the potential to reduce power delivery losses and limit the need to build new transmission or distribution line capacity.

In this work, we are primarily concerned with technical and policy challenges related to integration of medium sized generators ($\sim$ 1 MW) located in the distribution system

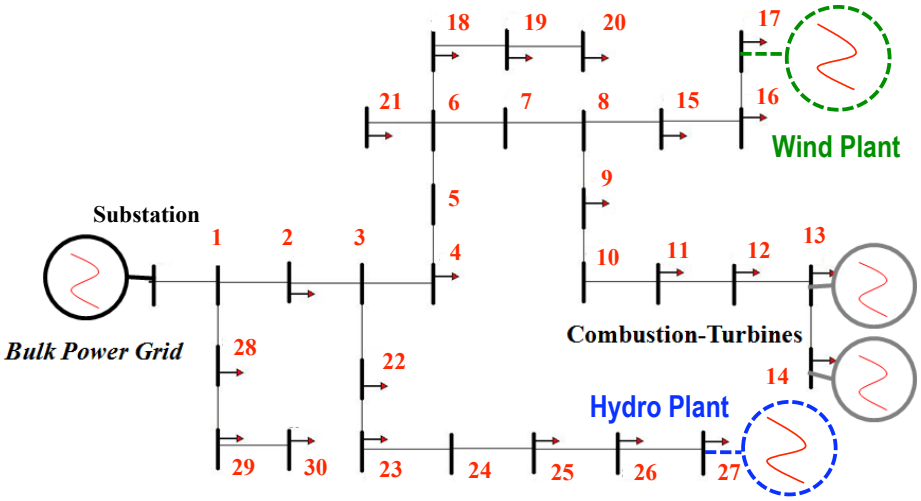

Figure 1.1: Schematics of the IEEE 30-node distribution system.

that supply a significant fraction of the power they generate to the system (as opposed to adjacent local loads).

Figure 1.1 illustrates the schematics of a real-world distribution system with DG units placed close to the end users. The system is created by modeling the IEEE 30-node distribution system in complementation with new DG units (71). Shown in black is a point of connection between the transmission and distribution system, modeled as an ideal power source. For illustration purpose represented in grey are two combustion turbines (CT) connected to nodes 13 and 14. In the future the same system might be expected to have a small hydro plant and/or a small wind plant.

1.1.1 Problem Formulation

As the penetration level of distributed generators increases, many uncertainties lie ahead. For instance, how will the deployment of a large number of distributed generators affect the planning, operation and control of legacy distribution systems? Can today's operating models and interconnection standards support a large penetration of DG sending power back to the distribution grid? How small and how localized DG should be before one worries about its technical impacts on the system? In fact, introduction of micro-grid and plug-and-play solutions to integrating highly distributed energy resources of 1kW order such as micro-CHPs and PV panels is currently not

perceived to cause technical problems. The question is whether this is indeed true with a very high penetration of such small devices or with deployment of larger DGs.

These are challenging tasks. This dissertation addresses these issues and illustrates the results using real-world-like distribution systems.

1.1.2 State of the Art

There are several studies concerning the effects of DG units on grid reinforcement requirements, power losses, on-peak operating costs, voltage profiles and load factors, deferring or eliminating system upgrades, and on system reliability (3, 4, 10, 11, 13, 33, 39, 54, 70).

A common strategy to optimally siting DG units on distribution systems is to minimize power delivery losses [5]. This strategy has been analyzed in many references with different approaches. For instance, references (58) and (33) introduce a power flow-based algorithm to find the optimal size of DGs at candidate nodes of a distribution system. In (39), the authors propose a tabu search method to obtain the minimum loss allocation and line loading of DGs. References (3) and (54) present analytical approaches to determining the optimal location for placing DGs in distribution systems, or in (13) a rule of thumb, often used in siting shunt capacitors, is presented to optimally place DG units on radial distribution feeders.

In addition, several authors including Angelo and Lopes (43), Guttromson (66), and Donnelly et al (47) have studied the effects of distributed generators on dynamic stability of transmission power systems. Cardell et al (30, 31) have investigated the frequency performance of distribution systems that have multiple small scale distributed generators. The authors propose a price-based control which enables independent distributed generators to participate in both the energy and the ancillary service markets. In (37) the effects of PV integration on voltage stability in distribution feeders are studied. The authors show that interconnected PV panels can create over-voltage in distribution feeders.

In this dissertation, we recognize that in order to provide a sound support for efficient and robust integration of DG systems into the distribution grid it is essential to: (1) assess current operating and planning practices with respect to their ability to best integrate and utilize DG units; (2) identify potential technical challenges brought about by the DG deployment; (3) introduce a sufficiently detailed dynamic model to assess

dynamic stability of distribution systems with large penetration of distributed generators, (4) introduce technically innovative ways for facilitating the best integration of DG units without creating reliability and safety problems; and, (5) recommend policies and institutional arrangements in support of integrating potentially high number of small DG units in the existing electric distribution networks in technically acceptable ways.

1.1.3 Major Contributions

In this dissertation, we describe the likely future structure of distribution systems with DG, noting how they are different from today's systems. We explore the possibility that in the near future the role of centralized power plants may decrease as many smaller scale distributed generators close to the end users provide a larger portion of electricity.

We introduce a new notion of efficiency for distribution energy systems which is uniquely defined by the fact that DGs are mainly environmentally friendly and inexpensive power plants. Therefore, they are must-run generators and they do not need to participate in economic dispatch. This points to the fact that the main measure of efficiency is reducing power delivery losses. We analyze the long-term and short-term effects of DGs on system-wide efficiency of distribution systems. At the planning stage, efficiency improvement is achieved by strategically locating DGs. In operation, AC OPF-based voltage dispatch is done to adjust the voltage settings of DGs.

Next, we assess frequency and voltage stability of distribution energy systems. Our findings show that while DGs are adjusted for optimal steady state utilization, the system could become very sensitive (non-robust) even to very small perturbations around the scheduled operating point.

We show that where DG units are located can play a significant role in system-wide efficiency and dynamic stability of distribution systems. Our results illustrate that DG units connected in electrically close areas could oscillate against each other and that this could lead to frequency and/or voltage stability problems in distribution systems during normal conditions.

In this work, the main differences between the dynamic model of distribution energy systems and transmission power systems are analyzed. In particular, we show that due to large resistance to reactance line ratio (r/x), real-power and voltage dynamics are

strongly coupled in distribution systems. Therefore, it is no longer possible to use decoupled real-power/voltage dynamic model for assessing stability of these systems.

Table 1.1: Transmission Power Systems vs. Distribution Energy Systems

Transmission Power Systems		Distribution Energy Systems	
Central Generation (CG)	Slow Large inertia	Distributed Generation (DG)	Fast Low inertia
Transmission Network	Non-resistive Meshed High voltage	Distribution Network	Resistive Radial Low voltage

Next, we design a structure-based decentralized control framework for ensuring small-signal stability of distribution systems in response to perturbations from normal condition. The Block Gerschgorin Theorem and Liapunov function-based stability methods are applied to formally state sufficient conditions for stability of such systems.

Our technical results raise questions concerning policy making and institutional arrangements for siting and operation of high numbers of larger DGs in technically feasible and efficient ways. We propose that a reliable and efficient integration of distributed generation needs strategic planning and operation for distribution systems. We show that today's standards and operating models such as IEEE 1547 and plug-and-play cannot support a large penetration of DG units sending power to the distribution system. Finally, we propose a possible model-based adaptive policy and link methods engineers use to the policy design for achieving efficient and reliable performance.

1.1.4 Dissertation Outline

The remaining chapters of this dissertation is organized as follows. Note that the chapters were written separately, and each are intended to provide value independently.

Chapter 2 explores optimal location and method of utilization of DG units in distribution systems so as to improve efficiency and reduce power delivery losses. We stress that DG units are environmentally friendly and inexpensive power plants, therefore they need to be fully utilized for real-power. We introduce loss minimization as a quantifiable measure of efficiency of distribution systems. In order to maximize system-wide efficiency, at the planning stage the optimal locations of placing DGs are obtained using optimization methods. In operation, AC OPF-based voltage dispatch is done to

optimize voltage settings of DG units in coordination with other controllable devices in the distribution system.

In Chapter 3, a new dynamic model is proposed for distribution energy systems. The dynamic model is structural and it comprises local models of DGs and loads interconnected via the distribution grid. We highlight that due to large resistance to reactance line ratio, frequency and voltage dynamics are strongly coupled in distribution systems. This differentiates distribution energy systems from typical transmission power systems.

Chapter 4 examines voltage and frequency stability of distribution energy systems. It demonstrates that DGs connected in electrically close areas can destabilize frequency and/or voltage in local distribution networks. This phenomenon has only recently been observed and studied by several authors like Cardell et al (30, 31) and Guttromson (66). These instabilities are partially explained in terms of electromechanical oscillations caused by the presence of small synchronous generators. However, an in-depth precise explanation and effective solutions of this phenomenon have not previously been provided.

We analyze in depth the nature of voltage and frequency instability and determine the dependence of instability on the network's and DGs' parameters. We show that instability mainly depends on electrical distance between larger DGs supplying power to the system. Next, the sensitivity analysis of unstable eigenmodes with respect to parameters of DGs and the network parameters is presented. Based on the analysis, the nature of system instability is explained.

In Chapter 5, several methods for stabilizing voltage and frequency in distribution networks are proposed. In particular, locating DGs beyond critical electrical distance, deploying fast flywheel energy storage and designing advance automatic control systems are suggested as possible ways to enhance the robustness of distribution energy systems. Particular emphasis is placed on systematic control design for DG units which might otherwise contribute to instability.

Our technical results raise questions concerning policy making and institutional arrangements for reconciling in technically feasible ways the siting and operation of high numbers of small and/or medium-size DGs. In Chapter 6, we introduce a possible adaptive model-based policy to link the methods engineers use to policy design for ensuring reliable and efficient integration of DGs. We stress that because of complexity

of the effects of DGs on distribution systems, it is no longer possible to design one-size-fits-all policies. Instead policies need to be supported by models and software.

2

Potential for Efficiency Improvements in Distribution Energy Systems

2.1 Introduction

Today about 7% of the electricity transmitted in the United States is dissipated in transmission and distribution systems. This accounts for around 270 Million MWh energy losses per year and is 1.17 times greater than the annual net electricity generation of Pennsylvania (230 Million MWh in 2010) (69).

The dissipation of power delivery imposes large social and environmental costs. These costs are closely related to the average price of electricity, the characteristics of electric power systems, and the technology of the power plants. In isolated electric power systems these costs can be much higher than in continental power systems.

As an illustration, the average price of electricity on Flores Island, one of the western group islands of Azores Archipelago, is around $174 per MWh, while the average price of electricity in the US is about $94 per MWh. Therefore, a 1 MWh loss in the distribution system of Flores costs approximately 1.85 times more than a 1 MWh loss in the distribution system of the US.

There are several conventional approaches to minimizing power delivery losses. The most well-known and commercialized method is to implement a shunt and/or series capacitors in order to cancel out reactive currents through the lines. In this chapter,

we show that using capacitor banks reduces only a small portion of the power delivery losses, since reactive currents through the lines only contribute to about 20% of the losses. On the other hand, distributed generators, such as wind plants, can significantly reduce losses by producing both real and reactive power.

Note that DG units are often must-run power plants. They are environmentally friendly and inexpensive; therefore, they do not need to participate in economic dispatch. Because of the unique characteristics of distribution systems, which differentiate them from transmission systems, the conflicting interest between clean, inexpensive, and loss minimization does not exist. Therefore, minimizing power losses is the only quantifiable measure for efficiency of distribution systems.

Long-term efficiency can be achieved at the planning stage by optimally locating DG units in distribution systems. In operation stage distribution losses can be minimized by optimizing voltage settings of DG units. This results in short-term efficiency of the system.

In this chapter, we investigate loss minimization of two real-world-like distribution systems. We show that by strategically locating and optimally operating candidate distributed generators, more than 50% of power delivery losses can be reduced.

2.2 Power Delivery Losses on Flores Island

Flores Island is one of the smaller islands of the Azores Archipelago, the islands of Portugal. The population is approximately 4000 inhabitants, and its area is around 143 km^2 (17).

The electric network on Flores consists of a 15 kV radial distribution network with 46 nodes and 45 branches. Total demand on the island is around 2 MW. Four diesel power plants provide more than 50% of the electric energy. Around 35% of the demand is supplied by four hydro power plants, and two synchronous wind plants provide the rest ($\sim$ 15%). Figure 2.1 illustrates the schematic of the distribution network on Flores. In this model, the diesel generator is located at the reference node. The hydro plant is located next to the diesel generator, and the wind plant is located in the middle of the island.

Power flow analysis for Flores demonstrates that more than 2% of the power delivery is dissipated in the 15-kV distribution network. This accounts for approximately a 1

MWh loss of energy per day and therefore a 365 MWh waste of electric energy per year. Note that power delivery losses in 400-V distribution feeders are not accounted here.

Given the average price of electricity on the island ($174/MWh), 2% power delivery losses cost the island more than $61,000/yr. Table 2.1 illustrates the average cost of producing electricity for the different power plants. The 2% losses also create more than 117 tons of CO_2 emissions per year; the average CO_2 emissions on Flores are 0.32 tons/MWh.

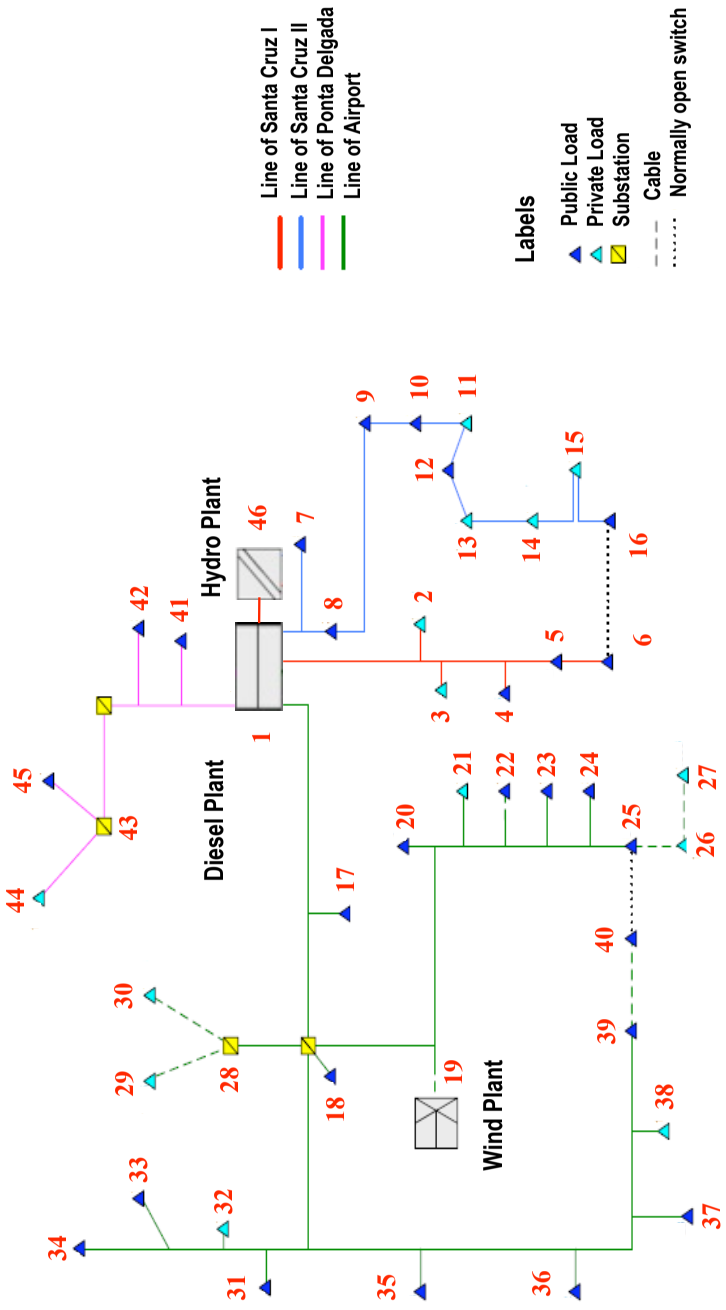

Figure 2.1: Schematic of the distribution network on Flores.

Table 2.1: Average cost of producing electricity for different power plants on Flores (8).

	Costs ($/MWh)
Diesel Plant	261
Hydro Plant	88
Wind Plant	87

2.3 Power Delivery Losses in the IEEE 30-node Distribution System

The second system studied in this chapter is the IEEE 23-kV-30-node distribution system (shown in Figure 2.2) (71). The overall fixed power load of the distribution system is 14.2 MW, which is the average consumption of a town of 20,000 people. About 9% of the delivery power is dissipated in the distribution system ($\sim$ 1.36 MW). This accounts for a 32.64 MWh waste of energy per day.

In the future, two combustion turbines (CT), represented in gray, whose real and reactive power capacity are 0.7 MW $\leq P_{DG} \leq$ 0.8 MW and -0.4 MVar $\leq Q_{DG} \leq$ 0.4 MVar will be connected to the system.

In the next section, we investigate possible approaches to minimizing power delivery losses on these real-world-like distribution systems.

2.4 Possible Approaches to Optimal Placement of DGs

In this section, three major approaches to determining the optimal combinations of placing DG units are studied: 1) exhaustive search for candidate locations, 2) model-based heuristic search; and, 3) sensitivity with respect to technical variables.

Note that placing DGs at optimal locations might violate the laissez-faire policy, under which private operators can install DG units wherever they choose. Therefore, it is essential for utilities and distribution system operators (DSOs) to promote incentive mechanisms in order to entourage DG owners to participate in optimization process and to place their DGs at optimal locations. This needs fundamental changes in planning of today's distribution networks. In Chapter 6, we investigate possible approaches to implement such incentive mechanisms.

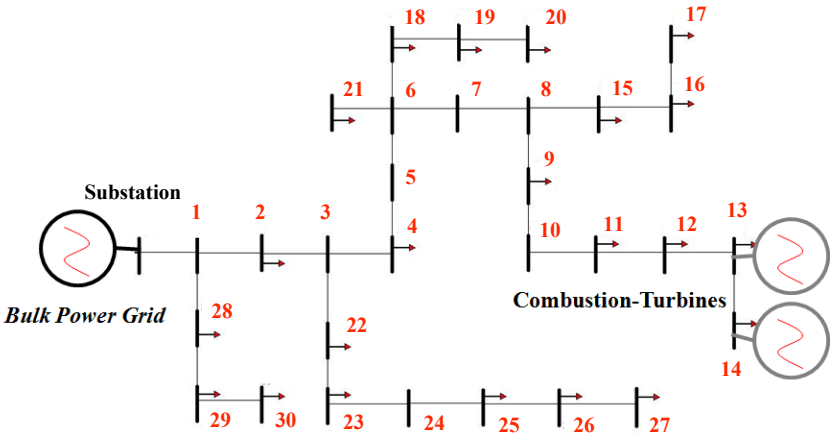

Figure 2.2: Schematic of the IEEE 23-kV-30-node distribution system with new DGs.

2.4.1 Exhaustive Search for Candidate Locations

The exhaustive search approach is motivated by the fact that only a sub-set of nodes in a distribution system is given for candidate locations of placing DG units. Therefore the combinatorial search is reduced to a selective search.

In this approach, first power flow analysis is done for all possible combinations of placing DG units. In the next step, the voltage profile of the system is obtained for all combinations. If voltage exceeds the acceptable limit, the corresponding locations are considered as problematic locations for placing DGs.

Next, power delivery losses are computed for all scenarios and candidate locations are ranked based on loss reduction. If the optimal location is among problematic locations, capacitor banks need to be installed to compensate voltage.

2.4.2 Model-based Heuristic Search

In general, distribution systems have a radial structure which gives them special features. For instance, there is only one route between two nodes of the system. The radial distribution networks are constructed by paths, which connect the substation to the end of the network. Figure 2.3 demonstrates a schematic of a 12-node radial distribution network constructed by 6 paths. That is, path 1: 650-632-633; $\cdots$ and; path 6: 650-632-671-684-611.

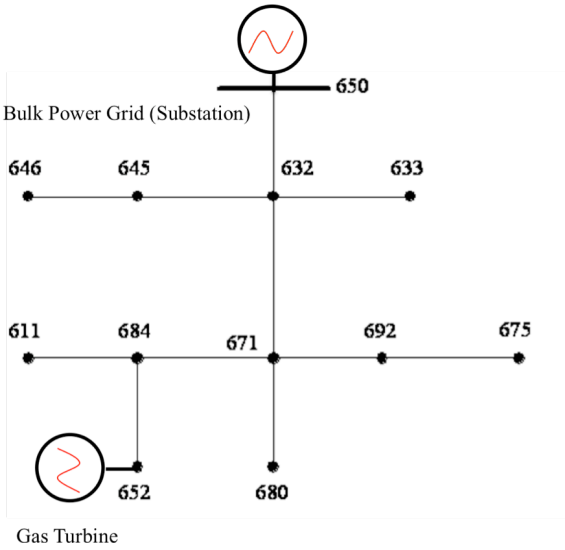

Figure 2.3: 12-node radial distribution network [22].

Due to the unidirectional structure of distribution networks, active and reactive currents through a path decrease by moving toward the end point. This implies that if DG's placement results in current reduction in a line of a path, it causes current reduction in all the lines located above the DG. In this condition, the amount of loss reduction due to DG is calculated as follows:

$$\begin{aligned} \Delta P_L &= \sum_{\substack{j=1 \\ i \in P}}^{j} \left[J_i^2 - \left(J_i cos(\varphi_i) - I_{DG} cos(\varphi_{DG}) \right)^2 - \left(J_i sin(\varphi_i) - I_{DG} sin(\varphi_{DG}) \right)^2 \right] R_i \\ &= \sum_{\substack{j=1 \\ i \in P}}^{j} \left[2 J_i I_{DG} cos(\Delta\varphi_i) - I_{DG}^2 \right] R_i \end{aligned} \tag{2.1}$$

where J_i and R_i are the apparent current and resistance of the i^{th} line, P is the route between the node where DG is located and the substation (e.g. lines 652, 684, 671, and 632 in Figure 2.3), and $\Delta\varphi_i$ is the difference between DG's and lines' power factor angles. Note that here the effect of overall voltage improvement due to loss reduction is neglected.

Given the unique characteristics of distribution systems, a model-based heuristic

algorithm is introduced to determine the optimal locations of placing DGs. This method has two general steps: (1) the optimal location of DG in each path is obtained. The results of this step gives the local optimal solutions. (2) the global optimal location is obtained by ranking the local optimal solutions.

If DG's placement at the i^{th} node results in power loss reduction in the i^{th} line (e.g. the line 652), loss reduction will occur through all the lines located above the i^{th} line (e.g. lines 684, 671 and 632). This implies that the optimal location of the DG at each path is the node where if the DG is located, power losses decrease through the line above the DG. If the DG is located at the node right below the optimal node, power losses increase through that line. The mathematical representation of these conditions is as follows:

$$\Delta P'_{L_i} \leq \Delta P_{L_i} \tag{2.2}$$

$$\Delta P'_{L_{i+1}} > \Delta P_{L_{i+1}} \tag{2.3}$$

where ΔP_{L_i} and $\Delta P'_{L_i}$ are power loss at the i^{th} line before and after adding the DG. Also, the $i+1$ line is the line right below the i^{th} line and closer to the end of the path. Recalling from Equation (2.1), the criteria for the optimal location can be re-written as follows:

$$\left[J_i^2 + I_{DG}^2 - 2J_i I_{DG} cos(\Delta\varphi_i)\right] \leq J_i^2 R_i \tag{2.4}$$

$$\left[J_{i+1}^2 + I_{DG}^2 - 2J_{i+1} I_{DG} cos(\Delta\varphi_{i+1})\right] > J_{i+1}^2 R_{i+1} \tag{2.5}$$

Or

$$I_{DG} \leq 2J_i cos(\Delta\varphi_i) \tag{2.6}$$

$$I_{DG} > 2J_{i+1} cos(\Delta\varphi_{i+1}) \tag{2.7}$$

Equations (2.6 and 2.7) imply that at the optimal location, the output current of DG is less than or equal to two times of the current of the line above the DG multiplied by the power factor differences of the DG and line. This implicitly suggests that the optimal location of DG is often at the end of distribution systems, since generally DG is

designed to serve local consumers and therefore its output current is smaller compared with the current through the lines.

When the optimal location is obtained, power flow analysis is done to compute the overall loss reduction. When two or more DGs are considered to be located in the system, the first step of the optimization process needs to be modified.

In this condition, DGs already located in the network are treated as negative loads. Then, the optimization algorithm is done for the new DG, asking to be connected. If the path in which DGs are located has a decreasing current profile, conditions (2.6 and 2.7) hold. Otherwise, power flow analysis needs to be done for all the candidate nodes in the non-decreasing part of the path. The global optimal node is obtained by ranking local optimal solutions.

2.4.3 Sensitivity with Respect to Technical Variables

In this approach the sensitivity of power losses with respect to changes in voltages and phase angles is analyzed. We start by recognizing that the system power losses are equal to the sum of total power injected.

$$P_L = \sum_{i,j}^{N} V_i V_j \left(G_{i,j} cos(\delta_{i,j}) + B_{i,j} sin(\delta_{i,j}) \right) \tag{2.8}$$

where N is the total number of nodes.

When a DG is located on the i^{th} node, the voltage and phase angle of the node change respectively. Therefore, the power losses change due to changes in voltage and phase angle (36).

$$\begin{aligned} \Delta P_L^i \quad &= \sum_{i,j}^{N} V_j \left(G_{i,j} cos(\delta_{i,j}) + B_{i,j} sin(\delta_{i,j}) \right) \Delta V_i \\ &+ \sum_{i,j}^{N} V_i V_j \left(-G_{i,j} sin(\delta_{i,j}) + B_{i,j} cos(\delta_{i,j}) \right) \Delta \delta_i \end{aligned} \tag{2.9}$$

If ΔP_L^i is negative, it implies that by locating DG at the i^{th} node power delivery losses decreases. At the optimal location, ΔP_L^i is minimum.

2.5 AC Optimal Power Flow-Based Voltage Dispatch

The second step in minimizing power delivery losses is to optimizing voltage settings of DG units in coordination with other controllable devices. The mathematical representation of the optimization algorithm is presented as follows:

$$\underset{V_G}{\text{Minimize}}\ P_L = \sum_{i=1}^{N_G} P_{DG}^{(i)}\left(\delta_G, \delta_L, V_G, V_L\right) - \sum_{j=1}^{N_L} P_L^{(j)}\left(\delta_G, \delta_L, V_G, V_L\right) \tag{2.10}$$

Subject to:

$$P_i - V_i^2 G_{ii} - \sum_{\substack{j=1 \\ j \neq i}}^{N_G+N_L} \left|V_i\right|\left|V_j\right|\left(G_{ij}cos(\delta_i - \delta_j) + B_{ij}sin(\delta_i - \delta_j)\right) = 0 \tag{2.11}$$

$$Q_i + V_i^2 B_{ii} - \sum_{\substack{j=1 \\ j \neq i}}^{N_G+N_L} \left|V_i\right|\left|V_j\right|\left(G_{ij}sin(\delta_i - \delta_j) - B_{ij}cos(\delta_i - \delta_j)\right) = 0 \tag{2.12}$$

$$P_{DG}^{(i)} = P_{DG_{max}}^{(i)} \quad \forall\, i \in N_G \tag{2.13}$$

$$Q_{DG_{min}}^{(i)} \leq Q_{DG}^{(i)} \leq Q_{DG_{max}}^{(i)} \quad \forall\, i \in N_G \tag{2.14}$$

$$P_{DG_i}^2 + Q_{DG_i}^2 \leq S_{DG_i}^2 \quad \forall\, i \in N_G \tag{2.15}$$

$$V_{min}^{(j)} \leq \left|V_j\right| \leq V_{max}^{(j)} \quad \forall\, j \in N_G + N_L \tag{2.16}$$

Here N_G is the number of generator nodes, and N_L is the number of load nodes in the system. In addition, V_L and δ_L are the voltages and phase angles of the system loads.

2.6 Power Delivery Losses Minimization

Our results illustrate that more than 57% of the distribution losses on Flores Island could be reduced by optimally locating a new wind plant and optimizing the voltage setting of the wind plant in coordination with other generators. This would mean more than 208 MWh energy savings per year, which would save Flores more than $36,000 per year and reducing CO_2 emissions by 70 tons per year. Figure 2.4 shows the potential optimal locations for the new wind plant, highlighted by the green rectangle.

Placing the new wind plant at the optimal location (at node 40) would also increase the reliability of the island. For example, if the line connecting the diesel plant to the center of the island is disconnected (Line 1-17 or 17-18), the wind power plants can supply loads in the center and southern parts of the island. Note that in this condition the wind plants need to be combined with energy storage and/or adaptive load management for ensuring system stability.

Since the average cost of producing electricity with diesel generators is about 3 times larger than that with wind power plants, offsetting 20% of the diesel generation with wind generation, furthermore, would result in a 10% reduction in the total cost of electricity. Therefore, the total dollar savings to the island would be more than $250,000 per year. About 15% of the overall savings is due to reducing the delivery losses, and the other 85% is due to the offsetting of diesel generation with wind generation. Moreover, overall CO_2 emissions would be reduced by about 1300 tons per year. Around 5% of the reduction would be due to reducing the delivery losses and more than 95% would be due to the offsetting of diesel generation with wind generation.

Our results of optimization for the IEEE 30-node system also indicate the optimal combinations of locating two CTs at nodes 13^{th} and 14^{th} (shown in Figure (2.2). Our findings also illustrate that strategic placement and optimal dispatch of voltage settings of two CTs result in about 47% of total loss reduction or about 5,600 MWh/yr energy savings when only 10% of the demand is supplied by CTs.

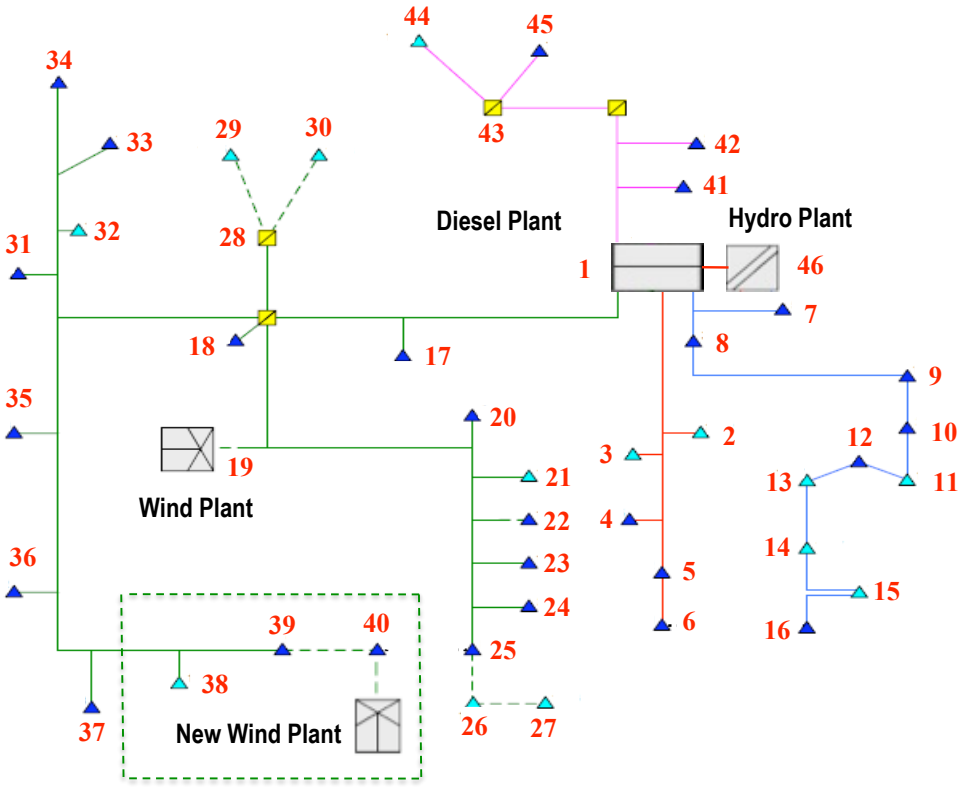

Figure 2.4: Schematics of the optimal area for locating new wind plants.

2.6.1 Comparison between Distributed Generation and Capacitor Banks

In this sub-section, we show that shunt and/or series capacitors cannot notably reduce power delivery losses, whereas small-scale power plants, such as synchronous wind plants, can significantly reduce losses by offsetting real and reactive currents. To this end, we explore first the effects of active and reactive currents on power delivery losses of Flores Island. We see in Figure 2.5 that active currents through the distribution lines of Flores are about two times larger than reactive currents. Since power delivery losses are related to the square of the current, the losses due to active currents (P_x) are four times larger than the losses due to reactive currents (P_r).

In other words, reactive currents contribute to only 20% of the losses; active currents cause the rest ($\sim$ 80%). This implies that installing a shunt and/or series capacitors, which compensate for reactive currents only, can eliminate only a small portion of the power delivery losses.

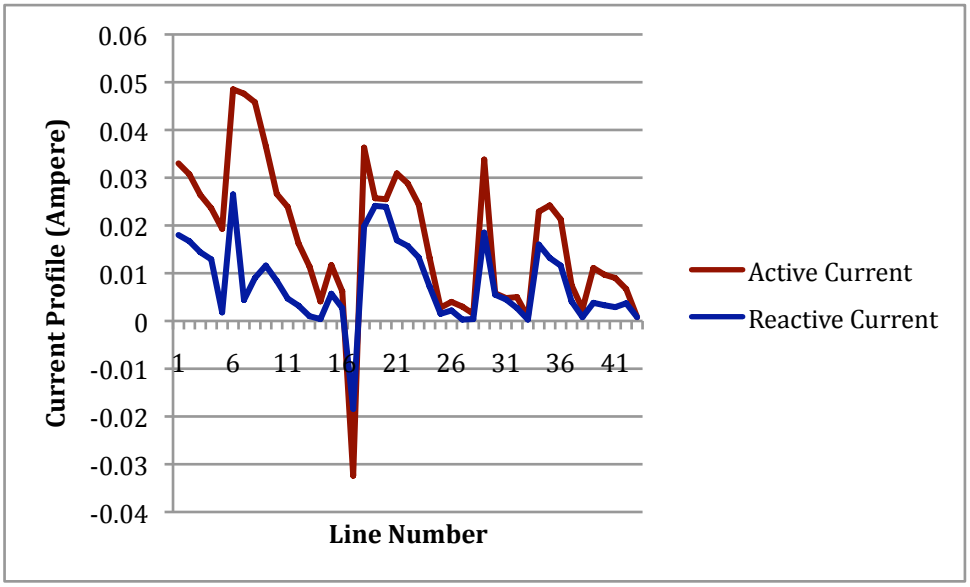

Figure 2.5: Active and reactive current profile through the lines.

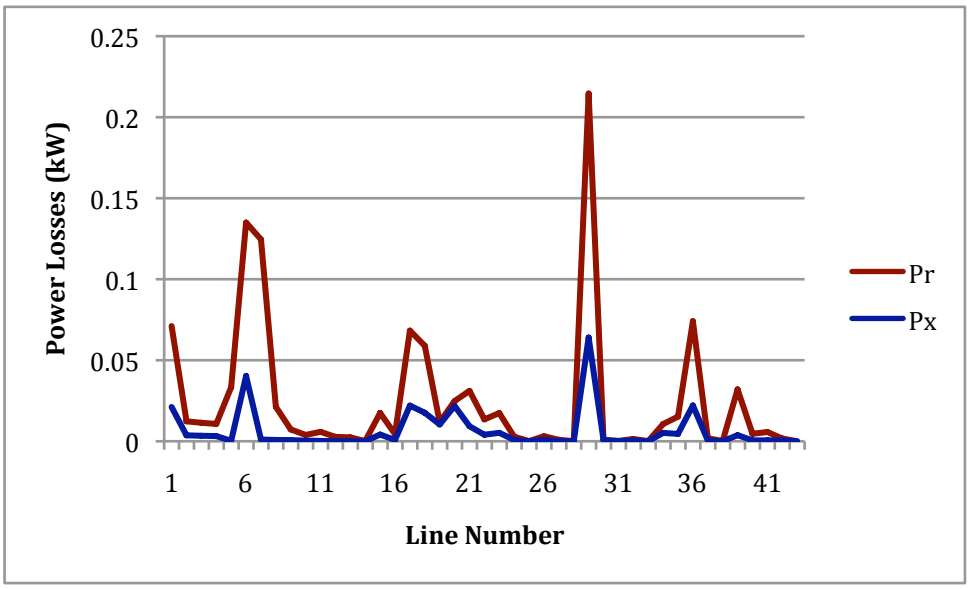

Figure 2.6: Distribution losses due to active and reactive currents.

On the other hand, DG power plants can offset both real and reactive currents through the lines and therefore eliminate a large portion of losses. We have shown in the previous section that by producing 10% of the demand with strategically placed and optimally operated DG units, about 50% of the power losses can be reduced.

In general minimizing power delivery losses has profound social and environmental advantages. Therefore, using AC OPF-based dispatch to gain such advantages, which would otherwise not be possible, is an indispensable step toward enhancing efficiency of distribution systems. To this end, DSOs need to implement both SCADA and computer tools such as AC OPF for computing on-line voltage adjustments of the distributed generators. Given that today the distribution power systems do not rely on on-line monitoring and dispatch, it is essential to understand the necessity of doing this in order to allow the transformation of these systems into the most efficient enablers of distributed generation.

2.7 Conclusions

In this chapter we highlight that by strategically placing and optimally operating DG units, about 50% of the power delivery losses can be reduced from the distribution system on Flores Island and from the IEEE 30-node distribution system. In this condition, annually more than 208 MWh energy can be saved on Flores. It would also save the island more than $250,000 per year and reduce CO_2 emissions by 1300 tons per year.

Our technical findings furthermore illustrate that loss reduction highly depends on the location and voltage settings of DG units. We show that capacitor banks can eliminate only a small portion of the power delivery losses, while distributed generators with automatic voltage control can significantly reduce power delivery losses by offsetting both the real and reactive currents through the lines.

We propose that while the utility studies are being carried out, and new candidate DGs are being considered, it is essential to develop a systematic framework that assesses the optimal locations and utilization methods for the new DG units in order to minimize power delivery losses and maximize system-wide efficiency.

3

Dynamic Models for Distribution Energy Systems

3.1 Introduction

Distributed generators cause major changes in dynamic stability of distribution systems. In particular, voltage and frequency stability may become a major concern for distribution system operators.

In this chapter, we show that due to large resistance to reactance line ratio, the real/reactive power decoupling assumption is not valid for distribution systems. This differentiates dynamic stability of distribution systems from that of traditional transmission power systems.

We first propose a new coupled real-power voltage dynamic model to assess voltage and frequency stability of distribution energy systems. This model is derived by combing dynamic models of real-power/frequency dynamics and reactive power/voltage dynamics for a small electric machine DG. The system-level model is further derived by subjecting this coupled DG model to the linearized real/reactive power network constraints. This ultimately leads to a standard state-space formulation of a dynamic model for a general distribution network system.

In Section 3.4 the main differences between the dynamic model of transmission power systems with large centralized generation (CG) and distribution energy systems with DG units are investigated. We show that because of low inertia and fast dynamic response of DGs, coupling between DG units is often stronger compared with that

between CG units.

3.2 Revisiting Real/Reactive Power Decoupling Conditions for Distribution Energy Systems

One of the major assumptions routinely made in today's transmission power systems is that real and reactive power dynamics are largely decoupled. Under this condition, the governor control and excitation control of generators can be designed in a fully decoupled fashion (61).

We show in this chapter that the decoupling assumption is not valid for distribution energy systems. Therefore, if the primary control of DG units is designed based on the decoupled model, small-signal stability problems may occur in distribution systems.

We start with revisiting the generalized decoupling conditions for today's transmission power systems and extending the conditions for distribution energy systems. In general, the relationship between changes in voltage and phase angles due to changes in real and reactive power is defined by linearizing the load flow equations around the operating point (shown in Equation 3.1) (46).

$$\begin{bmatrix} P \\ Q \end{bmatrix} = \begin{bmatrix} \frac{\partial P}{\partial \delta} & \frac{\partial P}{\partial V} \\ \frac{\partial Q}{\partial \delta} & \frac{\partial Q}{\partial V} \end{bmatrix} \begin{bmatrix} \delta \\ V \end{bmatrix} \tag{3.1}$$

Based on the Block Gerschgorin Theorem, fully elaborated in (5), changes in voltage have insignificant effects on changes in real-power, if the sensitivity of real-power with respect to change in voltage is much smaller compared with the sensitivity of real-power with respect to change in phase angle. Therefore, the decoupling condition for real-power and voltage dynamics can be expressed as follows:

$$\left\| \frac{\partial P}{\partial \delta} \right\|_\infty \gg \left\| \frac{\partial P}{\partial V} \right\|_\infty \tag{3.2}$$

where $\| \, . \, \|_\infty$ represents the infinity norm of the indicated matrix. In a similar fashion, the decoupling condition for reactive power and frequency dynamics is derived as:

$$\left\| \frac{\partial Q}{\partial V} \right\|_\infty \gg \left\| \frac{\partial Q}{\partial \delta} \right\|_\infty \tag{3.3}$$

The above conditions have generic structures, which is not explicitly expressed in

terms of the characteristics of electric power systems. In this section, we illustrate the decoupling conditions in terms of the conductances and susceptances of the grid.

Generally, the sensitivity of the real-power of the i^{th} node with respect to changes in the voltage and phase angle of the j^{th} node can be expressed as follows (32):

$$\frac{\partial P_i}{\partial \delta_j} = V_i V_j \left(G_{ij} sin(\delta_i - \delta_j) - B_{ij} cos(\delta_i - \delta_j) \right) \tag{3.4}$$

and

$$\frac{\partial P_i}{\partial V_j} = V_i \left(G_{ij} cos(\delta_i - \delta_j) + B_{ij} sin(\delta_i - \delta_j) \right) \tag{3.5}$$

Assuming voltages are close to 1 pu and the phase angle difference between nodes is small, the sensitivity of real-power with respect to changes in phase angles and voltages can be shown as:

$$\frac{\partial P_i}{\partial \delta_j} \approx -B_{ij} \tag{3.6}$$

and

$$\frac{\partial P_i}{\partial V_j} \approx G_{ij} \tag{3.7}$$

Similarly, the sensitivity of the reactive power with respect to changes in phase angles and voltages can be derived based on the conductances and susceptances of the grid.

$$\frac{\partial Q_i}{\partial \delta_j} \approx -G_{ij} \tag{3.8}$$

and

$$\frac{\partial Q_i}{\partial V_j} \approx -B_{ij} \tag{3.9}$$

By combining Equations (3.6) to (3.9) with Equation (3.1), the Jacobian matrix is expressed in terms of conductance and susceptance matrices.

$$\begin{bmatrix} P \\ Q \end{bmatrix} \approx \begin{bmatrix} B & G \\ -G & B \end{bmatrix} \begin{bmatrix} \delta \\ V \end{bmatrix} \tag{3.10}$$

It follows from Equations (3.6) to (3.10) that the decoupling conditions are valid if the resistance to reactance line ratio is negligible . That is,

$$\left\| B \right\|_\infty \gg \left\| G \right\|_\infty \tag{3.11}$$

In general, for high voltage transmission systems the $\frac{r}{x}$ ratio is small. Therefore,

Table 3.1: Average resistance to reactance ratio ($\frac{r}{x}$) for three real world distribution systems

The distribution system of Flores Island	3.17 (pu)
The distribution system of Sao Miguel Island	1.92 (pu)
IEEE 30-node distribution system	2.27 (pu)

the decoupling assumption might be acceptable during normal operating conditions. On the other hand, for distribution systems this ratio is not negligible at all. Table 3.1 illustrates the average resistance to reactance ratio for three real world distribution systems. As shown in Table 3.1, the resistance of distribution lines is even larger than the reactance of the lines. Therefore, the decoupling conditions are strongly violated for distribution systems.

It summary, the results of this section claim that the real-power and voltage dynamics are strongly coupled in distribution energy systems. Therefore, the commonly-used decoupled real-power/frequency dynamic model cannot be used to assess stability of distribution systems with DG units.

In the next section, we propose a new coupled real-power voltage dynamic model for distribution energy systems. This model builds on the model first introduced in (44). The proposed model offers an intuitive insight into the decentralized nature of distribution systems where each DG represent a sub-system of the whole system.

3.3 Coupled Real-Power Voltage Dynamic Model of Distribution Energy Systems

In general, a distribution energy system consists of a group of distributed generators and many loads which are interconnected via the distribution network. Grid connected distribution systems have a connection to the bulk power grid, typically modeled as an ideal generator with infinite inertia.

Dynamics of a small electric machine DG is considered as two parts, which represent the electromechanical and electromagnetic aspects of the DG (44). For conventional technologies such as a diesel plant the electromechanical part is dominated by a prime

mover, rotating mass, and a governor control (GC). Equation (3.12) illustrates the closed-loop state space model of the electromechanical part of a diesel plant.

$$\begin{aligned}\frac{d}{dt}\begin{bmatrix}\delta_G\\ \omega_G\\ m_B\\ \rho_C\end{bmatrix} &= \begin{bmatrix}0 & \omega_0 & 0 & 0\\ 0 & \frac{-D_d}{2H_d} & \frac{C_c}{2H_d} & 0\\ 0 & \frac{-C_dK_d}{T_cR_c} & \frac{-1}{T_c} & \frac{-C_dK_d}{T_c}\\ 0 & -K_I & 0 & -K_D\end{bmatrix}\begin{bmatrix}\delta_G\\ \omega_G\\ m_B\\ \rho_C\end{bmatrix}\\ &+ \begin{bmatrix}0\\ \frac{-1}{2H_d}\\ 0\\ 0\end{bmatrix}P_G + \begin{bmatrix}0\\ 0\\ 0\\ K_I\end{bmatrix}\omega_G^{ref}\end{aligned} \tag{3.12}$$

In this model, δ_G is the phase angle, ω_G is the frequency, m_B is the fuel rate, and ρ_C is the governor control of the diesel plant. In addition, ω_0 is the synchronous speed, and H_d and D_d are the inertia and damping coefficients, respectively. C_d and K_d are the transfer function coefficients for the fuel system, T_c is the time constant of the fuel system, and K_I and K_P are the integral gain and the proportional gain of the GC system. Moreover, ω_G^{ref} is the reference value for the generator frequency (14, 51).

The electromagnetic dynamics of the DG is coupled to the electromechanical dynamics by the magnetic field in the machine air gap (44). Depending on the technology of the DG, the electromagnetic part is modeled as a third or fourth order dynamic model. For a diesel generator, the electromagnetic part consists of a synchronous machine and an excitation control, shown in Equation (3.13).

$$\begin{aligned}\frac{d}{dt}\begin{bmatrix}V_R\\ e_{fd}\\ e'_q\\ V_F\end{bmatrix} &= \begin{bmatrix}\frac{-1}{T_a} & \frac{-K_aK_f}{T_aT_f} & \frac{-K_a}{T_a} & \frac{K_a}{T_a}\\ \frac{1}{T_e} & \frac{-(K_e+S_e)}{T_e} & 0 & 0\\ 0 & \frac{1}{T_d} & -\frac{1}{T_d} & 0\\ 0 & \frac{k_f}{T_f^2} & 0 & \frac{-1}{T_f}\end{bmatrix}\begin{bmatrix}V_R\\ e_{fd}\\ e'_q\\ V_F\end{bmatrix}\\ &+ \begin{bmatrix}0\\ 0\\ \frac{-(x_d-x'_d)}{T_d}\\ 0\end{bmatrix}i_d + \begin{bmatrix}\frac{K_a}{T_a}\\ 0\\ 0\\ 0\end{bmatrix}V_G^{ref}\end{aligned} \tag{3.13}$$

Here, V_R is the regulator voltage, e_{fd} is the field excitation, e'_q is the machine voltage behind the direct transient impedance, and V_F is the feed-back voltage (the voltage of the compensator). In addition, i_d is the reactive current out of the generator and V_G^{ref} is the reference value for the generator terminal voltage (44, 73). Note that if the

effects of damper winding is neglected, then $V_G = e'_q$ since $V_G = \sqrt{{e'_q}^2 + {e'_d}^2}$ and $e'_d = 0$ (73).

Considering Equations (3.12) and (3.13), the general state space model of the electromechanical and electromagnetic sub-systems of a DG take on the following form:

$$\frac{dx^P_{LC}}{dt} = A^P_{LC}x^P_{LC} + C_P P_G + B_P \omega^{ref}_G \tag{3.14}$$

$$\frac{dx^Q_{LC}}{dt} = A^Q_{LC}x^Q_{LC} + C_Q i_d + B_Q V^{ref}_G \tag{3.15}$$

Here x^P_{LC} and x^Q_{LC} are the internal state variables of the electromechanical and electromagnetic parts of the DG. For the diesel power plant the internal state variables is denoted in the following way:

$$x^P_{LC} = \begin{bmatrix}\delta_G & \omega_G & m_B & \rho_C\end{bmatrix}^T \; x^P_{LC} = \begin{bmatrix}V_R & e_{fd} & e'_q & V_F\end{bmatrix}^T$$

P_G and i_d are the coupling variables between the DG and the rest of the system.

It follows from Equations (3.14) and (3.15) that independent of the type of DG, its state-space model can be expressed in terms of its internal state variable (x^P_{LC} and x^Q_{LC}), while the coupling variables are real-power and reactive current (P_G and i_d) generated by the DG. For diesel plants internal state variables are different than for hydro plants, and are function of power generation type. However, the coupling variables between a diesel power plant, or a hydro power plant is the same (46). It is important to observe that models (3.14) and (3.15) are of the same form for any type of DG. The numerical parameters will determine robustness of the DG with respect to disturbances.

3.3.1 Distribution Network Constraints

The distribution network is modeled by a set of power flow equations (31). Changes in phase angle and voltage are related to changes in real and reactive power by a Jacobian matrix (32). We re-order the Jacobian matrix by grouping the generator nodes (G) and the load nodes (L) together. The new Jacobian matrix takes on the form:

$$\left[\begin{array}{c} P_G \\ Q_G \\ \hline P_L \\ Q_L \end{array}\right] = \left[\begin{array}{c|c} J_1 & J_2 \\ \hline J_3 & J_4 \end{array}\right] \left[\begin{array}{c} \delta_G \\ V_G \\ \hline \delta_L \\ V_L \end{array}\right] \tag{3.16}$$

where

$$J_1 = \begin{bmatrix} \frac{\partial P_G}{\partial \delta_G} & \frac{\partial P_G}{\partial V_G} \\ \frac{\partial Q_G}{\partial \delta_G} & \frac{\partial Q_G}{\partial V_G} \end{bmatrix} \approx \begin{bmatrix} B_{GG} & G_{GG} \\ -G_{GG} & B_{GG} \end{bmatrix} \tag{3.17}$$

$$J_2 = \begin{bmatrix} \frac{\partial P_G}{\partial \delta_L} & \frac{\partial P_G}{\partial V_L} \\ \frac{\partial Q_G}{\partial \delta_L} & \frac{\partial Q_G}{\partial V_L} \end{bmatrix} \approx \begin{bmatrix} B_{GL} & G_{GL} \\ -G_{GL} & B_{GL} \end{bmatrix} \tag{3.18}$$

$$J_3 = \begin{bmatrix} \frac{\partial P_L}{\partial \delta_G} & \frac{\partial P_L}{\partial V_G} \\ \frac{\partial Q_L}{\partial \delta_G} & \frac{\partial Q_L}{\partial V_G} \end{bmatrix} \approx \begin{bmatrix} B_{LG} & G_{LG} \\ -G_{LG} & B_{LG} \end{bmatrix} \tag{3.19}$$

$$J_4 = \begin{bmatrix} \frac{\partial P_L}{\partial \delta_L} & \frac{\partial P_L}{\partial V_L} \\ \frac{\partial Q_L}{\partial \delta_L} & \frac{\partial Q_L}{\partial V_L} \end{bmatrix} \approx \begin{bmatrix} B_{LL} & G_{LL} \\ -G_{LL} & B_{LL} \end{bmatrix} \tag{3.20}$$

Recalling from previous section that $V_G = e'_q$, the reactive current out of generator nodes and the reactive current into load nodes can be expressed as follows:

$$i_d = \frac{Q_G}{V_G} \qquad i_L = \frac{Q_L}{V_L}$$

Let i_d be the normalized reactive power into the grid from generator nodes and i_L be the normalized reactive power into load nodes. Therefore, Equation (3.16) can be re-written as follows:

$$\left[\begin{array}{c} P_G \\ i_d \\ \hline P_L \\ i_L \end{array}\right] = \left[\begin{array}{c|c} J_1 & J_2 \\ \hline J_3 & J_4 \end{array}\right] \left[\begin{array}{c} \delta_G \\ V_G \\ \hline \delta_L \\ V_L \end{array}\right] \tag{3.21}$$

By solving (3.21) for $\begin{bmatrix} P_L \\ i_L \end{bmatrix}$, an important relationship is obtained.

$$\begin{bmatrix} P_G \\ i_d \end{bmatrix} = K_{PQ} \begin{bmatrix} \delta_G \\ V_G \end{bmatrix} + D_{PQ} \begin{bmatrix} P_L \\ i_L \end{bmatrix} \tag{3.22}$$

Where

$$K_{PQ} = \begin{bmatrix} K_{PQ_{11}} & K_{PQ_{12}} \\ K_{PQ_{21}} & K_{PQ_{21}} \end{bmatrix} = J_1 - J_2 J_4^{-1} J_3 \tag{3.23}$$

and

$$D_{PQ} = \begin{bmatrix} D_{PQ_{11}} & D_{PQ_{12}} \\ D_{PQ_{21}} & D_{PQ_{21}} \end{bmatrix} = J_2 J_4^{-1} \tag{3.24}$$

Equation (3.22) specifies the dependence of generator real and reactive powers on the voltage and phase angle of generators and on the real and reactive powers of loads. Furthermore, Equation (3.22) illustrates that the coupling variables between generators

(P_G and i_d) can be expressed in terms of internal state variables of generators (δ_G and V_G) and deviations in the system loads.

Note that K_{PQ} is the coupling matrix of the interconnected generators. It can be expressed in terms of the reduced susceptance and conductance of the interconnected generators (38).

$$K_{PQ} \approx \begin{bmatrix} B_r & G_r \\ -G_r & B_r \end{bmatrix} \tag{3.25}$$

Assuming the resistance to reactance ratio is negligible ($\|B_r\|_\infty \gg \|G_r\|_\infty$), the coupling matrix can be defined as follows:

$$K_{PQ} \approx \begin{bmatrix} B_r & 0 \\ 0 & B_r \end{bmatrix} \tag{3.26}$$

3.3.2 Dynamic Model of the Interconnected Distribution System

As shown in Equation (3.22), the coupling variables between DG units are not exogenous variables. In fact, the coupling variables of the i^{th} DG can be expressed in terms of its own internal state variables ($\delta_G^{(i)}$ and $V_G^{(i)}$), in terms of the internal state variables of other DGs ($\delta_G^{(j)}$ and $V_G^{(j)}$), and in terms of the real and reactive powers of loads seen from the i^{th} DG.

$$\begin{aligned} P_G^{(i)} &= K_{PQ_{11}}^{(i,i)} \delta_G^{(i)} + K_{PQ_{12}}^{(i,i)} V_G^{(i)} \\ &+ \sum_{\substack{j=1 \\ j \neq i}}^{N} \left(K_{PQ_{11}}^{(i,j)} \delta_G^{(j)} + K_{PQ_{12}}^{(i,j)} V_G^{(j)} \right) \\ &+ \sum_{k=1}^{M} \left(D_{PQ_{11}}^{(i,k)} P_L^{(k)} + D_{PQ_{12}}^{(i,k)} i_L^{(k)} \right) \end{aligned} \tag{3.27}$$

and

$$\begin{aligned} i_d^{(i)} &= K_{PQ_{21}}^{(i,i)} \delta_G^{(i)} + K_{PQ_{22}}^{(i,i)} V_G^{(i)} \\ &+ \sum_{\substack{j=1 \\ j \neq i}}^{N} \left(K_{PQ_{21}}^{(i,j)} \delta_G^{(j)} + K_{PQ_{22}}^{(i,j)} V_G^{(j)} \right) \\ &+ \sum_{k=1}^{M} \left(D_{PQ_{21}}^{(i,k)} P_L^{(k)} + D_{PQ_{22}}^{(i,k)} i_L^{(k)} \right) \end{aligned} \tag{3.28}$$

Here N denotes the number of generator nodes and M represents the number of load nodes in the distribution system. By combining Equations (3.14) and (3.15) with (3.27) and (3.28), the desired coupled real-power voltage dynamic model for a distribution system with N DG nodes and M load nodes takes on the following form:

$$\begin{aligned}\frac{d}{dt}\begin{bmatrix} X_1 \\ \vdots \\ X_N \end{bmatrix} &= \begin{bmatrix} A_{1,1} & \cdots & A_{1,N} \\ \vdots & \ddots & \vdots \\ A_{N,1} & \cdots & A_{N,N} \end{bmatrix}\begin{bmatrix} X_1 \\ \vdots \\ X_N \end{bmatrix} \\ &+ \begin{bmatrix} B_1 & 0 & \cdots \\ 0 & \ddots & 0 \\ \vdots & 0 & B_N \end{bmatrix}\begin{bmatrix} U_1 \\ \vdots \\ U_N \end{bmatrix} \\ &+ \begin{bmatrix} D_{1,1} & \cdots & D_{1,M} \\ \vdots & \ddots & \vdots \\ D_{N,1} & \cdots & D_{N,M} \end{bmatrix}\begin{bmatrix} d_1 \\ \vdots \\ d_M \end{bmatrix}\end{aligned} \tag{3.29}$$

In this model, the whole system is divided into N sub-systems. Each sub-system represents the dynamics of the electromechanical and electromagnetic parts of the corresponding DG. The state variables of sub-systems (X_i) are defined as:

$$X_i = \begin{bmatrix} X_{LC}^{P(i)} \\ X_{LC}^{Q(i)} \end{bmatrix}$$

The diagonal terms of the system matrix ($A_{i,i}$) represent the system matrix of the i^{th} DG. The off-diagonal terms of the system matrix ($A_{i,j}$) represent the coupling matrix between the i^{th} DG and the j^{th} DG. The matrices are defined as follows:

$$A_{i,i} = \begin{bmatrix} A_{LC}^{P(i)} + C_P^{(i)} K_{PQ_{11}}^{(i,i)} S_{\delta_G^{(i)}} & C_P^{(i)} K_{PQ_{12}}^{(i,i)} S_{V_G^{(i)}} \\ C_Q^{(i)} K_{PQ_{21}}^{(i,i)} S_{\delta_G^{(i)}} & A_{LC}^{Q(i)} + C_Q^{(i)} K_{PQ_{22}}^{(i,i)} S_{V_G^{(i)}} \end{bmatrix} \tag{3.30}$$

and

$$A_{i,j} = \begin{bmatrix} C_P^{(i)} K_{PQ_{11}}^{(i,j)} S_{\delta_G^{(j)}} & C_P^{(i)} K_{PQ_{12}}^{(i,j)} S_{V_G^{(j)}} \\ C_Q^{(i)} K_{PQ_{21}}^{(i,j)} S_{\delta_G^{(j)}} & C_Q^{(i)} K_{PQ_{22}}^{(i,j)} S_{V_G^{(j)}} \end{bmatrix} \tag{3.31}$$

Where $S_{\delta_G^{(i)}}$ and $S_{V_G^{(i)}}$ are row vectors including 0's and 1's. They are relating $\delta_G^{(i)} = S_{\delta_G^{(i)}} X_{LC}^{P(i)}$ and $V_G^{(i)} = S_{V_G^{(i)}} X_{LC}^{Q(i)}$ respectively.

By combining Equations (3.25), (3.12) and (3.13) with (3.30) and (3.31), the system matrix can be expressed in terms of the parameters of the distribution system and

those of DGs such as the reduced susceptance and conductance of the interconnected generators and the inertia of DGs.

$$A_{i,i} \approx \begin{bmatrix} A_{LC}^{P(i)} + \frac{-1}{2H_i} B_r^{(i,i)} S_{\delta_G^{(i)}} & \frac{-1}{2H_i} G_r^{(i,i)} S_{V_G^{(i)}} \\ \frac{x_d^{(i)} - x_d'^{(i)}}{T_d^{(i)}} G_r^{(i,i)} S_{\delta_G^{(i)}} & A_{LC}^{Q(i)} - \frac{x_d^{(i)} - x_d'^{(i)}}{T_d^{(i)}} B_r^{(i,i)} S_{V_G^{(i)}} \end{bmatrix} \tag{3.32}$$

and

$$A_{i,j} \approx \begin{bmatrix} \frac{1}{2H_i} B_r^{(i,j)} S_{\delta_G^{(j)}} & \frac{1}{2H_i} G_r^{(i,j)} S_{V_G^{(j)}} \\ -\frac{x_d^{(i)} - x_d'^{(i)}}{T_d^{(i)}} G_r^{(i,j)} S_{\delta_G^{(j)}} & \frac{x_d^{(i)} - x_d'^{(i)}}{T_d^{(i)}} B_r^{(i,j)} S_{V_G^{(j)}} \end{bmatrix} \tag{3.33}$$

The second part of the Equation (3.29) illustrates the local control of DGs, which consists of the governor control and excitation control systems. As shown in Equation (3.29), each DG has a decentralized control which responds to perturbations in the local frequency and terminal voltage of the DG. The control signal (U_i) and the control matrix (B_i) of the i^{th} DG is defined as follows:

$$U_i = \begin{bmatrix} \omega_G^{ref^{(i)}} \\ V_G^{ref^{(i)}} \end{bmatrix} \tag{3.34}$$

and

$$B_i = \begin{bmatrix} B_P^{(i)} & 0 \\ 0 & B_Q^{(i)} \end{bmatrix} \tag{3.35}$$

The third part of the Equation (3.29) illustrates the effects of the real and reactive power load deviations on the frequency and voltage dynamics of the DGs. Note that, deviations in the system loads are exogenous variables modeled as disturbances to the grid. The disturbance matrix $D_{i,k}$ accounts for the effects of the load deviations in the k^{th} load node on the frequency and voltage stability of the i^{th} DG. The disturbance variables and the disturbance matrices are defined as:

$$d_k = \begin{bmatrix} P_L^{(k)} \\ i_d^{(k)} \end{bmatrix} \tag{3.36}$$

and

$$D_{i,k} = \begin{bmatrix} E_{\omega_G^{(i)}} D_{PQ_{11}}^{(i,k)} & E_{\omega_G^{(i)}} D_{PQ_{12}}^{(i,k)} \\ E_{V_G^{(i)}} D_{PQ_{21}}^{(i,k)} & E_{V_G^{(i)}} D_{PQ_{22}}^{(i,k)} \end{bmatrix} \tag{3.37}$$

Where $E_{\omega_G^{(i)}}$ and $E_{V_G^{(i)}}$ are column vectors including 1's for the frequency ($\omega_G^{(i)}$) and terminal voltage ($V_G^{(i)}$) of the i^{th} DG respectively and including 0's for other state variables of the i^{th} DG.

3.4 Distribution Energy Systems vs. Transmission Power Systems

In this section, we recognize the main differences between the dynamic model of distribution energy systems with DGs and that of transmission power systems with large centralized power plants.

Recalling from earlier sections, if $\frac{r}{x}$ is negligible, the coupling matrix is only expressed in terms of the reduced susceptance matrix of the interconnected generators. Therefore, for high-voltage transmission systems with small resistance to reactance line ratio, the system matrix takes on the following form:

$$A_{i,i} \approx \begin{bmatrix} A_{LC}^{P(i)} + \frac{-1}{2H_i} B_r^{(i,i)} S_{\delta_G^{(i)}} & 0 \\ 0 & A_{LC}^{Q(i)} - \frac{x_d^{(i)} - x_d^{\prime(i)}}{T_d^{(i)}} B_r^{(i,i)} S_{V_G^{(i)}} \end{bmatrix} \tag{3.38}$$

and

$$A_{i,j} \approx \begin{bmatrix} \frac{1}{2H_i} B_r^{(i,j)} S_{\delta_G^{(j)}} & 0 \\ 0 & \frac{x_d^{(i)} - x_d^{\prime(i)}}{T_d^{(i)}} B_r^{(i,j)} S_{V_G^{(j)}} \end{bmatrix} \tag{3.39}$$

As shown in Equations (3.38) and (3.39), the real-power dynamics is decoupled from voltage dynamics.

Another main difference between the dynamic model of distribution energy systems and that of transmission power systems is that DG units are faster and smaller power plants compared with CG units. Therefore, the inertia and time constant of DGs are smaller compared with those of CGs. Table 3.2 compares dynamic parameters of a small diesel plant on Flores Island and those of a large synchronous power plant installed in continental Portugal.

As shown in Table 3.2, the inertia of CG is more than 630 times larger than that of DG. In addition, DG is more than two times faster than CG. In (52) we have calculated the strength of electrical interaction between power plants based on the norm of the off

Table 3.2: Dynamic parameters of a small diesel plant and a large synchronous power plant

	DG	CG
S_n (MVA)	1	900
M (MJ/Hz)	0.216	137.5
T_d	2.35	5

diagonal terms of the system matrix ($\sum_{j \neq i} \parallel A_{ij} \parallel_\infty$). For distribution energy systems the strength of electrical interaction between the i^{th} DG and the rest of the system is calculated as:

$$\sum_{j \neq i} \parallel A_{ij} \parallel_\infty = \sum_{j \neq i} Max \left(\frac{B_r^{(i,j)} + G_r^{(i,j)}}{2H_i}, \frac{|x_d^{(i)} - x_d'^{(i)}|}{T_d^{(i)}} (B_r^{(i,j)} + G_r^{(i,j)}) \right) \tag{3.40}$$

As shown in Equation (3.40), the strength of electrical interaction depends on the electrical distance between DGs ($B_r^{(i,j)} + G_r^{(i,j)}$), the inertia of DGs and/or the time constant of DGs.

For transmission power systems the strength of electrical interaction between the i^{th} CG and the rest of the system is calculated as follows:

$$\sum_{j \neq i} \parallel A_{ij} \parallel_\infty = \sum_{j \neq i} Max \left(\frac{B_r^{(i,j)}}{2H_i}, \frac{|x_d^{(i)} - x_d'^{(i)}|}{T_d^{(i)}} B_r^{(i,j)} \right) \tag{3.41}$$

As Equations (3.40) and (3.41) indicate, because of low inertia of DG units and due to negligible resistance to reactance ratio of distribution lines the strength of electrical interaction between DG units is often larger compared with that between CG units.

3.5 Conclusions

In this chapter, we first derive the decoupling conditions of real and reactive power dynamics in terms of the susceptance and conductance matrices of the grid. We show that in general the decoupling assumption is not valid for distribution energy systems due to large resistive to reactance line ratio.

Next, a new coupled real-power voltage dynamic model is introduced to demonstrate this inter-dependency of real and reactive power dynamics. We analyze the fundamental

differences between the dynamic model of distribution energy systems and that of transmission power systems. In the next chapter, we confirm our theoretical findings on the distribution systems on Azores Islands.

4

Small-Signal Stability Analysis of Distribution Energy Systems

4.1 Introduction

A system is small-signal stable if it has the ability to retain its steady state following a small perturbation (62). In electric systems, perturbations occur due to changes in the loads, fluctuations in intermittent resources, or variations in the output power of the conventional power plants. If an electric power system cannot maintain its stability, an overall blackout can occur.

Small-signal stability is an essential issue for the robustness and resilience of modern electric energy systems. It is more critical for systems with a high penetration of renewable energy resources, since the intermittency of these resources can intensify frequency oscillations. The electric energy systems in the Azores Archipelago are real-world examples of modern electric energy systems with a large penetration of renewable energy resources such as wind, hydro, and geothermal. In fact, small-signal stability is a major concern when renewable energy resources provide a large portion of the electricity. There have been several reports of outage in the islands brought on by stability issues (8) and (55).

The severity of dynamical problems in specific distribution systems with DGs depends on the technology and control of DGs and on the electrical distances between the DGs. Typical DGs are either synchronous machines or induction machines whose inertia may be much smaller than the inertia of large generators. Their local con-

trol may range from no control, through well-understood governor-excitation control of synchronous machines, through power electronically controlled inverters of synchronous and/or induction machine type DGs (power system stabilizers (PSS) and/or doubly fed induction machines (DFIG)).

In order to ensure the dynamic stability of distribution systems, it is essential to: A) introduce a sufficiently detailed dynamic model to assess the small-signal stability of the systems with their large penetration of distributed generators; B) determine potential instability problems and identify the main causes of the instabilities; and C) design an automatic control to enable the large penetration of DGs while at the same time ensuring the electrical stability of the islands. This chapter intends to analyze the small-signal stability of the two islands of Flores and Sao Miguel and the IEEE 30-node distribution system.

In Section 4.2, four scenarios concerning the dynamic stability of Flores are studied: 1) assuming the decoupling of real-power and voltage dynamics and treating fluctuations of wind as a bounded real-power disturbance to the system; 2) assuming the decoupling of real-power and voltage dynamics and modeling the dynamics of the wind plant as a synchronous generator; 3) assuming the coupling of real-power and voltage dynamics and treating fluctuations of wind as a bounded real-power disturbance, and; 4) assuming the coupling of real-power and voltage dynamics and including the dynamic model of the wind plant.

Our technical findings illustrate that small-signal instability can occur when the governor control (GC) and excitation control of the DGs are tuned without accounting for interactions between the electromechanical and electromagnetic dynamics.

In Section 4.3, the small-signal stability of Sao Miguel is investigated assuming the decoupling of real-power and voltage dynamics. The results illustrate that slow modes of oscillation exist in the system. This is attributed to the weak inter-connection between the thermal plants (diesel/geothermal) and hydro plants.

In section 4.4, small-signal stability of the IEEE 30-node system is investigated. The results show that CTs can oscillate against each other and can destabilize the distribution system.

In Section 4.6, the Block Gerschgorin Theorem and Liapunov function-based stability criteria are used to formally state sufficient conditions for stability of such distri-

bution systems with decentralized control. We show that if the coupling between real and reactive power flows is neglected, two methods result in the same conditions.

4.2 The Small-Signal Stability of Flores

The main focus of this section is the problem of small-signal stability on Flores on a typical winter day with a sufficient availability of wind and hydro power. As shown in Figure 4.1, wind and hydro are the two main sources of energy during the winter on Flores, and more than 50% of the electricity is produced by these resources. Due to the intermittent nature of these resources, however, the distribution system is more vulnerable to frequency and/or voltage instability.

In order to assess the frequency and voltage dynamics in response to small disturbances, it is essential to model the distributed generators first.

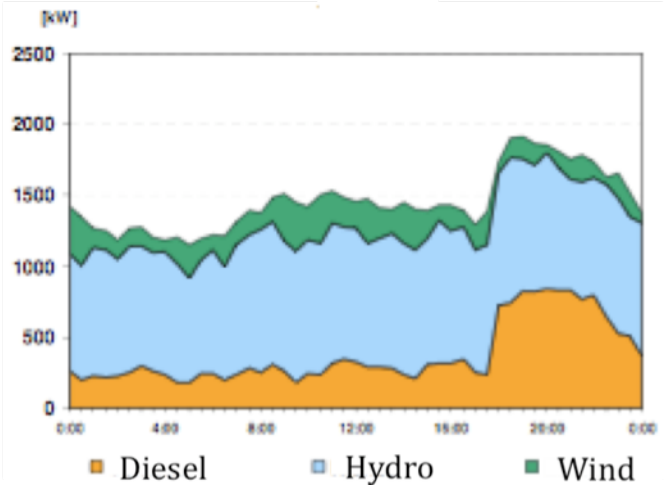

Figure 4.1: Illustration of the availability of wind and hydro power on a typical winter day (8).

4.2.1 Distributed Generator Models Used

The dynamics of the generators are represented with state space models. In general, a generator includes an electromechanical and an electromagnetic part. For conventional plants such as a hydro generator, the electromechanical part consists of a prime mover, rotating mass, and a governor control (GC) system. Equation 4.1 illustrates the state

space model of the electromechanical part of a hydro plant.

$$\frac{d}{dt}\begin{bmatrix}\omega_G\\ q\\ v\\ a\end{bmatrix} = \begin{bmatrix}\frac{-D_h}{2H_h} & \frac{K_q}{2H_h} & 0 & \frac{-K_w}{2H_h}\\ \frac{1}{T_f} & \frac{-1}{T_d} & 0 & \frac{1}{T_w}\\ 0 & 0 & \frac{-1}{T_e} & \frac{r'}{T_e}\\ \frac{-1}{T_s} & 0 & \frac{1}{T_s} & \frac{-(r_h+r')}{T_s}\end{bmatrix}\begin{bmatrix}\omega_G\\ q\\ v\\ a\end{bmatrix} + \begin{bmatrix}\frac{-1}{2H_h}\\ 0\\ 0\\ 0\end{bmatrix} P_G + \begin{bmatrix}0\\ 0\\ 0\\ \frac{1}{T_s}\end{bmatrix}\omega_G^{ref} \tag{4.1}$$

Here, q is the penstock flow, v is the governor droop, and a is the gate position. Moreover, T_a, T_f, and T_d are the time constants of the hydro plant. T_s is the time constant of the servomotor, and r_h and r' are the permanent and transient speed droop, respectively (31).

The electromagnetic part of the hydro plant is coupled to the electromechanical sub-system by the magnetic field of the machine air gap (44). For a hydro generator, the electromagnetic part consists of a synchronous machine and an excitation control. Equation 4.2 represents the state space model of the electromagnetic sub-system.

$$\frac{d}{dt}\begin{bmatrix}V_R\\ e_{fd}\\ e'_q\\ V_F\end{bmatrix} = \begin{bmatrix}\frac{-1}{T_a} & \frac{-K_aK_f}{T_aT_f} & \frac{-K_a}{T_a} & \frac{K_a}{T_a}\\ \frac{1}{T_e} & \frac{-(K_e+S_e)}{T_e} & 0 & 0\\ 0 & \frac{1}{T_d} & -\frac{1}{T_d} & 0\\ 0 & \frac{k_f}{T_f^2} & 0 & \frac{-1}{T_f}\end{bmatrix}\begin{bmatrix}V_R\\ e_{fd}\\ e'_q\\ V_F\end{bmatrix} + \begin{bmatrix}0\\ 0\\ \frac{-(x_d-x'_d)}{T_d}\\ 0\end{bmatrix} i_d + \begin{bmatrix}\frac{K_a}{T_a}\\ 0\\ 0\\ 0\end{bmatrix} V_G^{ref} \tag{4.2}$$

In this model, V_R is the regulator voltage, e_{fd} is the field excitation, e'_q is the machine voltage behind the direct transient impedance, and V_F is the feed-back voltage (the voltage of the compensator) (73). In addition, i_d is the reactive current out of the generator and V_G^{ref} is the reference value for the generator terminal voltage (73). Likewise, the dynamics of the electromechanical and electromagnetic parts of a diesel plant are presented in Chapter 3.

A wind plant is a synchronous machine connected to the grid through a power electronic interface. The electromechanical part of the plant consists of a rotating mass and a wind turbine with a pitch control system. Equations (4.3) and (4.4) illustrate the dynamics of the rotating mass and the wind turbine, respectively. As shown in Equation (4.5) the electromagnetic part includes a synchronous machine without excitation

control.

$$\frac{d\omega_G}{dt} = \frac{1}{2H_w}P_m - \frac{D_w}{2H_w}\omega_G - \frac{1}{2H_w}P_G \tag{4.3}$$

where

$$P_m = -K_m\omega_G \tag{4.4}$$

and

$$\frac{de'_q}{dt} = \frac{-1}{T_d}e'_q + \frac{-(x_d - x'_d)}{T_d}i_d \tag{4.5}$$

Here, P_m is the mechanical power, D_W is the damping coefficient, and K_m is the proportional gain of the pitch control system (35). The data for the state space models shown in Equations (4.1) to (4.5) are available in Appendix B.

4.2.2 Decoupled Real-Power Frequency Dynamic Model: Treating Wind as a Disturbance

Considering a decoupling of real-power and voltage dynamics, and neglecting the dynamics of the wind plant, result in a simple dynamic model for the island:

$$\frac{d}{dt}\begin{bmatrix} X'_1 \\ X'_2 \end{bmatrix} = \begin{bmatrix} A'_{11} & A'_{12} \\ A'_{21} & A'_{22} \end{bmatrix}\begin{bmatrix} X'_1 \\ X'_2 \end{bmatrix} + \begin{bmatrix} \gamma'_1 \\ \gamma'_2 \end{bmatrix} \tag{4.6}$$

where X'_i, A'_{ii}, A'_{ij} and γ'_i are defined as

$$X'_i = \begin{bmatrix} x_{LC}^{P(i)} \\ P_G^{(i)} \end{bmatrix} \tag{4.7}$$

$$A'_{ii} = \begin{bmatrix} A_{LC}^{P(i)} & C^{P(i)} \\ Kp_G^{(ii)}S_{\omega_G} & 0 \end{bmatrix} \tag{4.8}$$

$$A'_{ij} = \begin{bmatrix} 0 & 0 \\ Kp_G^{(ij)}S_{\omega_G} & 0 \end{bmatrix} \tag{4.9}$$

$$\gamma'_i = \begin{bmatrix} 0 \\ Dp_L^{(i)}\frac{dP_L}{dt} \end{bmatrix} \tag{4.10}$$

Matrices Kp_G and Dp_L are described as (73)

$$Kp_G = J_{GG} - J_{GL}J_{LL}^{-1}J_{LG} \tag{4.11}$$

$$Dp_L = -J_{GL}J_{LL}^{-1} \tag{4.12}$$

where

$$J_{GG} = \frac{\partial P_G}{\partial \delta_G}\ J_{GL} = \frac{\partial P_G}{\partial \delta_L}\ J_{LG} = \frac{\partial P_L}{\partial \delta_G}\ J_{LL} = \frac{\partial P_L}{\partial \delta_L}$$

The numerical data of the dynamic models are available in Appendix B. Note that the governor control of each plant is designed so that the system matrix of the stand alone plant (A'_{ii}) is stable in response to small perturbations.

An eigenvalue analysis of the system in this scenario shows that all the eigenvalues lie in the left hand side of the complex plane. Figure 4.2 illustrates the oscillations in frequency of the diesel and hydro plants after a small disturbance on the island. The disturbance is a 0.01 pu decrease in wind power.

As shown in Figure 4.2, the frequency of the hydro generator oscillates around its operating point, but it settles gradually. The oscillations result in smaller fluctuations in the frequency of the diesel plant. After the disturbance, the diesel generator increases its output power to balance the real-power mismatch. On the other hand, the hydro plant cannot ramp up rapidly, but it oscillates around the equilibrium point due to its non-minimal phase margin property. Figure 4.3 illustrates the deviations in the output power of the plants. The results illustrate that the system is oscillatory stable.

In order to measure strength of the electrical interaction between the plants, the coupling matrix (Kp) is calculated. Figure 4.4 demonstrates the 3-D plot of the coupling matrix. The depth and horizontal axes of the Figure represent the x and y axis of the coupling matrix, respectively. The z axis illustrates the strength of the coupling (Kp_{ij}). As shown in Figure 4.4, the diesel and hydro plants are strongly coupled. This explains why oscillations in the hydro plant makes the diesel generator oscillatory as well.

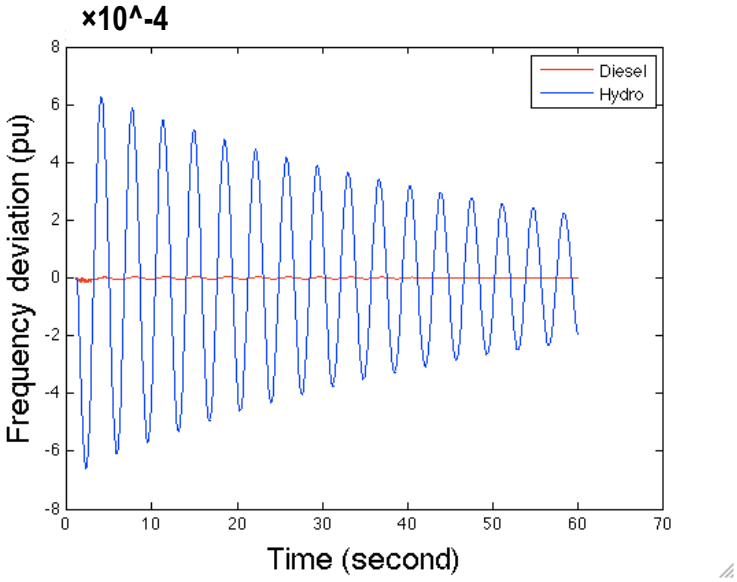

Figure 4.2: Frequency deviation in the diesel and hydro plants after a small perturbation (0.01 pu).

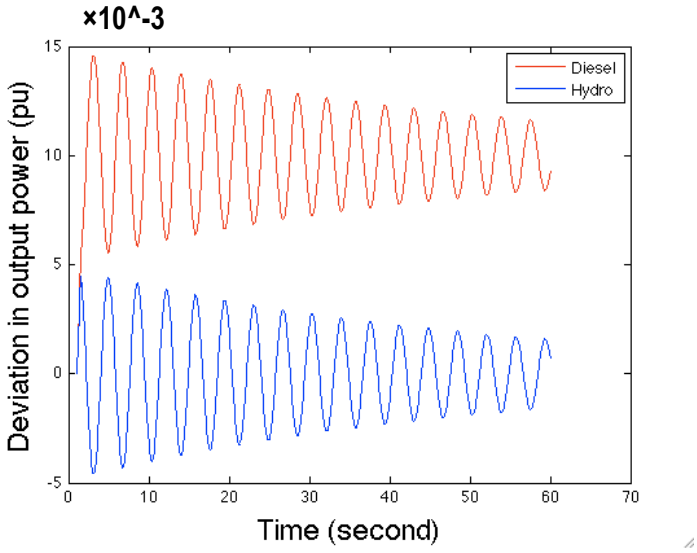

Figure 4.3: Deviations in output power of the DGs after the perturbation in wind power.

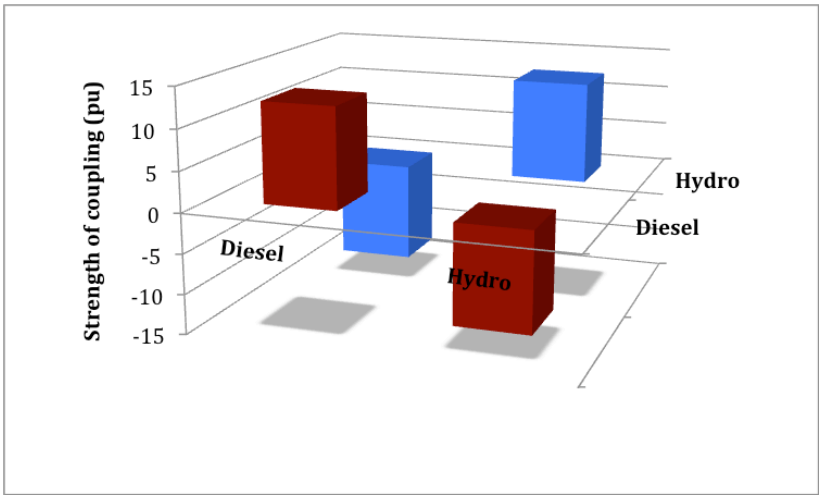

Figure 4.4: 3-D plot of the coupling matrix for the decoupled real-power voltage dynamic model.

4.2.3 The Decoupled Real-Power Frequency Model

In this subsection, the small-signal stability of the island is studied by modeling the dynamics of the synchronous wind plant shown in Equations (4.3) and 4.4). The results illustrate that when the wind plant is poorly tuned or has no pitch control system, the overall fluctuations of frequency are exaggerated (shown in Figure 4.5). In general, implementing a pitch control system increases the damping of the wind plant and lessens frequency oscillations. Figures 4.6 and 4.7 demonstrate the deviations of output power and the frequency of the DGs when the wind plant has a proportional pitch control system (gain = 2 pu). The results illustrate that the system has stable oscillatory response.

As shown in Figure 4.6, after a small disturbance (a 0.01 pu increase in load), the frequency of the wind plant deviates, but it returns to the equilibrium point gradually. The hydro plant shows a different dynamic behavior. Due to its non-minimal phase margin characteristics, it has fast oscillations around the equilibrium point, and damps very sluggishly. On the other hand, the diesel plant has robust dynamic behavior because of its fast integral control system. The diesel plant is compensating real-time oscillations in real-power.

In general, using the diesel generator for frequency regulation and to compensate for fast fluctuations of real-power can cause wear-and-tear in the governor control of

the plant. It can also increase the operating and maintenance costs of the plant and increase emissions. In (72) it is shown that if gas turbines are operated to compensate for fast fluctuations of intermittent energy resources such as wind, their CO_2 emissions may increase up to 20% and their NO_x pollutions rise by 50-70% compared to full power steady-state operation levels. Similarly, it is expected that in a fast ramping of the diesel plant, its CO_2 and NO_x emissions increase significantly.

In order to investigate the effect of the electrical interaction between the plants on system stability, a coupling matrix is calculated. Figure 4.8 illustrates the 3-D plot of the coupling matrix, and shows that the electrical interaction between the wind and diesel plants is weak, but that the diesel and hydro plants are strongly coupled.

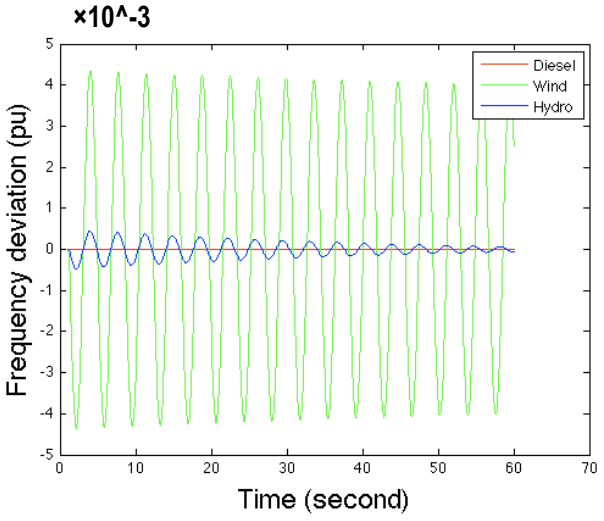

Figure 4.5: Frequency deviation of DGs when the wind plant has no pitch control system.

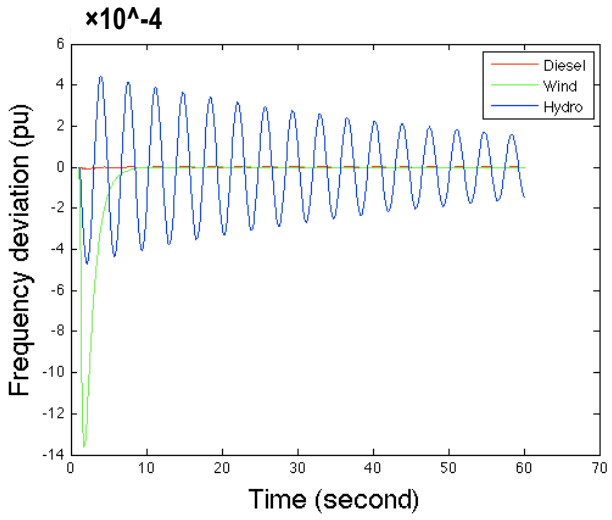

Figure 4.6: Frequency deviation of DGs when the wind plant is equipped with a proportional pitch control system.

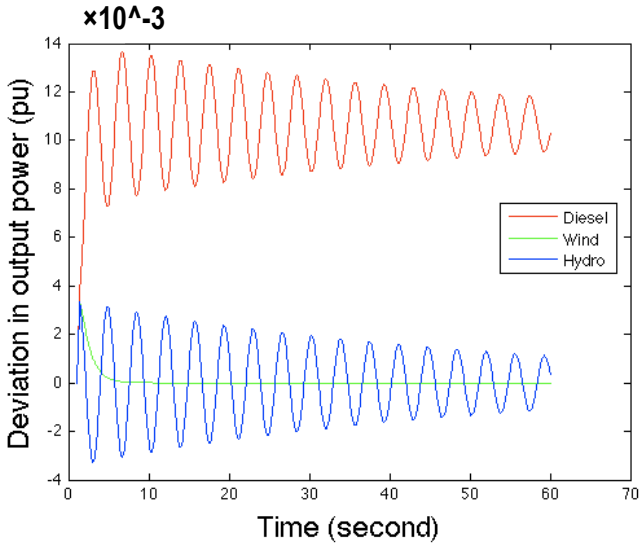

Figure 4.7: Deviations in output power of DGs when the wind plant is equipped with a proportional pitch control system.

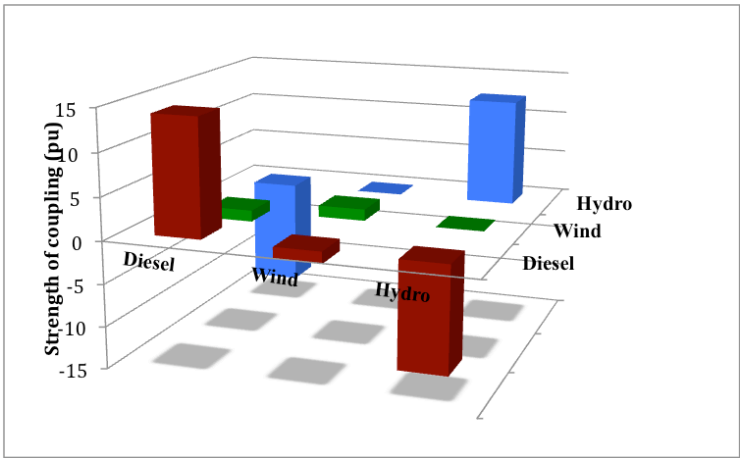

Figure 4.8: 3-D plot of the coupling matrix for the decoupled real-power voltage dynamic model.

4.2.4 The Coupled Real-Power Voltage Dynamic Model: Treating Wind as a Disturbance

Neglecting the coupling between real-power and voltage dynamics may lead to an optimistic assessment of system stability. This section examines the small-signal stability of Flores considering a coupling of real-power and voltage dynamics. The wind plant is treated as a negative load and its dynamics are neglected. Note that the governor of the plants is designed based on the decoupled model.

The result of stability analysis demonstrates that with a small disturbance (a 0.01 pu increase in load), the frequency of the hydro plant deviates from the equilibrium point (50 Hz). These oscillations are exacerbated due to the strong interaction between the electromechanical and electromagnetic parts of the plant. This leads to a frequency instability of the hydro plant. As shown in Figures 4.9 and 4.10, the instabilities of the hydro plant make the diesel generator unstable. Therefore, the full system is unstable in response to small perturbations.

In order to determine the main cause of the instability, a participation factor-based analysis, fully elaborated in (6), is carried out. The results show that the coupling variables (P_G and i_d^G) play the main role in the instability. Comparing the coupling matrix of the system with the decoupled scenario illustrates that the coupling between the plants is stronger in the coupled model.

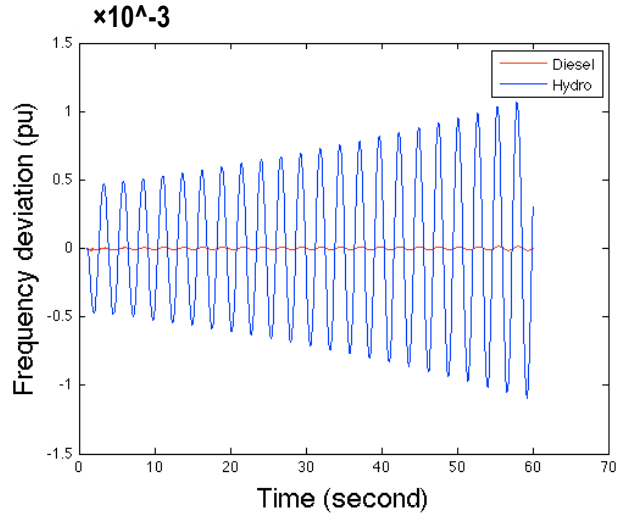

Figure 4.9: Frequency deviation of DGs after a small disturbance in the system.

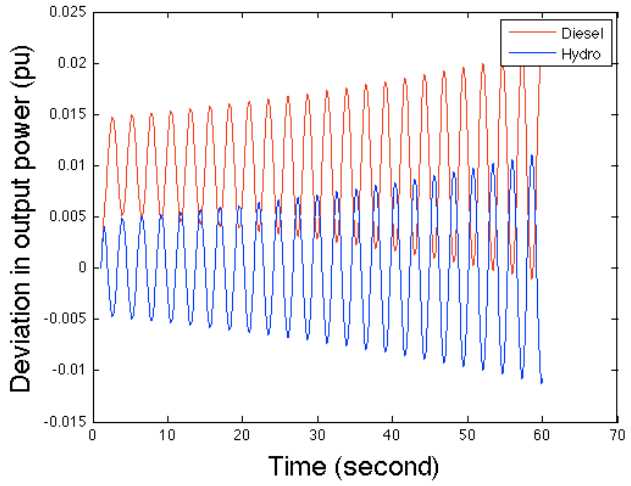

Figure 4.10: Deviations in the output power of DGs after the disturbance.

4.2.5 The Coupled Real-Power Voltage Dynamic Model with Wind Power Dynamics Included

In this subsection, the coupled real-power voltage dynamic model on Flores containing the dynamics of all the plants is investigated. Here, the wind plant is modeled as a synchronous generator with a proportional pitch control system. The governor of the diesel and hydro power plants are designed based on the decoupled model.

The result of eigenvalue analysis illustrates that the stand-alone hydro plant has two eigenvalues in the right hand side of the complex plane. These eigenvalues appear in the eigenvalues of the full system and lead to unstable response for the entire island. Similar dynamic behavior is reported in (55).

The interaction between the electromagnetic and electromechanical parts of the hydro plant exaggerates the oscillations and makes the plant unstable. This instability penetrates across the island and leads to system-wide instability. Figures 4.11 and 4.12 demonstrate variations in the frequency and output power of DGs after a disturbance occurs on the island. The instabilities found in these scenarios can be avoided by carefully designing the governor control of the plants based on the coupled real-power voltage dynamic model.

Comparing the coupling matrix of the island with the earlier scenarios illustrates that the coupling between the plants (Kp_{ij}) and the self-coupling Kp_{ii} are larger if the interaction between real-power and voltage dynamics is considered. In summary, our findings demonstrate that if the governor control and excitation control of the plants are tuned without considering the coupling between real-power and voltage dynamics, small-signal instability may occur in the system.

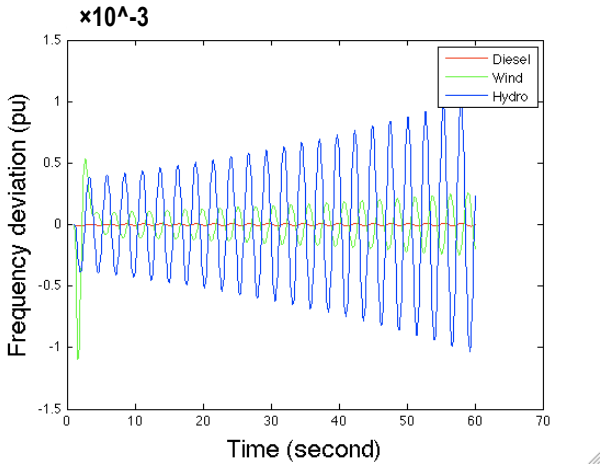

Figure 4.11: Dynamic response of the diesel, hydro, and wind generators after the disturbance.

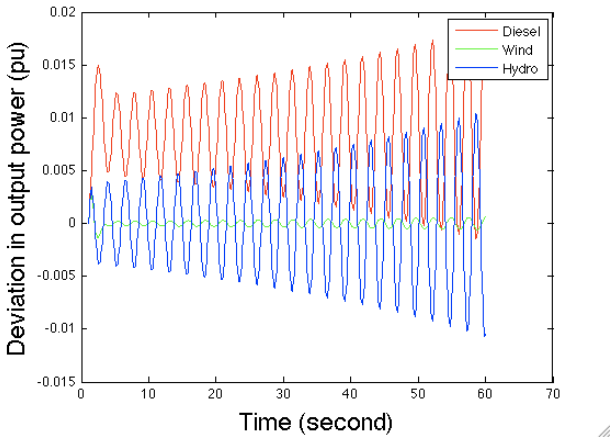

Figure 4.12: Deviations in the output power of DGs after the disturbance.

4.3 Small-Signal Stability on Sao Miguel

Sao Miguel is the largest island in the Azores Archipelago with an average demand of around 65 MW. Three large diesel generators, two medium-size geothermal plants, and 10 small hydro plants supply the demand. The hydro plants are run-of-river hydroelectric generators and provide electricity based on the availability of the stream. These plants do not have advanced governor control and cannot participate in frequency regulation. The geothermal plants produce electricity based on the availability of steam. Both the hydro and geothermal plants supply base-load power. Figure 4.13 illustrates the role of each technology in providing the daily electricity of the island during the spring. As shown in Figure 4.13, around 40% of the electricity is provided by renewable sources of energy, and the rest is provided by conventional power plants (the diesel generators).

The diesel plants are the only fully controllable generators on the island. They balance the supply and demand and regulate frequency. In order to model the dynamics of the island, it is essential to pose the dynamics of each power plant first by modeling its prime mover, governor control, excitation control, and synchronous machine. The diesel plants have similar state space models to the ones shown in Equations (4.1) and (4.2). On the other hand, the geothermal and hydro plants have no governor control and excitation control systems. Therefore, their electromechanical part contains of a rotating mass, and their electromagnetic sub-system includes a synchronous machine.

Equations (4.13) and (4.14) represent the general structure of the state space model of these plants.

$$\frac{d\omega_G}{dt} = \frac{1}{M}P_m - \frac{D}{M}\omega_G - \frac{1}{M}P_G \tag{4.13}$$

$$\frac{de'_q}{dt} = \frac{-1}{T_d}e'_q + \frac{-(x_d - x'_d)}{T_d}i_d \tag{4.14}$$

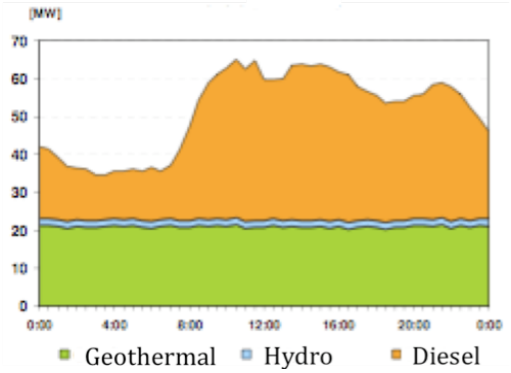

Figure 4.13: Illustration of the availability of geothermal and hydro power on a typical spring day [3].

On Sao Miguel, loads are modeled as non-controllable elements and their dynamics are modeled as a disturbance to the system. The dynamics of the generators are coupled via the distribution network. The strength of the coupling between generators is calculated by the sensitivity of active and reactive power with respect to rotor angle and voltage. This is similar to calculating the Jacobin matrix of the island. Since the dynamics of loads are neglected, a reduced Jacobin matrix needs to be calculated in order to obtain the coupling between generators. Figure 4.14 illustrates the 3-D plot of the reduced coupling matrix.

As shown in Figure 4.12, there is strong coupling between the diesel generators and the geothermal plants. However, the hydro plants have very weak coupling to either of these plants. Some hydro plants are strongly coupled to each other, but some are weakly connected to the rest of the system. In general, the coupling between generators is identified by the location of the generators and the electrical distance between the plants. Those plants electrically close to each other are strongly coupled, and those

electrically far from each other are weakly coupled.

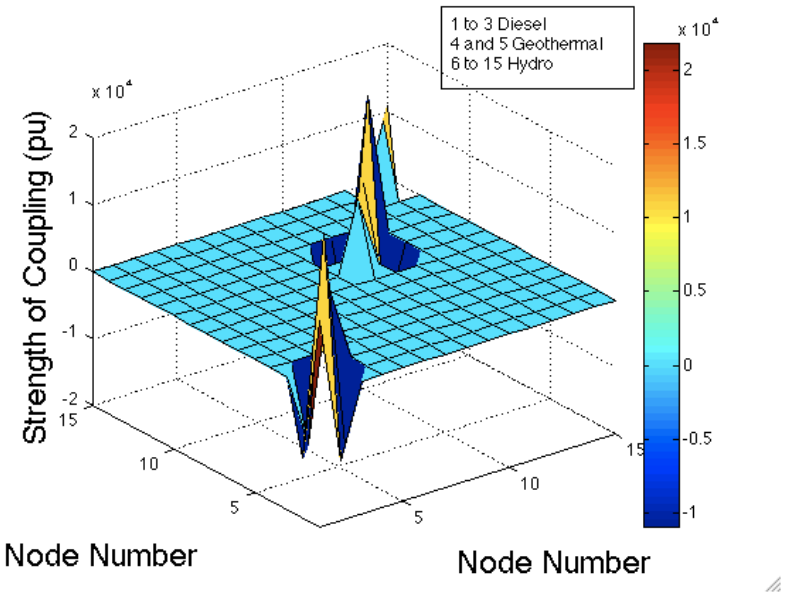

Figure 4.14: 3-D plot of the coupling matrix of Sao Miguel for the decoupled real-power voltage dynamic model.

Figure 4.13 illustrates the schematic of the one-line diagram of Sao Miguel. This model presents the reduced dynamic model of the island. The equivalent admittance between the plants is equal to the coupling between them ($Yeq_{ij} = Kp_{ij}$). In Figure 4.15, the equivalent admittance is colored in red for strong coupling ($Kp_{ij} > 100$), green for moderate coupling ($7 < Kp_{ij} < 100$), and white for weak coupling ($Kp_{ij} < 7$). In addition, the equivalent admittance is neglected for very weak coupling ($Kp_{ij} < 0.05$).

Simulating the small-signal stability of the island demonstrates that due to weak coupling between the hydro plants and the thermal plants (diesel/geothermal), a slow mode of oscillation exists between the two clusters. Figures 4.16 and 4.17 demonstrate the variations in frequency and output power of the plants after a small perturbation on the island.

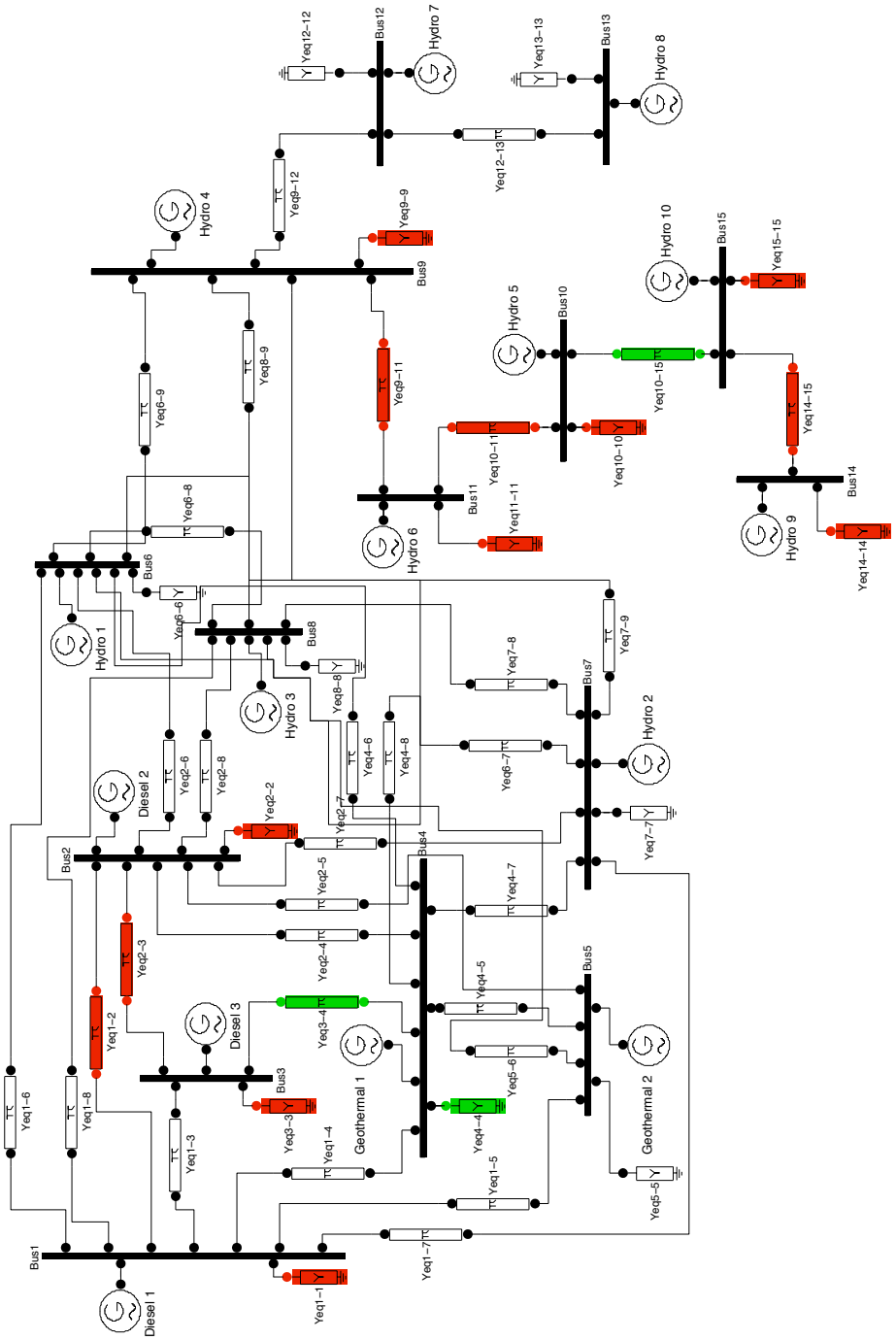

Figure 4.15: One-line diagram of Sao Miguel.

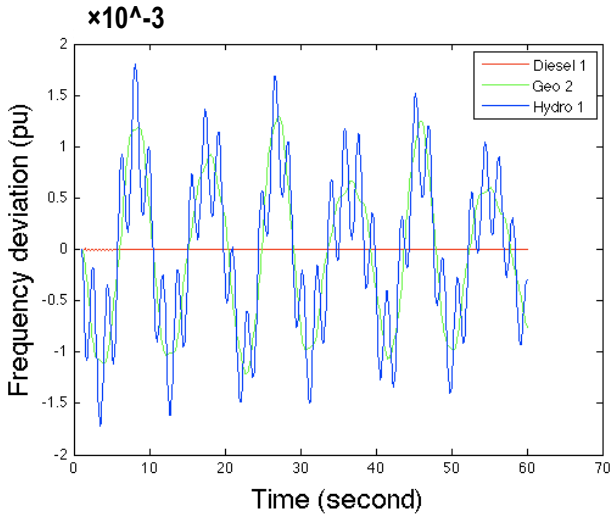

Figure 4.16: Deviations in the output power of the generators after the disturbance.

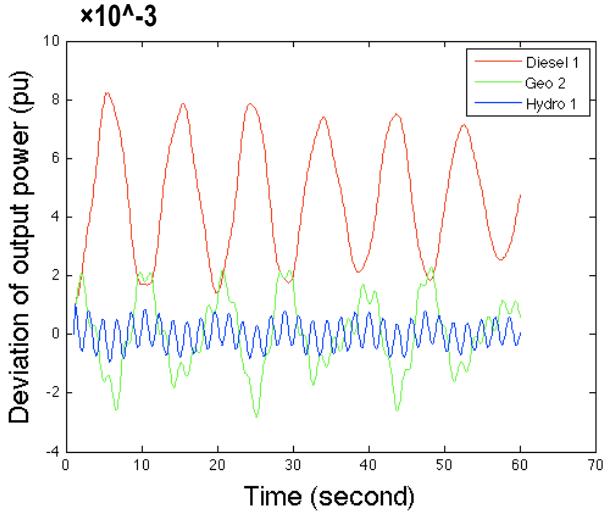

Figure 4.17: Deviations in the output power of the generators.

4.4 Small-Signal Stability on IEEE 30-node System

In this subsection we investigate small-signal stability of the 30-node distribution system. Our results show that the optimal placement-distribution system with CTs located at nodes 13^{th} and 14^{th} is indeed small-signal unstable. Note that, instabilities of the CTs remain local and cannot penetrate in the bulk power grid due to its immense in-

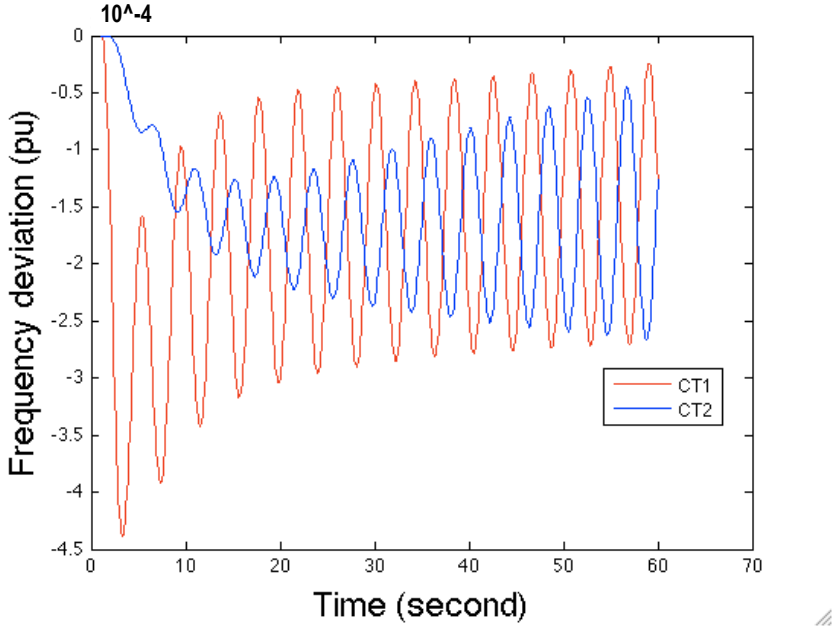

Figure 4.18: Unstable system response with conventional governor control.

ertia. Unstable DGs can detriment frequency stability of the local distribution system. Figure 4.18 shows after a small disturbance (equal to 0.01 pu increase in load) occurs at node 15^{th}, CTs placed at optimal locations become unstable .

In order to determine fundamental causes of potential frequency instabilities, participation factor-based analysis, fully elaborated in (6), is carried out. A participation factor p_{ij} is described as the sensitivity of eigenvalues with respect to state variables (6).

$$p_{ij} = c_{ij} v_{ij}$$

where v_{ij} is the i^{th} entry in the j^{th} right eigenvector, and c_{ij} is the equivalent for the left eigenvector (6).

The results illustrate that the coupling variable between DGs (P_G) and the state variables of the GC system (W_F and W_{Fd}) are mostly participating in frequency instability. Figure 4.19 illustrates the results of participation factor-based analysis for the first CT.

By increasing electrical distance (impedance) between DGs, the system becomes stable. For instance, by moving away the first DG (located on node 13^{th}) from the

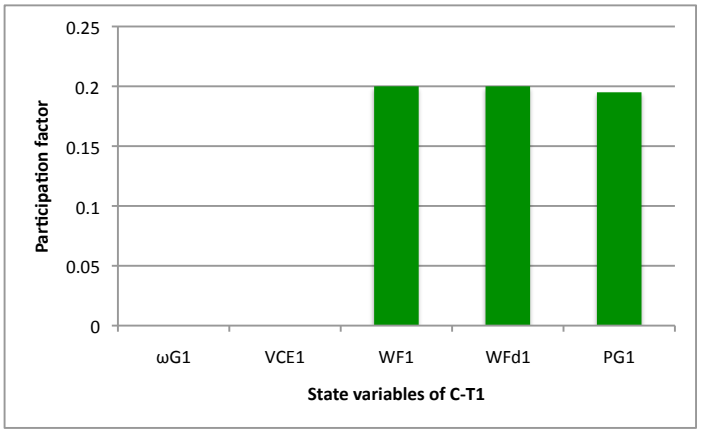

Figure 4.19: Illustration of the critical state variables of the first CT, located at node 13^{th}.

second one and locating the first DG on node 11^{th} or 10^{th}, the stability of the system is restored.

Investigating the diagonal and off-diagonal matrices of the optimal placement-distribution system furthermore illustrates that the full system matrix is not block diagonal dominant. That is, the following inequality does not hold.

$$\left(\left\|A_{ii}^{-1}\right\|_{\infty}\right)^{-1} \geq \sum_{\substack{j=1 \\ j \neq i}}^{N} \left\|A_{ij}\right\|_{\infty} \quad i \in N \tag{4.15}$$

This implies that DGs are strongly coupled to each other. As shown in this subsection, two stable DGs can fight against each other, if their GCs are not designed to cancel out interactions between DGs.

The physical explanation of this phenomenon is that, due to short electrical distance between DGs, their GCs are strongly coupled. This causes interruption in operation of local GCs, which have no communication with each other or the rest of the system. Therefore, given any perturbation in the system, both generators work against each other while attempting to compensate for their local power mismatch; however, they do not observe that the nearby generator is also reacting to the perturbation. Thus, they suddenly observe another perturbation in the system because of the nearby DG, so they again try to react to the new perturbation and this cascading phenomenon makes both unstable.

4.5 Stability Conditions with Decentralized Control

In this section, we identify fundamental causes of potential system instabilities in terms of the strength of electrical interactions between DGs and the damping magnitude (real part of the eigenvalue) contributed by the state variables of DG units.

To this end, we use the decoupled dynamic model of distribution energy systems. Note that the results can be generalized for the coupled real-power/voltage dynamic model.

Recalling from earlier, the coupling variable of a DG is its real-power output. Moreover, since the coupling variables of all power plants are subject to the real-power flow network constraints, it is possible to express their dynamics in terms of local state variables of the DGs, in particular their frequencies ($\omega_G^{(i)}$) (73).

$$\frac{dP_G^{(i)}}{dt} = \sum_{j=1}^{N} Kp_{ij}\omega_G^{(i)} \tag{4.16}$$

By combining the dynamics of the distribution system with the dynamics of DG units, a full system model representing dynamics of the distribution system with N DGs is obtained as (30):

$$\frac{d}{dt}\left[\begin{array}{c} X_{LC}^{(1)} \\ \vdots \\ \hline P_G^{(1)} \\ \vdots \end{array}\right] = \left[\begin{array}{ccc|cc} A_{LC}^{(1)} & & 0 & C_M^{(1)} & 0 \\ & \ddots & & 0 & \ddots \\ 0 & & & & \\ \hline Kp_{11}S_{\omega_G^{(1)}} & \cdots & & 0 & \cdots \\ \vdots & \ddots & & \vdots & \ddots \end{array}\right] \left[\begin{array}{c} X_{LC}^{(1)} \\ \vdots \\ \hline P_G^{(1)} \\ \vdots \end{array}\right] + \left[\begin{array}{c} 0 \\ \vdots \\ \hline Dp^{(1)} \\ \vdots \end{array}\right] \frac{dP_L}{dt} \tag{4.17}$$

Where the matrix $S_{\omega_G^{(i)}}$ includes 0's and 1 and relates $\omega_G^{(i)} = S_{\omega_G^{(i)}} X_{LC}^{(i)}$. In addition, $\frac{dP_L}{dt}$ represents changes in loads modeled as disturbances to the grid.

The desired system model is obtained by changing the order of state variables of (4.17) and by ordering the state variables as internal state variables of DGs and their coupling variable (real-power out of the corresponding DG).

$$\frac{d}{dt}\begin{bmatrix} X_1 \\ X_2 \\ \vdots \end{bmatrix} = \begin{bmatrix} A_{11} & A_{12} & \cdots \\ A_{21} & A_{22} & \cdots \\ \vdots & \vdots & \ddots \end{bmatrix} \begin{bmatrix} X_1 \\ X_2 \\ \vdots \end{bmatrix} + \begin{bmatrix} \gamma_1 \\ \gamma_2 \\ \vdots \end{bmatrix} \frac{dP_L}{dt} \tag{4.18}$$

where

$$X_i = \begin{bmatrix} X_{LC}^{(i)} \\ P_G^{(i)} \end{bmatrix} \; A_{ii} = \begin{bmatrix} A_{LC}^{(i)} & C_M^{(i)} \\ Kp_{ii} S_{\omega_G^{(i)}} & 0 \end{bmatrix} \; A_{ij} = \begin{bmatrix} 0 & 0 \\ Kp_{ij} S_{\omega_G^{(j)}} & 0 \end{bmatrix} \; \gamma_i = \begin{bmatrix} 0 \\ Dp^{(i)} \end{bmatrix}$$

4.5.1 Gerschgorin Stability Conditions

As noted earlier, the particular interest is to identify sufficient conditions for stability of new distribution systems with DGs. These conditions are obtained by applying Block Gerschgorin Theorem to the new system model presented in (4.18) (5) .

$$\left(\parallel (A_{ii} - sI_i)^{-1} \parallel_\infty \right)^{-1} \sum_{\substack{j=1 \\ j \neq i}}^{n} \parallel A_{ij} \parallel_\infty \quad \forall i \in [1, n] \tag{4.19}$$

where $\parallel . \parallel_\infty$ represents the infinity norm of the indicated matrix. The left hand side of (4.19) represents the set of complex-valued numbers that all the eigenvalues of the full system matrix lie in the union of these sets (5). Also, the right hand side of (4.19) is calculated by adding the infinity norms of the off-diagonal matrices.

In particular, off diagonal matrices denote the coupling matrix between the i^{th} DG and other DGs in the system. By inspection, it can be simply obtained that the infinity norm of off-diagonal matrices equals to the norm of their coupling variables. That is,

$$\parallel A_{ij} \parallel_\infty = \mid Kp_{ij} \mid$$

where $\mid Kp_{ij} \mid$ denotes the electrical interaction between the i^{th} and the j^{th} DGs. Hence, (4.19) can be re-written as follows:

$$\min \left\{ \mid s - \lambda_{i,1} \mid \cdots \mid s - \lambda_{i,m} \mid \right\} \leq \sum_{j \neq i} \mid Kp_{ij} \mid \quad \forall i \in [1, n] \tag{4.20}$$

Here m denotes the number of state variables for the i^{th} sub-system (A_{ii}). Condition (9) states that eigenvalues of the full system lie within the circles centered at eigenvalues of a sub-system and with the radius equals to the sum of the electrical interaction between the sub-system and other sub-systems. Figure 4.20 demonstrates the schematic of the circles in which eigenvalues ($\lambda_i = r_i + jv_i$) of the full system lie. The blue crosses represent eigenvalues of sub-systems (A_{ii}).

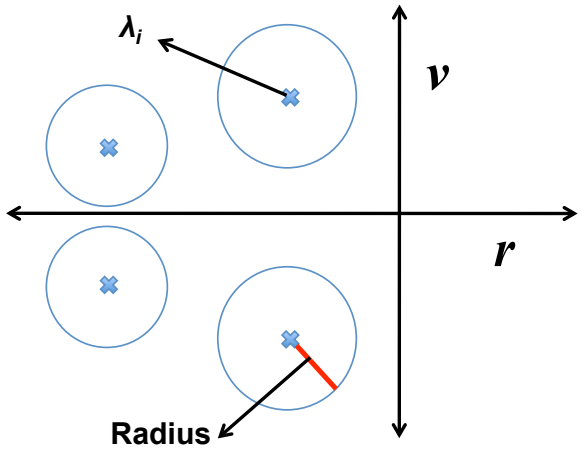

Figure 4.20: Illustration of Gerschgorin Circles in which eigenvalues of the full system matrix lie.

One can simply conclude from Figure 4.20 that stability of the full system is satisfied when all the circles lie in the left hand side of the complex plane. That is;

1) Eigenvalues of all sub-systems lie in the left hand side of the complex plane (sub-systems are asymptotically stable).

2) The real part of the slowest eigenvalue of a sub-system (the closest eigenvalue to the imaginary axis) is greater than the sum of the electrical interaction between the sub-system and other sub-systems.

The physical interpretation of this theorem is that when local DGs are asymptotically stable and the strength of electrical interaction between DGs is less than the damping magnitude (real part) of the slowest eigenmode of DGs, then the whole system always remains asymptotically stable. This also implies that the main cause of frequency instability in distribution systems with DGs is: 1) low damping magnitude of the eigenmode of local DGs; and, 2) strong coupling between DGs. In general, low damping results from poor tuning of the governor control of DGs. Furthermore, strong coupling between DGs is caused by strong electrical interaction between them. Coupling between DGs is measured by the norm of the off-diagonal terms of the coupling matrix ($\sum_{j \neq i} \mid Kp_{ij} \mid$). If this value is greater than the damping magnitude of the i^{th} DG, then the DG is strongly coupled to other generators.

4.5.2 Liapunov Stability Conditions

An alternative approach to determine sufficient conditions for stability is using Liapunov stability method, fully elaborated in (7). In this section the Block Gerschgorin Theorem-based and Liapunov-based stability criteria are compared and it is shown that these conditions are identical when the Liapunov equation is defined using the knowledge of system eigenvalues.

To this end, Equation (4.18) is re-arranged by using nonsingular transformation ($X_i = T_i\hat{X}_i$). Furthermore, the energy function and the Liapunov equation of the system are introduced as follows (7):

$$\frac{d\hat{X}_i}{dt} = \Lambda_{ii}\hat{X}_i + \sum_{j\neq i} \Delta_{ij}\hat{X}_j \quad \forall i \in [1, n] \tag{4.21}$$

$$v_i(\hat{X}_i) = \left(\hat{X}_i^T \hat{H}_i \hat{X}_i\right)^{\frac{1}{2}} \tag{4.22}$$

$$\Lambda_{ii}^T \hat{H}_i + \hat{H}_i \Lambda_{ii} = -\hat{G}_i \tag{4.23}$$

where

$$\Lambda_{ii} = T_i^{-1} A_{ii} T_i \qquad \Delta_{ij} = T_i^{-1} A_{ij} T_j$$

The solution to (4.23) is obtained as

$$\hat{H}_i = I_i \quad \text{and} \quad \hat{G}_i = -2diag\left\{\sigma_1, \sigma_2, \cdots, \sigma_m\right\}$$

where σ_i is the absolute real part of the i^{th} eigenvalue of A_{ii}. The sufficient condition for stability of the system shown in (10) is satisfied when W-matrix is Metzler. The W-matrix for the choice of Liapunov function takes on the form (7):

$$w_{ij} = \begin{cases} -\sigma_M^i & i = j \\ \lambda_M^{\frac{1}{2}}(\Delta_{ij}^T \Delta_{ij}) & i \neq j \end{cases} \tag{4.24}$$

Here σ_M^i denotes the maximum real part of the eigenvalues of A_{ii} and λ_M represents the maximum eigenvalue of the indicated matrix. Since the second term of the W-

matrix is the Euclidean norm of Δ_{ij}, it is possible to re-written Equation (4.24) as follows:

$$w_{ij} = \begin{cases} -\sigma_M^i & i = j \\ \parallel \Delta_{ij} \parallel_2 & i \neq j \end{cases} \tag{4.25}$$

As transformation matrices (T_i and T_j) are unity matrices, the Euclidean norm of Δ_{ij} is the same as the Euclidean norm of A_{ij}. By inspection, it is trivial to show that $\parallel A_{ij} \parallel_2 = \mid KP_{ij} \mid$. Therefore, the W-matrix takes on the form

$$w_{ij} = \begin{cases} -\sigma_M^i & i = j \\ \mid KP_{ij} \mid & i \neq j \end{cases} \tag{4.26}$$

The new W-matrix is Metzler if the following conditions hold.

$$\begin{cases} -\sigma_M^i < 0 \\ \mid \sigma_M^i \mid > \sum\limits_{j \neq i} \mid KP_{ij} \mid \end{cases} \tag{4.27}$$

4.6 Conclusions

This chapter shows that a large penetration of DG units sending power back to the grid could cause frequency and/or voltage stability problems. In addition, our findings illustrate that neglecting the strong interactions between the electromagnetic and electromechanical parts of the plants can lead to an overly optimistic assessment of system stability. These interactions exaggerate overall frequency oscillations. Therefore, if the governor control and excitation control of DGs are designed based on the decoupled model, the distribution systems may become very sensitive to even small perturbations.

Our results in this chapter also claim that both Block Gerschgorin Theorem-based and Liapunov-based criteria are equivalent when the Liapunov equation is defined using the knowledge of system eigenvalues. Furthermore, both conditions have an intuitive physical interpretation of mathematical conditions which state that as long as local control reacts sufficiently fast to counteract the dynamics of interactions with the rest of the system, the decentralized control will be sufficient to stabilize the system frequency and voltage.

5

Potential Robustness Enhancement Approaches

5.1 Introduction

There are at least three possible major approaches to assuring system stability in distributed energy systems: A) placing DGs beyond critical electrical distance, B) installing fast energy storage devices; and, C) designing enhanced decentralized control systems. In this chapter these three methods are summarized.

5.2 Placing DGs Beyond Critical Electrical Distance

Given the findings in preceding chapters, it should be possible to establish guidelines for assuring the robustness of distributed networks based on the critical electrical distance between DG units. In other words, DG units need to be located such that the electrical distance between them is more than the critical value.

For instance, in the 30-node distribution system, when CTs are located at optimal static locations, the GCs of DGs are fighting against each other and causing frequency stability problems. However, by increasing the electrical distance between them, frequency stability is restored. Thus, when CTs are located at nodes 11^{th} and 14^{th} or 10^{th} and 14^{th}, they are stable. Figure 5.1 illustrates a schematic of the distribution system in which two CTs are located at nodes 10^{th} and 14^{th}. Figure 5.2 also shows how frequency of two CTs becomes stable when they are electrically far from each other.

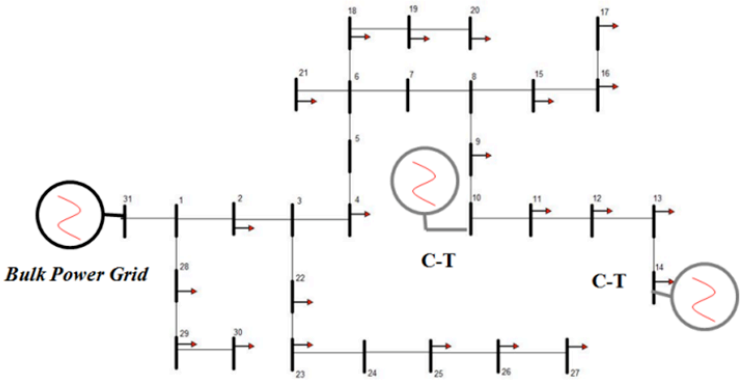

Figure 5.1: A schematic of the distribution system in which two C-Ts are located at nodes 10^{th} and 14^{th}.

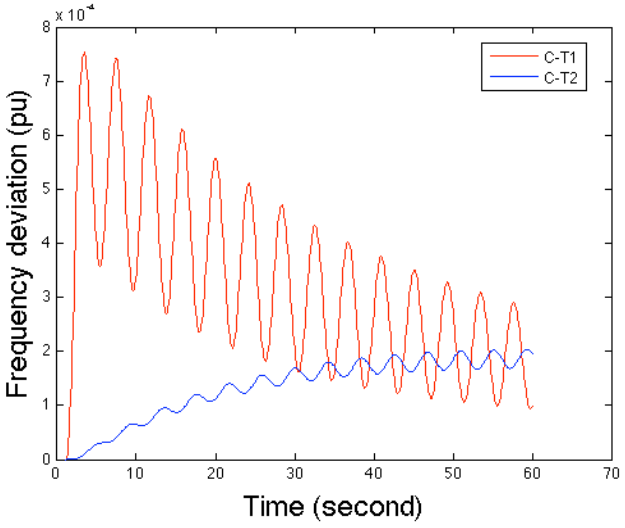

Figure 5.2: Illustration of the dynamic response of C-Ts, located at buses 10^{th} and 14^{th}, when small perturbation occurs in the system.

5.3 Installing Fast Energy Storage System

Another possible way to enhance robustness of distribution systems with DGs is to increase overall damping by installing fast energy storage systems such as flywheels. When flywheels are responding to frequency oscillations, they would contribute enhanced damping to the system. The state space model of a flywheel system is described as:

$$2H_F \frac{d\omega_G}{dt} = P_M - P_G \tag{5.1}$$

where

$$P_M = f_F(\omega_G - \omega_G^{ref})$$

In this model, f_F is the gain of the proportional control, H_F is the inertia of the flywheel, and ω_G^{ref} is the reference value for the flywheel frequency. As shown in Equation (5.1), the mechanical power of the flywheel (P_M) linearly varies by changes in frequency. When frequency drops in the system the flywheel would increase its mechanical power and if frequency increases the flywheel would decrease its mechanical power.

By combining Equations (4.18) and (5.1), the general structure of a stand alone DG with a flywheel is denoted in the following way.

$$\frac{dx_{LC}^{(i)}}{dt} = A_{LC}^{(i)} x_{LC}^{(i)} + \frac{f_F}{2H_F} E'_{\omega_G^{(i)}} x_{LC}^{(i)} + C_{LC}^{(i)} P_G^{(i)} + B_{LC}^{(i)} \rho^{(i)} \tag{5.2}$$

with $E'_{\omega_G^{(i)}}$ relating $\omega_G^{(i)} = E'_{\omega_G^{(i)}} x_{LC}^{(i)}$.

Implementing flywheels can also change the structure of the diagonal matrices of the full system as follows:

$$A_{ii} = \begin{bmatrix} A_{LC}^{(i)} + \frac{f_F}{2H_F} E'_{\omega_G^{(i)}} + B_{LC}^{(i)} \rho^{(i)} & C_{LC}^{(i)} \\ K p_{ii} E_{\omega_G^{(i)}} & 0 \end{bmatrix} \tag{5.3}$$

Therefore, by designing an appropriate gain for flywheels, the block diagonal dominant structure of the full system matrix can be maintained.

In order to improve robustness of the IEEE 30-node distribution system and the distribution system on Flores, we investigate scenarios when a 2.5-MW/4-MWh and a 300-kW/0.6-MWh flywheel is implemented on the IEEE 30-node system and on Flores

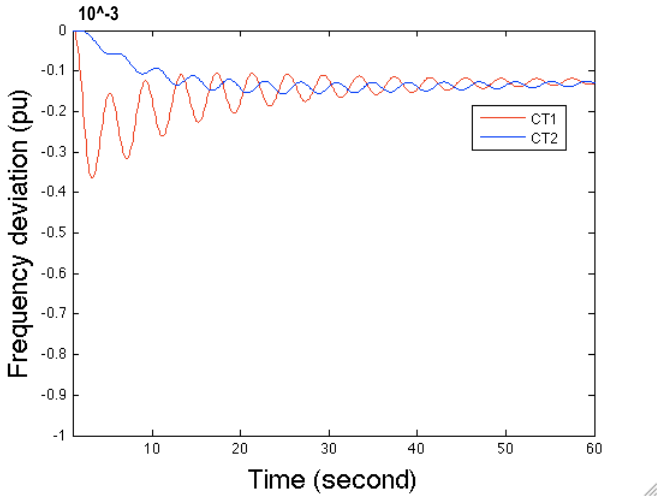

Figure 5.3: Illustration of the dynamic response of the CTs after installing the flywheel.

respectively. The results indicate that the new systems would be robust with respect to small perturbations. Figures 5.3 and 5.4 illustrate the frequency response of the systems after installing the flywheels.

5.4 Designing Enhanced Decentralized Control Systems

Given the findings in the previous chapters, dynamic stability problems can occur in distribution energy systems when the primary control of DGs are designed without considering strong interactions between DGs. Thus, another approach to enhancing robustness of distribution systems is designing enhanced decentralized control with Gerschgorin logic.

The new control is designed based on shifting all the Gerschgorian Circles of the full system to the left hand side of the complex plain. Equation (5.4) illustrates the mathematical formulation of the proposed control system.

$$\frac{dX_i}{dt} = A_{ii}X_i + B_iU_i + \sum_{j \neq i} A_{ij}X_j \quad \forall i \in [1, n] \tag{5.4}$$

where

$$U_i = -K_iX_i$$

and

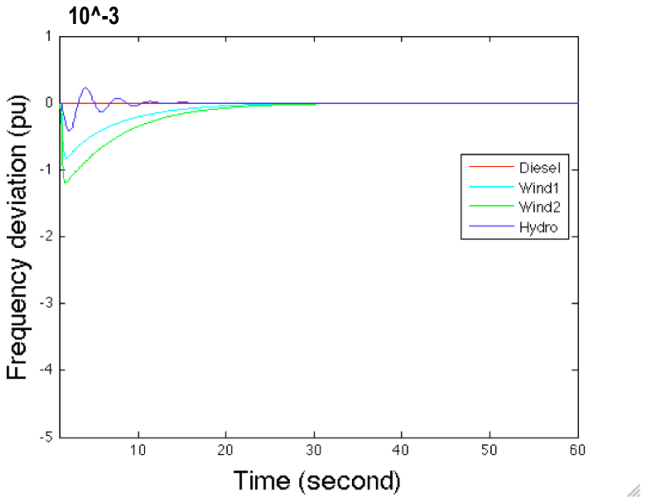

Figure 5.4: Illustration of the dynamic response of the generators on Flores after implementing the flywheel.

$$\mid \sigma_M(A_{ii} - B_i K_i) \mid > \sum_{j \neq i} \parallel A_{ij} \parallel_\infty = \sum_{j \neq i} \mid Kp_{ij} \mid$$

For the CTs the control signal inputs to the fuel control state ($V_{CE}^{(i)}$) and therefore the control matrix takes on the form

$$B_{CT} = \begin{bmatrix} 0 & 1 & 0 & 0 & 0 \end{bmatrix}^T$$

Likewise, for the plants on Flores the control matrices are obtained as:

$$B_{Diesel} = \begin{bmatrix} 0 & 0 & 1 & 0 \end{bmatrix}^T \quad B_{Wind} = \begin{bmatrix} 1 & 0 \end{bmatrix}^T \quad B_{Hydro} = \begin{bmatrix} 0 & 0 & 0 & 1 & 0 \end{bmatrix}^T$$

The decentralized control signal is superposed to the primary control of DGs and it responds to both disturbances of the internal state variables $X_{LC}^{(i)}$ as well as the coupling variable. Figure 5.5 demonstrates a block diagram of the existing closed-loop dynamics improved by the enhanced decentralized control loop.

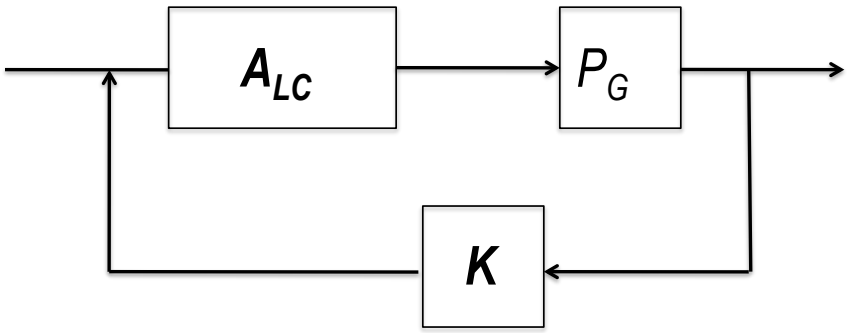

Figure 5.5: The block diagram of the new control system.

Applying the new control strategy to the CTs of the IEEE 30-node system demonstrates that the system will restore its dynamic stability and can satisfy stability criteria. In this condition, interactions between CTs are cancelled out by the advanced control system. This implies that when each DG is stabilized, the entire system remains stable. Figure 5.6 illustrates the frequency response of the CTs with the enhanced control.

In the next step, the dynamic stability of Flores is investigated, while the enhanced control is implemented on the DG units. The results indicate that the island has a well-damped stable response even with high penetration of renewable energy resources. Figure 5.7 demonstrates the frequency response of the island.

As shown in Figures 5.6 and 5.7, the proposed control can enhance both stability and dynamic performance of distribution systems.

5.5 Conclusions

Our technical findings illustrate that where larger DGs are located can play a significant role in determining the stability of distribution energy systems. We find that short electrical distance between DGs, and poor tuning of their primary control system are the major causes of dynamic stability problems in distribution systems.

Based on our technical findings we recommend consideration of three major methods to enhancing robustness: 1) placing DGs beyond critical electrical distance, 2) installing fast flywheel energy storage systems, and 3) designing enhanced decentralized control for DGs.

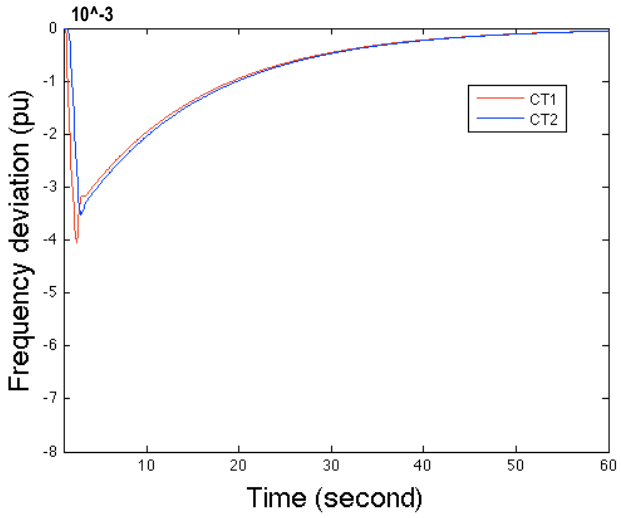

Figure 5.6: Frequency response of the IEEE 30-node system after implementing the enhanced control.

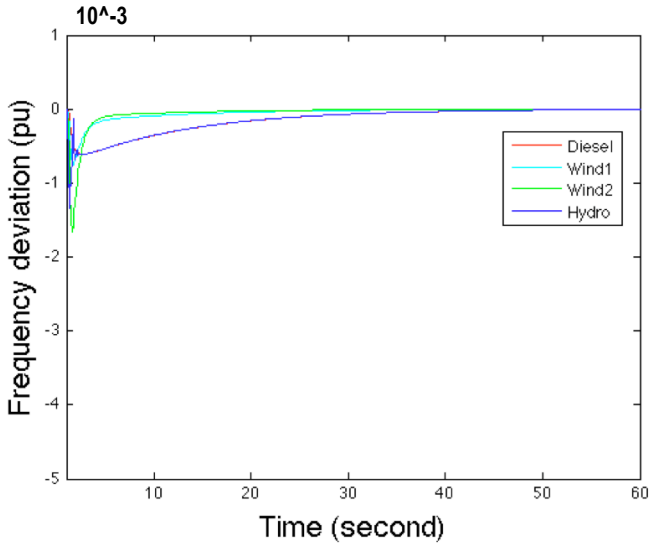

Figure 5.7: Frequency response of the power plants on Flores after implementing the enhanced control.

The proposed decentralized control with Gerschgorin logic enables flexibility of DGs and brings many advantages such as:

1. Simple control systems;
2. No need for system-wide sensing and communications; and,
3. Relatively inexpensive control equipment.

However, decentralized control has inherent drawbacks such as it requires that all decentralized controllers operate as expected. Failure of some decentralized controllers to respond could lead to system-wide instabilities. The deployment of AMI (Automatic Meter Infrastructure) could resolve the problem by metering the actual actions of controllers. AMI enables two-way communication between DGs and SCADA (control center and data acquisition).

6

Adaptive Model-based Policy Design for Integration of Distributed Generation

6.1 Introduction

Despite all the benefits of distributed generation, DG is still relatively rare and growth rates are modest. Today distributed generation makes up less than 0.3% of the generation capacity of the United States (69). While a number of State and Federal initiatives promote the greater use of DG (26, 27), obstacles such as difficulties in interconnection (2), and regulations that establish exclusive service territories, inhibit the growth of micro-grids that could take advantage of DG economies of scale.

Here we assume that all of those obstacles can be overcome and explore the technical and regulatory issues that will arise if there is wide-spread deployment of DG in distribution systems. Deployment of many DGs could lead to unacceptable voltage and frequency fluctuations in distribution systems. Indeed, interconnected PV panels have already created over-voltage in some distribution systems (37). Today's policies do not adequately address these challenges: in particular the complexity of the effects of a large penetration of DGs is such that no one-size-fits-all policy is appropriate.

In this chapter we propose models that distribution system operators and regulators can use to assess the effects of DGs, and to design effective communication/control systems capable of ensuring acceptable quality of service (QoS). We illustrate possible

use of such models for defining technical and policy objectives concerning quality of service in distribution systems with high DG penetration.

In Section 6.2, we review today's standards and operating models for interconnecting DG units to distribution power systems. The main focus is on a plug-and-play operating model and IEEE standard 1547. This IEEE family of standards outlines technical requirements and test specifications for interconnecting distributed resources to electric power systems with aggregate capacity of 10 MVA or less (68).

In Section 6.3, we explore potential quality of service problems that may arise in distribution systems with high penetration of DGs. We show that when the penetration of DGs increases, it is essential for at least larger DGs to participate in frequency regulation and stabilization. Otherwise, frequency deviations may exceed acceptable limits. We highlight the risk that DGs connected in electrically close areas may oscillate against each other and may cause small-signal stability problems.

In Section 6.4 we propose a possible model-based adaptive policy design for efficient integration of DG units at acceptable QoS. The model uses sets of software to support: 1) quantifiable policy design, and; 2) approval of possible options for specific candidate deployments.

Today the deployment of most smaller DG units is done using a plug-and-play approach without quantifiable recommendations for the necessary control/communications. An obvious policy question is how, and at what point, should distribution system operators and regulators switch from the present regime to a more systematically planned approach and what equity and other issues are raised by such transition. These issues are briefly addressed in Section 6.5.

6.2 Operating Models and Interconnection Standards for Distributed Generation

In the past, electric power distribution systems were passive networks with generation only coming from the sub-station and transmission systems. Integration of DG in distribution systems changes the planning, operation, and control design of the existing systems.

To propose some necessary enhancements, we first review in this section today's operating models and interconnection standards for distributed generation. We highlight

some of the main drawbacks of available standards and illustrate why these interconnection standards cannot support a large penetration of DG units sending power back to the grid.

6.2.0.1 Plug-and-Play Approach in Today's Distribution systems

A plug-and-play approach is a common operating practice in systems with DGs. The approach allows to locating small DGs at any point in the distribution system without needs for changing the planning, operation and control design of the system. This gives DGs the same functionality and flexibility as that of residential loads (65). The main advantage of such plug-and-play operation is that adopting distributed generation is fast and easy for both customers and utilities (9).

When DGs operate according to plug-and-play rules, they do not communicate with the control center. Therefore, DGs are effectively unpredictable negative loads as seen by the supervisory control and data acquisition (SCADA). Lack of predictability poses new technical challenges to the operation and control of electric power systems. For instance, random behavior of plug-and-play DGs may cause imbalance in real-power. This imbalance, when significant, will lead to frequency deviations from the desired normal frequency of 60 Hz. In addition, DGs with power electronic interfaces contribute less inertia to the grid. Therefore, imbalance in real-power has larger effects on frequency deviations.

Generally fast ramping power plants such as gas turbines or hydro power plants regulate the frequency of the grid by balancing supply and demand. These plants are equipped with speed droop governor control to regulate frequency. Since the proportional speed droop control does not eliminate the real-power imbalance, the frequency of the grid drifts away from the desired normal frequency. The secondary level control responds to frequency deviations every 15 to 30 minutes.

The maximum penetration of plug-and-play DGs could be defined based on the acceptable range of frequency deviation (Δf_{max}), the droop constant of fast power plants (R) and the accuracy of predicting demand. Equation (6.1) illustrates the dependence of the penetration of plug-and-play DGs on the equivalent droop constant of the power plants (R_{eq}), unpredicted load deviation (ΔP_{Load}), and the acceptable range

of frequency deviation.

$$P_{DG}^{max} = -\frac{\Delta f_{max}}{R_{eq}} - \Delta P_{Load} \tag{6.1}$$

where

$$\frac{1}{R_{eq}} = \frac{\sum_{j=1}^{N} \frac{S_i}{R_i}}{S_{eq}} \tag{6.2}$$

In this model, P_{DG}^{max} is the maximum penetration level of plug-and-play DG, N is the number of fast ramping power plants, S_i and R_i are the rated power and droop constant of the i^{th} power plant, and S_{eq} is the sum of the rated power of the power plants.

Random fluctuations in real-power due to plug-and-play DGs will not degrade the quality of frequency by more than Δf_{max} as long as $(P_{DG}^{max} + \Delta P_{Load})$ is larger than or equal to R_{eq}.

6.2.1 IEEE 1547 Series of Interconnection Standard

The IEEE 1547 series of interconnected standards has been developed by the IEEE Standards Coordinating Committee 21 for interconnecting distributed resources such as distributed generation and energy storage to the electric power systems.

In the first version, IEEE 1547.1 provides guidelines for test procedures and technical requirements for interconnecting distributed resources to low voltage distribution feeders. In the second version, IEEE 1547.2 provides application details to support the understanding of IEEE 1547 series of interconnected standards. IEEE 1547.3 provides recommended practices for monitoring and control of distributed resources connected to the electric power systems. In the fourth version, IEEE 1547.4 provides guidelines for operation and control of distributed resources connected to the island-type distribution system. In addition, IEEE 1547.6 provides recommended practices for interconnecting distributed resources to the secondary electric power distribution systems. The fifth version, IEEE 1547.5, has been withdrawn and the last two versions of IEEE 1547 series (IEEE 1547.7 and IEEE 1547.8) are still under development (68).

The IEEE 1547 standard only provides guidelines for interconnecting distributed generation smaller than 10 MVA that are connected to the distribution feeders or to the secondary distribution systems with operating voltage level 1 kV or less. Note that larger DGs are often placed in medium voltage distribution systems whose voltage level is higher than 1 kV.

The IEEE 1547 standard is technology neutral and does not provide a framework for planning, operating and safety of distribution systems with DGs larger than 10 MVA. The underlying assumption is that the reliable operation of DG units is independent of specific distribution system characteristics, level of DG penetration, DG technology, or their location in distribution systems. In what follows we show that these factors should be considered for reliable and efficient integration of distributed generation. Otherwise, technical problems such as small-signal instability could occur in distribution systems with DGs. In the next section, some of technical problems that may occur are discussed.

6.3 Possible Operating Problems and Potential Efficiency Improvement in Distribution Systems with Significant DG Penetration

6.3.1 Frequency Regulation for Distributed Generation

The IEEE 1547 standard does not require DG units to regulate frequency when they are connected to the electric power system. This may be acceptable in systems with a low penetration of DGs and it simplifies the control design of DG units. However, by increasing the penetration level of DG and by offsetting fast ramping centralized power plants with DGs, the ability of the electric power system to regulate frequency with in the pre-specified Δf_{max} decreases.

For instance, if 10% of fast ramping centralized generation is replaced by DG units, the equivalent droop constant of the system can increase up to 11%. Therefore, it follows from Equation (6.2) that the sensitivity of frequency with respect to changes in real-power increases by 11%. Here it is assumed that all centralized power plants have the same droop constant ($R_1 = R_2 = \cdots = R_N$). If power plants with lower droop constants are offset, the sensitivity of frequency increases, and vice versa.

Table 6.1: The IEEE 1547 Standard for disconnecting DGs in response to abnormal frequency (68).

DG size	Frequency range (Hz)
< 30 kW	< 59.3
> 30 kW	< 59.8

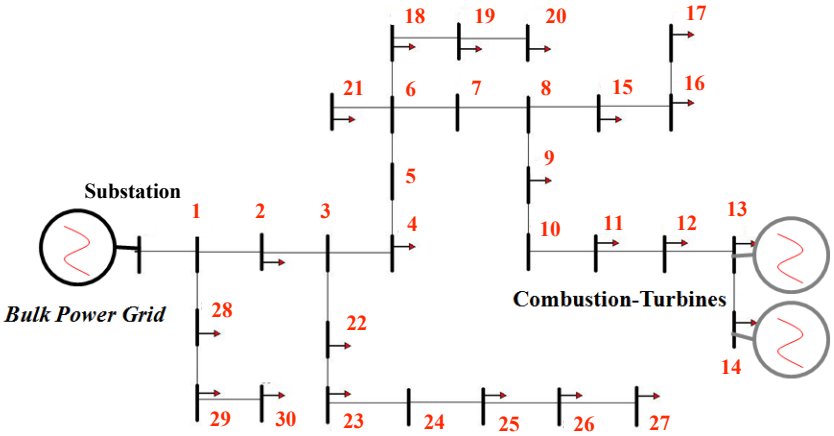

Figure 6.1: Schematics of IEEE 30-node system with two medium-size CTs (750 kW).

The IEEE 1547 standard requires DGs to discontinue energizing distribution systems when the frequency falls below the range given in Table 6.1 (68). Note that, when the frequency is lower than 60 Hz, disconnection of DG units will decrease overall generation and will likely lead to larger deviations in frequency. We propose that as the level of DG penetration increases at least larger DGs need to regulate frequency by means of automatic generation control.

6.3.2 Potential Small-Signal Stability Problems

A high penetration of DG units sending power back to the grid could create small-signal instabilities in distribution power systems. This chapter illustrates how larger DGs or a high number of smaller DGs connected in electrically close areas could create stability problems as reported in previous chapters.

We illustrate this problem on a representative distribution system with a high penetration of DGs. Two scenarios are studied. In the first scenario, two medium-size CTs (750 kW each) are connected to the IEEE 30-node distribution system (shown in Figure 6.1).

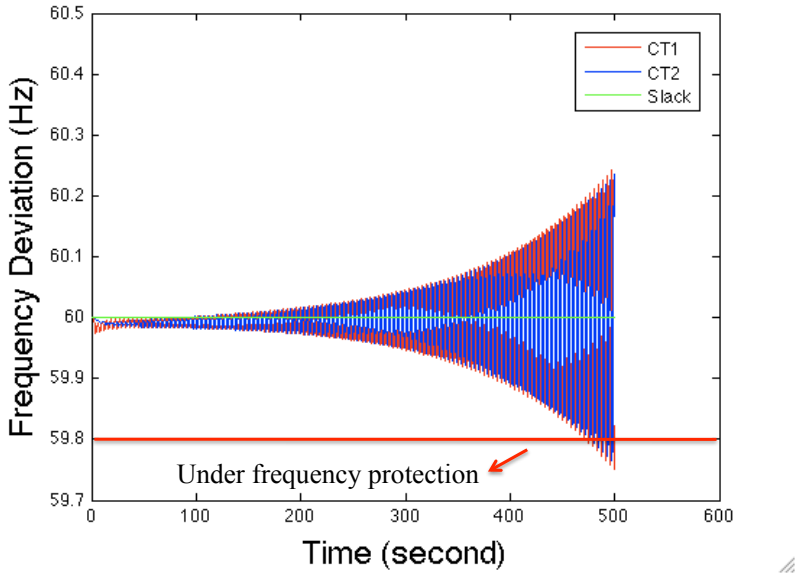

Figure 6.2: Strong mutual interactions between two medium-size CTs results in stability problems (DG penetration is 10%).

Both combustion turbines (CTs) have the same generation characteristics. They meet about 10% of the demand on the distribution system and the bulk power grid meets the rest of the demand. In previous chapters the dynamic model of CTs and that of the distribution system are introduced and the small-signal stability of the system is investigated. As described in Chapter 4, due to strong mutual interaction between CTs connected in electrically close areas, small-signal instability occurs in the system. Figure 6.2 illustrates frequency deviation of CTs after a small perturbation in the system. The perturbation is equal to 0.01 pu increase in load at node 15 (shown in Figure 6.3).

As shown in Figure 6.2, the two CTs oscillate against each other. This leads to the small-signal instability of CTs. After a few minutes, the oscillatory CTs will be disconnected from the grid by under frequency protection devices. In addition, these oscillations can cause disconnection of sensitive loads connected electrically close to CTs.

Note that due to the immense inertia of the bulk power grid compared with the inertia of DGs, instabilities remain local and are not seen at the substation level. For high penetration of DGs (e.g. $> 20\%$), these oscillations can cause blackout in the local

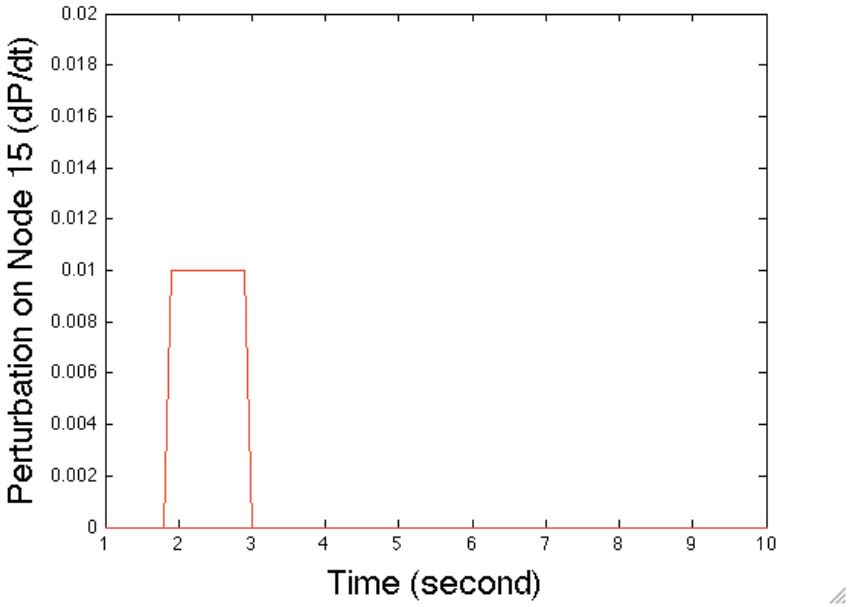

Figure 6.3: A perturbation at node 15 equal to 0.01 pu increase in load.

distribution system.

In the second scenario, fifteen small CTs ($\sim$ 100 kW each) with the same generation characteristics are connected to the IEEE 30-node distribution system. Small CTs provide 10% of the electric demand of the system. Figure 6.4 illustrates the schematics of the distribution system with small CTs.

As shown in Figure 6.4, CTs are arbitrarily placed in the system. Similar to the previous scenario, CTs connected in electrically close areas found to oscillate against each other. This results in a small-signal instability of CTs. Figure 6.5 illustrates the dynamic response of CTs located at nodes 8, 11 and 12 after the same perturbation at node 15.

In this condition, the CT on node 8 has larger deviations since it is closer to the perturbation. Under frequency protection will disconnect the CT connected to node 8 first. Other CTs will be disconnected when their frequency oscillation exceeds the acceptable Δf_{max} .

In the previous chapters we have shown that the main causes of instability are recognized as short electrical distance between DGs and poor tuning of the governor control of DGs. By increasing the electrical distance between DGs, system stability

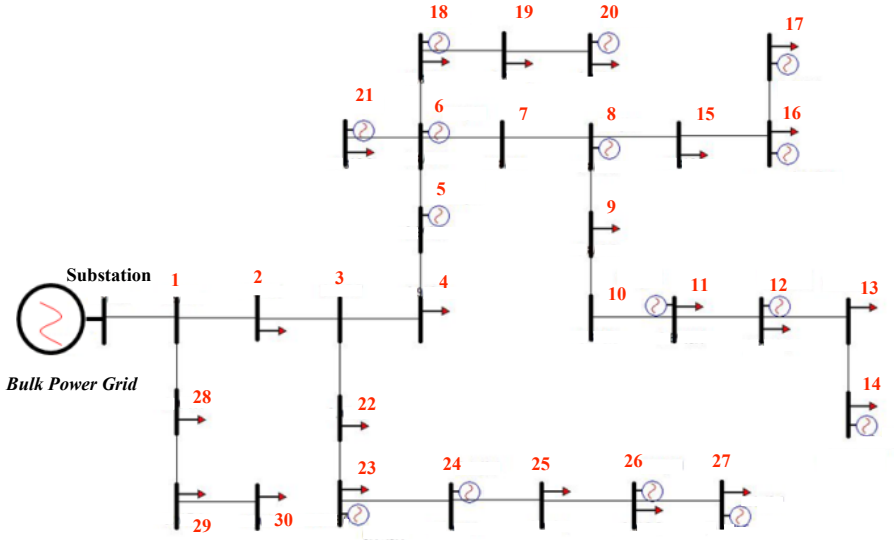

Figure 6.4: Schematics of IEEE 30-node distribution system with fifteen small CTs ($\sim$ 100 kW).

is restored. In addition, designing enhanced decentralized control, which cancels out interactions between DGs, can ensure system stability.

As described in this section, small-signal stability could become a major concern in distribution systems with a large penetration of DG units sending power back to the grid. This problem is not addressed by today's standards such as IEEE 1547. Based on IEEE 1547.4, system stability analysis is not required when connecting DGs in parallel with the grid. In addition, the Federal Energy Regulatory Commission (FERC) does not require stability analysis when connecting DGs whose aggregate capacity is 20 MW or less (28).

In what follows, we propose that there is no one-size-fits-all approach for reliable and efficient integration of distributed generation. For a low penetration of DGs, it is possible to apply today's standards or operating models such as IEEE 1547. However, as the level of DG penetration increases, it becomes necessary to design a model-based adaptive policy in order to avoid potential technical problems by providing technically innovative solutions for mitigating these problems.

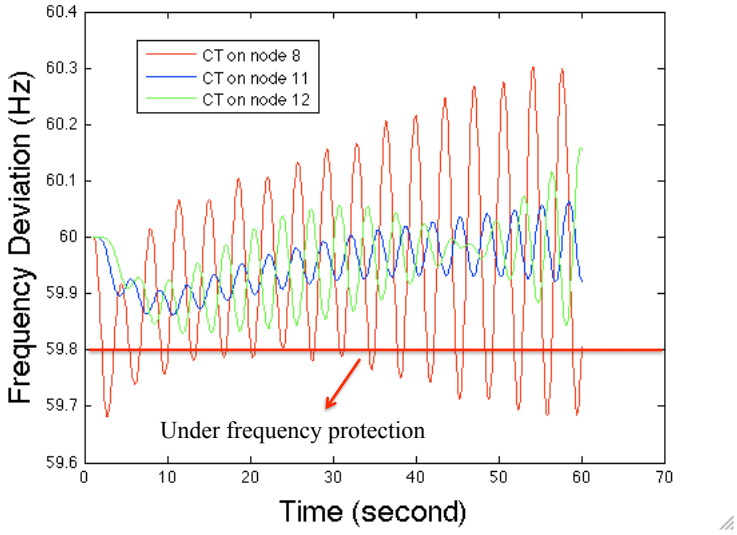

Figure 6.5: Strong interaction between small CTs results in stability problems (DG penetration is 10%).

6.3.3 Potential Low Voltage Problems in Distribution Systems with a High Penetration of DGs

The IEEE 1547 standard requires DGs to discontinue energizing distribution systems when the voltage level at the point of interconnection is in the range given in Table 6.2 (68). Voltage drop often occurs across long radial distribution lines. When DG is connected at the end of such distribution lines, an under voltage problem may occur. In this circumstance, under voltage protection will disconnect the DG from the grid if the voltage level at the DG is lower than the limit given in Table 6.2.

This problem is illustrated in the system shown in Figure 6.1. The system has long radial distribution lines. Voltage drop occurs at far-end nodes of the system such as nodes 13 and 14. Placing CTs at these nodes could create low voltage problem. As shown in Figure 6.6, when CTs are operating as constant sources of power (PQ Mode), their nodal voltage becomes lower than the acceptable limit shown in Table 6.2. Therefore, the under voltage protection will disconnect CTs even during normal conditions.

If the AVR (automatic voltage regulation) voltage set point of CTs are dispatched using coordinated AC Optimal Power Flow (AC OPF), the overall voltage level of the system is above the acceptable limit. Implementing AC OPF-based dispatch for

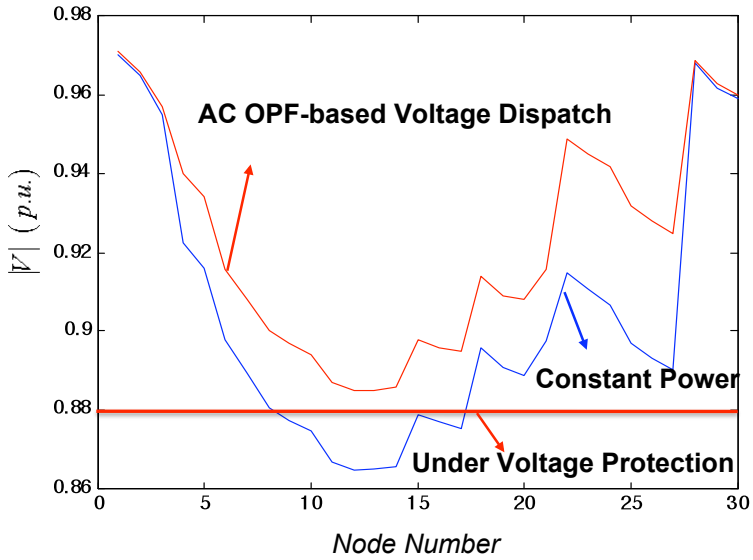

Figure 6.6: Eliminating under voltage problem by optimizing voltage settings of DGs

distribution systems with DG not only eliminate the risk for under voltage problem, but it also could improve the system-wide efficiency of distribution systems. This is discussed in Chapter 2 and is further elaborated in the next subsection.

Table 6.2: Rules for DG response to abnormal voltage (68).

Voltage level (% of base voltage)	Clearing time for disconnecting DG
V < 50	0.16 sec
50 < V < 88	2.0 sec
110 < V < 120	1.00 sec
V > 120	0.16 sec

6.3.4 The Role of Distributed Generation in Enhancing Efficiency

Today about 7% of the electricity transmitted in the United States is dissipated in transmission and distribution systems. According to the Energy Information Administrative (EIA) total transmission and distribution (T&D) losses in 2009 were around 270 Million MWh. This is 1.17 times greater than the annual net electricity generation of Pennsylvania (69). Figure 6.7 illustrates total T&D losses in the United States since 1949. It can be seen that the power delivery losses have gradually increased over the years.

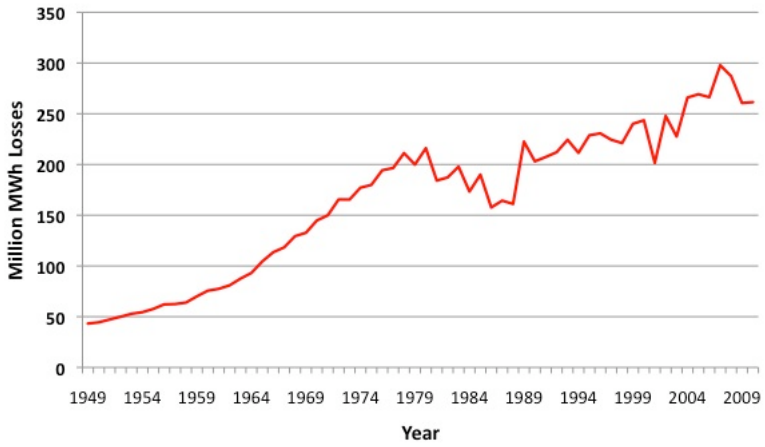

Figure 6.7: Total T&D losses in the United States since 1949 (69).

Distributed generation holds a major promise to enhance the efficiency of transmission and distribution systems by reducing power delivery losses. To this end, DGs should be strategically located and optimally utilized in distribution systems. This implies that for long-term planning the optimal placement of DGs should be determined and that DG operators should be given incentives to locate DGs at those locations. For short-term operation, coordinated AC OPF-based dispatch should be used to optimize voltage settings of DGs.

In order to determine how changing the location of DGs can affect system-wide efficiency, an exhaustive AC OPF analysis for 900 (30^2) possible combinations of locating CTs is carried out. Figure 6.8 illustrates the results of the exhaustive AC OPF analysis.

As shown in Figure 6.8, in some combinations such as nodes 13 and 14 over 45% of power delivery losses are reduced, while in some combinations such as nodes 1 and 2 almost no efficiency improvement is obtained. If CTs located at nodes 13 and 14 are operating as constant sources of power the overall loss reduction is about 42%. Note that CTs are only meeting 10% of the demand. Table 6.3 compares the performance of CTs at nodes 13 and 14 with and without voltage optimization. These results indicate that efficiency improvement highly depends on the locations of CTs.

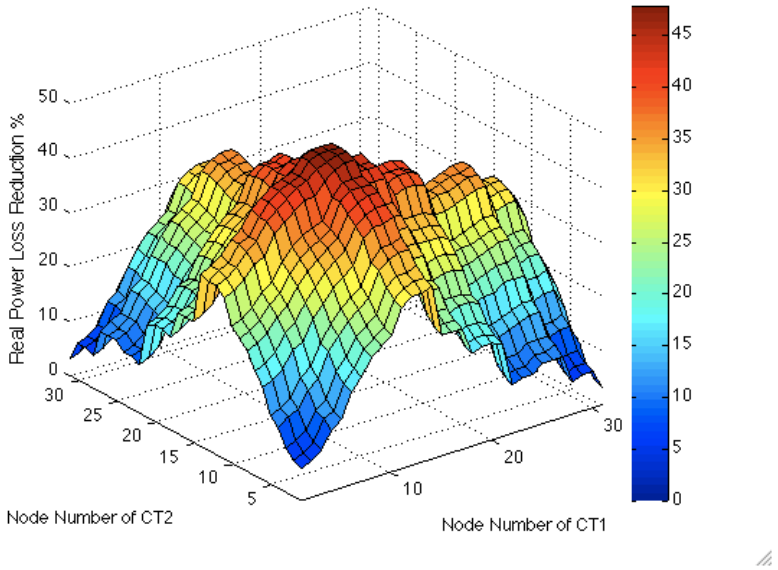

Figure 6.8: The dependence of loss reduction on the location of CTs.

Table 6.3: Loss reduction for the IEEE 30-node system with CTs at nodes 13th and 14th.

Without optimizing voltage	With optimizing voltage
0.65 MW	0.58 MW
42.3%	47.7%

Generally environmental and/or technical restrictions could limit feasible combinations of placing DGs. However, as our analytical results suggest finding the optimal feasible combinations of locating DGs and incentivizing DG operators to place DGs at those locations could significantly improve the overall efficiency of distribution energy systems.

In the next section, an example of model-based adaptive policy design is introduced in order to define quantifiable measures for the performance of DG units and to provide guidelines for reliable and efficient integration of DG units in distribution systems.

6.4 Model-Based Adaptive Policy Design For Reliable and Efficient DG Integration During Normal Condition

The main point of this chapter is that standards and policies for distributed generation should be proactive rather than reactive (67). Utilities, distribution system operators (DSOs), and regulatory commissions should assess possible undesired effects of distributed generation on legacy distribution power systems and adopt policies to support efficient and reliable integration of DGs.

Because of complexity of the effects of larger DGs or a large number of small DGs concentrated in electrically close areas, it is necessary to establish a set of models for assessing technical and economic effects of DGs requesting to be deployed and agreement needs to be reached on protocols used in these tools. Utilities could receive all the applications for interconnecting DGs once or twice a year and a neutral third party could conduct a systematic assessment using stability analysis and optimization tools such as ones discussed in previous chapters. The result of this assessment would be a set of recommended alternatives and necessities to deploy for efficient and robust integration of DGs.

DGs asking to be placed at optimal locations would be incentivized for enhancing efficiency. The incentive could be provided by Tax Credit or Feed in Tariff. On the other hand, DGs asking to be placed at the worst locations would be penalized for degrading efficiency. In the same fashion, DGs placed at problematic locations would be required to install protection equipment and/or advanced local control to ensure the system stability of the interconnected distribution system. If the advanced local control cannot ensure system stability or if DG operators are not willing to install the advanced local control, utilities need to implement centralized communication/control systems (IT) in order to ensure system stability. In this circumstance, problematic DGs would be approved only at IT cost. Figure 6.9 illustrates the schematics of the adaptive model-based policy flow chart.

The proposed model-based adaptive policy design would provide a detailed quantifiable measure to evaluate and optimize the short-term and long-term performance of DG units and distribution power systems. Note that available policies such as performance based- regulation only provide incentives for improving the long-term performance of distribution systems with DGs (e.g. every five years) (64). The long-run nature of

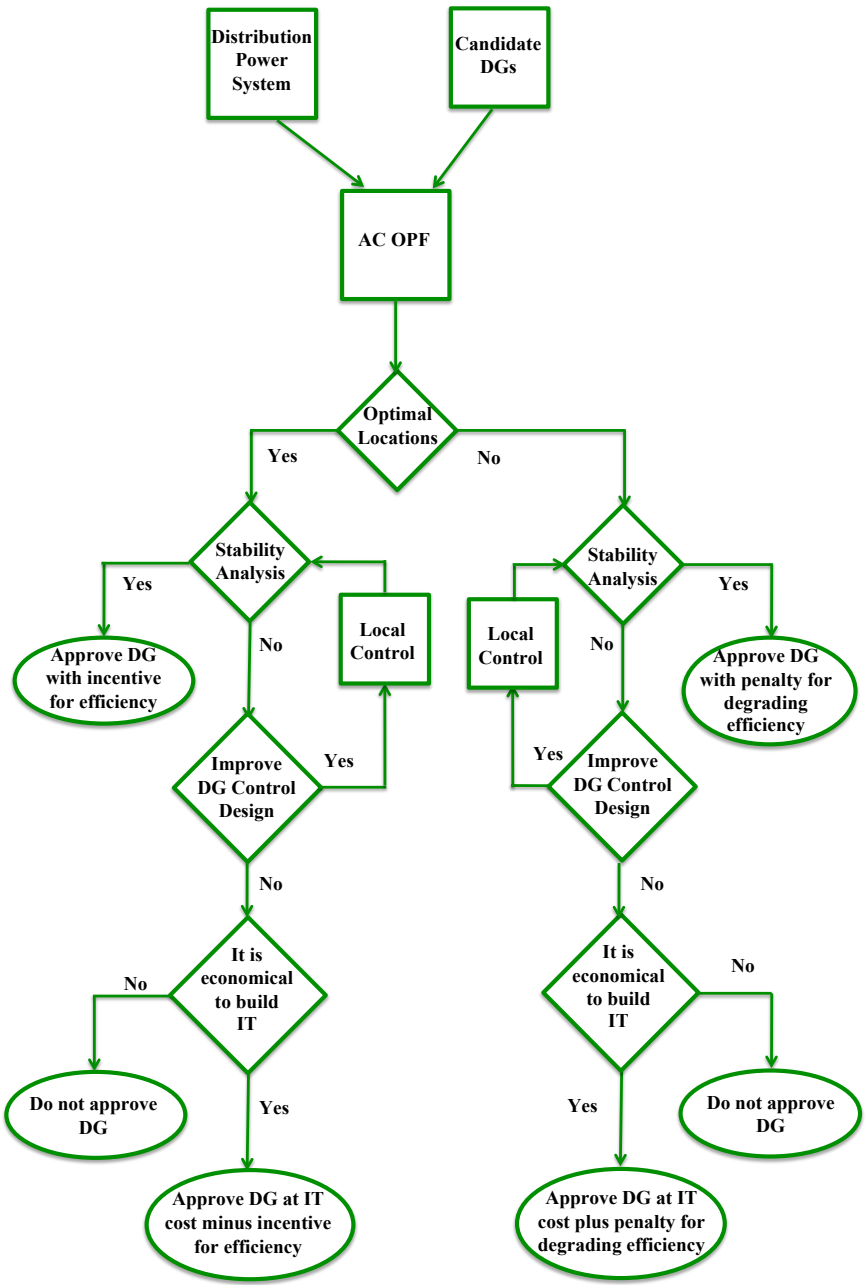

Figure 6.9: A possible model-based adaptive policy design process.

performance based-regulation discourages many DSOs and DG operators to invest in efficiency improvement.

6.5 Making the Transition

For a low penetration of DG units, it is possible to apply today's operating models such as plug-and-play. Under the plug-and-play regime the adoption of DGs is easier and faster. However, as the preceding discussion indicates, as the level of DG penetration increases, new technical challenges and new opportunities, not accounted for by today's standards and operating models, will arise. This raises two obvious policy questions: 1) at what point should distribution system operators and regulators make the transition from the present plug and play regime, to a more systematically planned and coordinated approach, and; 2) what equity issues, if any, arise between those operators who have installed DGs before the transition and those who install facilities after the change?

Because many distribution system operators view DGs run by other parties as a real problem, they will likely want the transition to be made as soon as possible. However, because central policy design will likely complicate what is already a difficult set of challenges faced by potential DG operators, parties interested in promoting higher adoption of DGs would presumably like to see the transition made as late as possible in the course of the build-out. In order to make the most out of DGs, it is essential to strategically place and optimally utilize DGs in distribution systems. As shown in the previous sections, a 10% penetration of DGs can reduce up to 50% of power delivery losses if DGs are optimally located and utilized in distribution systems. On the other hand, randomly placed DGs could degrade the quality of frequency and system stability.

The model-based adaptive policy design provides a systematic approach to quantify the performance of DG and to incentivizing DG to enhance efficiency and improve its effects on system stability. The incentive can provide added value to DG and can increase the willingness of DG operators to make the transition. In order to avoid complexity and to ease DG interconnection, we suggest that a neutral third party such as a consortium for distributed generation assesses the effects of DGs and provides guidelines for DG operators and DSOs. These consortiums could and should be helped by those capable of quantitative analysis.

If utilities approve DG on a first-come-first-serve basis, the first DG operators will face fewer limitations and will enjoy greater incentive for enhancing efficiency. Due to the effects of DGs on each other, the next DG operators may need to install advanced local control or may only be approved at the cost of installing centralized communication/control systems.

In order to avoid equity issues, we propose that the consortium for distributed generation should conduct an assessment for the entire candidate DGs asking to be connected once a year, or depending on the demand for interconnection, the assessment can be conducted twice or even three times per year. The main advantage of this approach is that the global optimal combinations of placing candidate DGs would be determined and the long-term efficiency of distribution energy systems would be maximized.

6.6 Conclusions

This chapter proposes that for efficient and reliable integration of DGs, it is essential to design a model-based adaptive policy to link the methods engineers use to policy design. This chapter particularly emphasizes that a large penetration of DGs sending power back to the grid could degrade the quality of frequency and system stability. For instance, the random behavior of plug-and-play DGs could cause large frequency deviations. In addition, DGs connected in electrically close areas could oscillate against each other and cause small-signal instability problems in distribution systems.

The chapter also points out that DGs hold the potential to significantly reduce power delivery losses and therefore improve system-wide efficiency, if they are strategically located and optimally dispatched in distribution systems. To this end, a neutral third party such as a consortium for distributed generation could conduct a systematic assessment using stability analysis and optimization tools in order to provide a set of recommended alternatives and necessities for reliable and efficient integration of DGs.

The key point of this chapter is that there is no one-size-fits-all policy to support efficient and reliable integration of distributed generation. Therefore, it is essential to design sets of models to analyze the effects of DGs asking to be deployed and to provide quantifiable measures for assessing the efficiency and reliability of distribution systems with DGs.

6. ADAPTIVE MODEL-BASED POLICY DESIGN FOR INTEGRATION OF DISTRIBUTED GENERATION

7

Conclusions

7.1 Policy Implications and Conclusions

In this dissertation, we have introduced a systematic framework needed for (1) assessing operating and planning practices for distribution systems with respect to their ability to best integrate and utilize DG units; (2) identifying potential technical problems brought about by deploying a high penetration of DGs; (3) introducing technically innovative ways for facilitating the best integration of DG units without creating stability and safety problems; and, (4) designing policies and institutional arrangements in support of integrating potentially high number of DG units in the existing electric distribution networks without creating technical problems. We have shown that today's standards such as IEEE 1547 and current operating practices such as plug-and-play cannot support a high penetration of DG units sending power to the distribution grid.

Our analysis shows that, strategically located and optimally dispatched DGs that meet a small portion of the electric demand ($\sim$10%) on a distribution feeder can result in a reduction of 50% or more in the power losses that arise in distribution and transmission lines. Hence, in order to make the most efficient use of distribution systems, it will be important to implement optimization algorithms, such as AC OPF, in planning and operating such systems. This goes beyond today's scenario studies by the utilities and the reliance on current interconnection standards such as IEEE 1547. In addition, larger DGs should regulate frequency and voltage in order to ensure QoS in distribution systems. Without these features, it will not be possible to realize many of the potential efficiency benefits. In contrast, most of the today's DG technologies are only equipped

with simple local control systems.

In general, DG owners can locate their generators wherever they choose unless DGs operation results in technical problems for grids. Hence, if efficiency improvement are one of the concerns of utilities, it is essential to develop strategies to encourage DG owners to participate in an optimization process and locate their DGs at optimal locations. This encouragement could be achieved either through direct control or licensing, via price signals for desirable locations, or via extra charges for locating in those that are problematic. In any case, some form of regulatory oversight will be needed to assure equitable treatment of both legacy utilities and the operators of new larger DG units.

Our technical findings demonstrate that where larger DGs are located can play a significant role in determining the stability of distribution energy systems. We find that short electrical distance between DGs and poor tuning of the primary control of DGs are the major causes of instability. If electrical distance between generators is less than a critical value, strong coupling between generators occurs and leads to overall instability. In addition, critical electrical distance is a function of DGs' and networks' parameters such as the inertia of DGs, the gain of GCs, the number of DGs in the system and the networks topology and characteristics.

Based on our technical findings we recommend consideration of three major methods of enhancing stability; 1) placing DGs beyond critical electrical distance; 2) installing fast ramping flywheel energy storage devices to provide enhanced damping to the system, and; 3) implementing advanced decentralized control system.

Depending on the nature of the control systems that are implemented, there may also be significant *order effects* as first one and then another large DG facility gets built. For example, there may be few constraints on the first one or two DG facilities that are installed, but if other entities later also want to install DG facilities, interactions may results. Methods, such as public notice and review, should be found to manage *first mover* benefits and equitably distribute benefits and costs among the legacy distribution system operator and the old and the new DG operators as power flows change and upgrade for controls become necessary.

Some of the issues that will be raised by the growth of DG might be addressed through the creation of new protocols (beyond IEEE 1547) that consider both efficiency and robustness. For instance, larger DGs might be required to have some minimum level of advanced control in order to affirm robustness of the system and they might be

required to have AVR to be able to participate in AC OPF-based voltage dispatch, so that efficiency of the system is certified. Furthermore, as the penetration of DGs in the legacy distribution networks increases, there will be a great need for communication standards for distribution control. The protocols should require distribution-connected generators to provide real-time technical information about themselves, such as output power, phase angle and terminal voltage, to system operators over secure communication channels. These requirements are far beyond the utilization methods of today's distribution networks.

8

Appendix A

8.1 Electrical Networks of the Azores Archipelago

The Azores Archipelago consists of nine islands located in the middle of the North Atlantic Ocean. The western group consists of Flores and Corvo islands; the central group consists of Graciosa, Terceira, Sao Jorge, Pico and Faial islands; and the eastern group consists of Sao Miguel and Santa Maria islands (16). The focus of this dissertation is on Flores and Sao Miguel. Therefore, their electrical networks are explained in detail.

8.1.1 Flores Island

Flores Island is one of the smaller islands of the Azores Archipelago. The population is approximately 4000 inhabitants, and its area is around 143 km^2 (17). Figure 8.2 is a satellite image of the island.

The electrical network of Flores consists of a 15 kV radial distribution network with 46 nodes and 45 branches. The total demand of the island is around 2 MW. More than 50% of the demand is concentrated in the town of Santa Cruz; around 37% of the load is situated in the vicinity of Lajes Das Flores; approximately 7% of the load is located in the town of Ponta Delgada, and the rest (2-3%) is dispersed throughout the rest of the island. Figure 8.1 illustrates the schematic of the distribution network of Flores Island.

Three small power plants supply the electrical demand. More than 50% of the electricity is provided by four diesel generators whose total capacity is 2.5 MW. Around 35% of the demand is supplied by four hydro power plants with an overall capacity of

1.65 MW. Two synchronous wind power plants with a total capacity of 0.65 MW provide the rest of the demand (15%). The hydro plants and diesel generators are located next to the town of Santa Cruz and the wind plants are located in the middle of the island far from the major load centers (8). Figure 8.3 demonstrates where the large loads and power plants are located and how real-power flows in the distribution system of the island. In (49), the steady-state characteristics of the nodes, loads, generators, and branches of Flores Island are presented in PTI 23 standard format (8).

Since the electrical network of the island is an AC system, active power needs to be balanced almost instantaneously. The hydro generator is a reservoir hydro plant with the ability to store energy. However, the hydro plant has slow dynamic response and cannot balance active power instantaneously. The synchronous wind power plant has no governor control and cannot regulate frequency. The diesel plant, as the only fully controllable power plant, balances demand and supply. The diesel plant also compensates for active and reactive losses occurring in the system. There is no control center on Flores Island. Therefore, the diesel generator regulates frequency locally.

On Flores Island, distribution lines have been over-built. Hence, contingencies due to the reaching of thermal limits are unlikely to occur. However, due to the strong interaction between the electromagnetic and electromechanical parts of the generators, small-signal instability can occur on the island.

One of the major flaws of the electrical network on Flores is the lack of (N-1) reliability criteria. Due to the radial structure of the distribution network, if the line connecting the diesel plant to the center of the island (Fonte de Frade) is disconnected, a local blackout occurs in the central and southern parts of the island. Similarly, if the line connecting the diesel plant to the north of the island (Ponta Delgada) is disconnected, a local blackout occurs in the northern part. The critical lines are presented in Table 8.1.

Table 8.1: Critical lines of Flores Island.

Ponta Delgada	Vicinity of Lajes Das Flores
Line 1-41	Line 1-17
Line 41-42	Line 17-18
Line 42-43	

In order to improve reliability, we suggest that new wind power plants be installed

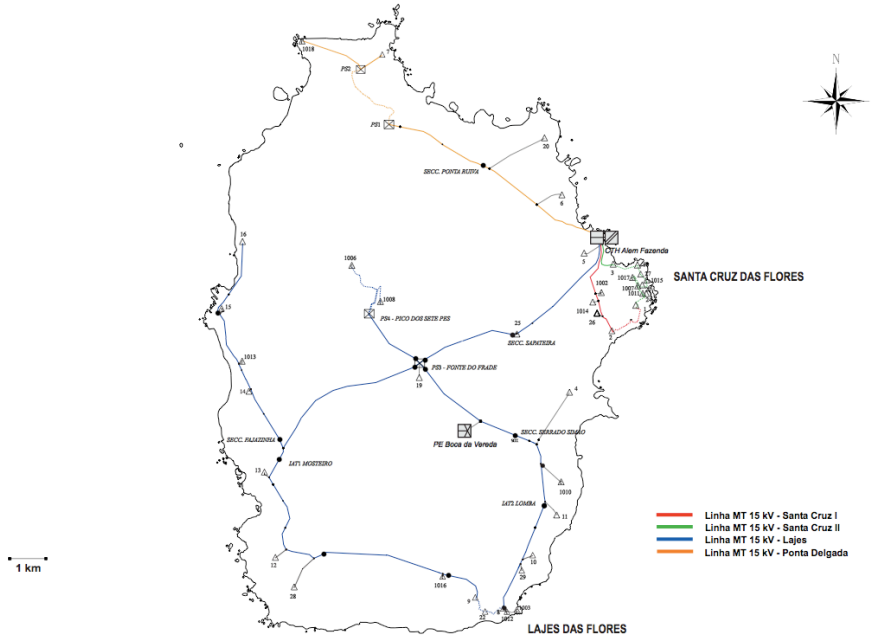

Figure 8.1: Electrical network of Flores Island (8).

in the central and northern parts of the island. Implementing normally open switches to connect the southern part of the island to the town of Santa Cruz, where the diesel and hydro plants are installed, could enhance reliability in the south.

8.1.2 Sao Miguel Island

Sao Miguel Island is the capital, and the largest, island of the Azores Archipelago. The population of this island is approximately 140,000 inhabitants and the area of the island is 744.55 km^2 (25). Figure 8.4 shows a satellite image of Sao Miguel.

The electrical system of Sao Miguel consists of a 60-kV transmission network, situated in the middle of the island, which connects the large power plants to large loads. Figure 8.5 illustrates how real-power flows in the transmission network. As shown in Figure 8.5, two large diesel generators located in the middle of the island (close to the large loads) produce 75% of the electrical demand. Two large geothermal plants provide more than 20% of the demand. The rest comes from ten small hydro plants with run-of-the-river hydro-power (8). The capital of the island (Ponta Delgada) is the largest load.

There is a 30-kV and a 10-kV ring distribution network located along the coastal

Figure 8.2: Satellite image of Flores Island.

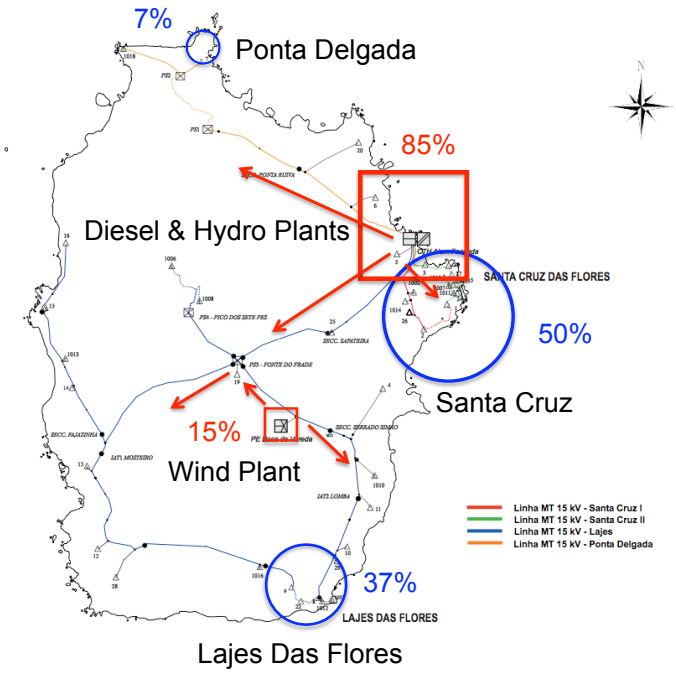

Figure 8.3: Illustrating the location of large loads and power plants and how real-power flows.

Figure 8.4: Satellite image of Sao Miguel Island.

area. Figure 8.6 shows the schematic of the distribution network of the island and where the largest loads are located. In (49), the steady-state characteristics of the nodes, loads, generators, and branches of Sao Miguel Island are presented in PTI 23 standard format.

Like the other islands of the Azores Archipelago, Sao Miguel has an all-AC electrical system. This requires an almost instantaneous balancing of active power. On Sao Miguel, the hydro and geothermal plants are non-controllable generators, so they provide base-load power only. It falls on the diesel plants to balance demand and supply almost instantaneously. In addition, the diesel generators compensate for active and reactive power losses occurring in the system. The parameters of the dynamic model of the generators are presented in Appendix B.

Sao Miguel Island has an advanced control center. The control center provides generation control and regulates frequency by communicating with the automatic generation control (AGC) of the diesel plants. The control center also provides the most economical dispatch for the diesel generators by minimizing their operating costs. The advanced control system helps the island to manage system operations during peak hours.

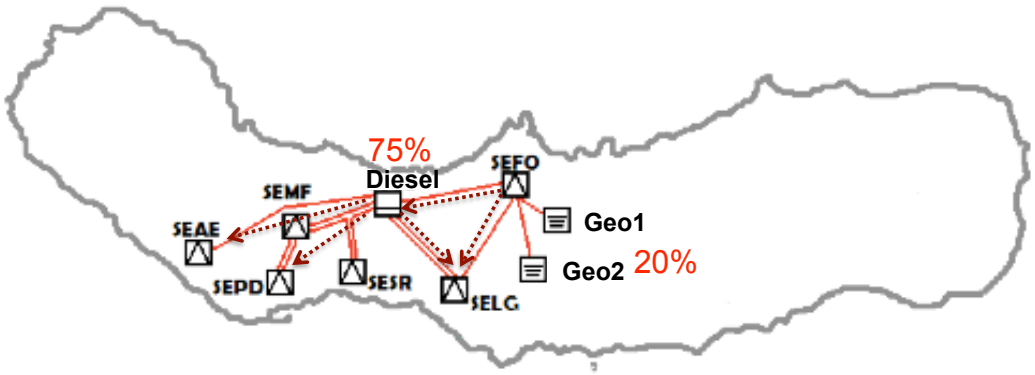

Figure 8.5: Transmission network of Sao Miguel Island (8).

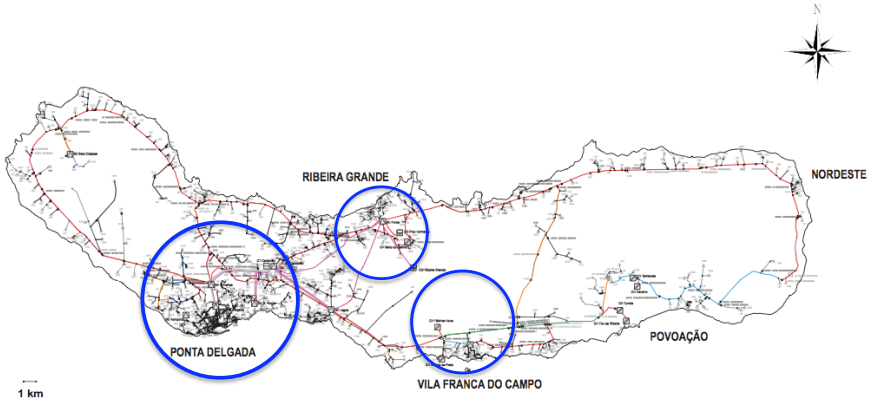

Figure 8.6: Distribution and transmission network of Sao Miguel Island (8).

9

Appendix B

Appendix B presents equilibrium point, coupling matrix (Kp), eigenvalues, and dynamic parameters of Flores and Sao Miguel Islands.

9. APPENDIX B

Table 9.1: Eigenvalues of the decoupled real-power voltage dynamic model

The Whole System	Diesel Generator	Wind Plant	Hydro Generator
1.0e+02 *	-0.6845 +31.3998i	-3.4586	1.0e+02 *
(-1.1772	-0.6845 -31.3998i	-0.8353	(-1.1772
-0.0068 + 0.3140i	-0.3086		-0.0002 + 0.0174i
-0.0068 - 0.3140i	-0.0000		-0.0002 - 0.0174i
-0.0346			-0.0133
-0.0002 + 0.0173i			-0.0050)
-0.0002 - 0.0173i			
-0.0133			
-0.0084			
-0.0030			
-0.0050			
0.0000)			

Table 9.2: Eigenvalues of the coupled real-power voltage dynamic model

The Whole System	Diesel Generator	Wind Plant	Hydro Generator
1.0e+02 *	-45.0995	-55.1861	1.0e+02 *
(-0.1100 + 0.9898i	-0.6271 +31.4737i	-1.4642 + 2.5122i	(-1.1772
-0.1100 - 0.9898i	-0.6271 -31.4737i	-1.4642 - 2.5122i	-0.1100 + 0.9898i
-1.1772	-4.0688 +17.2365i		-0.1100 - 0.9898i
-0.6805	-4.0688 -17.2365i		-0.0809
-0.0063 + 0.3149i	-0.3187		0.0014 + 0.0235i
-0.0063 - 0.3149i	-0.0499		0.0014 - 0.0235i
-0.3955	0.0000		-0.0136
-0.0406 + 0.1722i			-0.0050
-0.0406 - 0.1722i			-0.0002)
-0.0148 + 0.0251i			
-0.0148 - 0.0251i			
0.0002 + 0.0241i			
0.0002 - 0.0241i			
-0.0135			
-0.0118			
-0.0029 + 0.0047i			
-0.0029 - 0.0047i			
-0.0030			
-0.0050			
-0.0004			
-0.0000)			

Table 9.3: Coupling matrix of Flores Island in the decoupled scenario

	Bus 1	Bus 2	Bus 3
Bus 1	13.9058	-1.4076	-12.4982
Bus 2	-1.3464	1.3464	0
Bus 3	-12.5017	0	12.5017

Table 9.4: J_1 matrix of Flores Island in the coupled scenario

	J_1^{Bus1}	J_1^{Bus2}	J_1^{Bus3}
J_1^{Bus1}	13.9058	-1.4076	-12.4982
J_1^{Bus2}	-1.3464	1.3464	0
J_1^{Bus3}	-12.5017	0	12.5017

Table 9.5: J_2 matrix of Flores Island in the coupled scenario

	J_2^{Bus1}	J_2^{Bus2}	J_2^{Bus3}
J_2^{Bus1}	15.0207	-2.4883	-12.5017
J_2^{Bus2}	-2.5220	2.4887	0
J_2^{Bus3}	-12.4982	0	12.5018

Table 9.6: J_3 matrix of Flores Island in the coupled scenario

	J_3^{Bus1}	J_3^{Bus2}	J_3^{Bus3}
J_3^{Bus1}	-14.9806	2.4788	12.5017
J_3^{Bus2}	2.5126	-2.5126	0
J_3^{Bus3}	12.4982	0	-12.4982

Table 9.7: J_4 matrix of Flores Island in the coupled scenario

	J_4^{Bus1}	J_4^{Bus2}	J_4^{Bus3}
J_4^{Bus1}	13.9056	-1.4073	-12.4982
J_4^{Bus2}	-1.3461	1.3461	0
J_4^{Bus3}	-12.5017	0	12.5017

Table 9.8: Power flow solution (equilibrium point) of Flores Island

Bus number in the original system	Bus number in the equivalent system	Name	V [pu]	phase [rad]	P gen [pu]	Q gen [pu]
Bus 1	Bus 1	Diesel	1	0	0.06739	0.0747
Bus 19	Bus 2	Wind	1	-0.01225	0.06	0.05391
Bus 46	Bus 3	Hydro	1	0.00014	0.07	-0.06999

Table 9.9: Coupling matrix of Sao Miguel Island

	Bus1	Bus 2	Bus 3	Bus 4	Bus 5	Bus 6	Bus 7	Bus 8	Bus 9	Bus 10	Bus 11	Bus 12	Bus 13	Bus 14	Bus 15
Bus 1	10935	-10932	-0.61	-1.60	-0.22	-0.16	-0.08	-0.08	-0.03	-0.00	-0.00	-0.00	-0.00	-0.00	-0.00
Bus 2	-10932	21867	-10930	-4.15	-0.10	-0.07	-0.12	-0.12	-0.04	-0.00	-0.00	-0.00	-0.00	-0.00	-0.00
Bus3	-0.66	-10930	10938	-7.75	-0.02	-0.01	-0.00	-0.00	-0.00	-0.00	-0.00	-0.00	-0.00	-0.00	-0.00
Bus4	-1.60	-4.16	-7.75	16.15	-1.38	-0.98	-0.10	-0.10	-0.04	-0.00	-0.00	-0.00	-0.00	-0.00	-0.00
Bus5	-0.22	-0.10	-0.02	-1.38	4.03	-2.16	-0.04	-0.04	-0.04	-0.00	-0.00	-0.00	-0.00	-0.00	-0.00
Bus6	-0.16	-0.07	-0.01	-0.97	-2.16	3.58	-0.05	-0.05	-0.06	-0.00	-0.00	-0.00	-0.00	-0.00	-0.00
Bus7	-0.08	-0.12	-0.00	-0.10	-0.04	-0.05	2.38	-1.41	-0.52	-0.00	-0.00	-0.01	-0.00	-0.00	-0.00
Bus8	-0.08	-0.12	-0.00	-0.10	-0.04	-0.05	-1.41	2.37	-0.51	-0.00	-0.00	-0.01	-0.00	-0.00	-0.00
Bus9	-0.03	-0.04	-0.00	-0.04	-0.04	-0.06	-0.52	-0.51	10791	-0.00	-10789	-0.08	-0.03	-0.00	-0.00
Bus10	-0.00	-0.00	-0.00	-0.00	-0.00	-0.00	-0.00	-0.00	-0.00	10797	-10789	-0.00	-0.00	-0.00	-7.70
Bus11	-0.00	-0.00	-0.00	-0.00	-0.00	-0.00	-0.00	-0.00	-10789	-10789	21579	-0.00	-0.00	-0.00	-0.00
Bus12	-0.00	-0.00	-0.00	-0.00	-0.00	-0.00	-0.01	-0.01	-0.08	-0.00	-0.00	0.40	-0.27	-0.00	-0.00
Bus13	-0.00	-0.00	-0.00	-0.00	-0.00	-0.00	-0.00	-0.00	-0.03	-0.00	-0.00	-0.27	0.33	-0.00	-0.00
Bus14	-0.00	-0.00	-0.00	-0.00	-0.00	-0.00	-0.00	-0.00	-0.00	-0.00	-0.00	-0.00	-0.00	10789	-10789
Bus15	-0.00	-0.00	-0.00	-0.00	-0.00	-0.00	-0.00	-0.00	-0.00	-7.70	-0.00	-0.00	-0.00	-10789	10797

Table 9.10: Electromechanical parameters of the diesel plant on Flores

M_d (MJ/Hz)	D_d (MW/Hz)	T_2 (sec)	K_2 (pu)	Rd (pu)	Cd (pu)
0.216	0.005	0.6	40	0.03	1
KI (pu)	Cc (pu)				
10	1				

Table 9.11: Electromechanical parameters of the wind plant on Flores

M_w (MJ/Hz)	D_w (MW/Hz)	Kp_w (pu)
0.089	0.002	2

9.1 Dynamic Parameters of Flores

In this section, electromechanical and electromagnetic parameters of the power plants on Flores are presented. These parameters are estimated based on the data-set provided by Professor Pecas Lopes from INESC Porto and based on the models used in (31).The bases are Sbase = 10 MVA, Vbase = 0.4 kV, and fbase = 50 Hz.

9.2 Dynamic Parameters of Sao Miguel

In this section, electromechanical parameters of the power plants in Sao Miguel are presented. These parameters are estimated based on the data-set provided by Professor Pedro Carvalho from IST Lisbon and based on the models used in (31). The bases are Sbase = 100 MVA and fbase = 50 Hz.

Table 9.12: Electromechanical parameters of the hydro plant on Flores

M_h (MJ/Hz)	D_h (MW/Hz)	K_q (pu)	K_w (pu)	T_f (sec)	r_h (pu)
0.2749	0.02	2.78	1.52	-3.6	7
T_q (sec)	T_w (sec)	T_e (sec)	T_s (sec)	r_p (pu)	
0.72	4	2	0.06	0.06	

9. APPENDIX B

Table 9.13: Electromagnetic parameters of the diesel plant on Flores

Ta_d (sec)	Tf_d (sec)	Td_d (sec)	Ka_d (pu)	Xd_d (pu)	$X'd_d$ (pu)
0.2	0.65	2.35	25	8.1479	0.5917
R_d (pu)	Te_d (sec)	Ke_d (pu)	Se_d (pu)		
0.001	0.6544	1	0.105		

Table 9.14: Electromagnetic parameters of the wind plant on Flores

Td_w (sec)	Xd_w (pu)	$X'd_w$ (pu)	Rw (pu)
0.661	28.161	3.052	0.002

Table 9.15: Electromagnetic parameters of the hydro plant on Flores

Ta_h (sec)	Tf_h (sec)	Td_h (sec)	Ka_h (pu)	Xd_h (pu)	$X'd_h$ (pu)
0.05	0.9	3.5	400	2.399	0.3609
R_h (pu)	Te_h (sec)	Ke_h (pu)	Se_h (pu)		
0.001	0.9	1	0.035		

Table 9.16: Characteristics of the plants on Flores Island

Node number in the 46-node system	Node number in the reduced system	Capacity (MW)	Type of Plant
1	1	2.5	Diesel
19	2	0.6	Wind
46	3	1.5	Hydro

Table 9.17: Electromechanical parameters of the first diesel plant on Sao Miguel

M_{d1} (MJ/Hz)	D_{d1} (MW/Hz)	T_{d1} (sec)	K_{d1} (pu)	R_{d1} (pu)	C_{d1} (pu)
5.853	0.704	1.07	40	0.03	1
KI_1 (pu)	Cc_1 (pu)				
10	1				

Table 9.18: Electromechanical parameters of the second and third diesel plants on Sao Miguel

M_{d2} (MJ/Hz)	D_{d2} (MW/Hz)	T_{d2} (sec)	K_{d2} (pu)	R_{d2} (pu)	C_{d2} (pu)
6.473	0.352	1.25	40	0.03	1
KI_2 (pu)	Cc_2 (pu)				
10	1				

Table 9.19: Electromechanical parameters of the first geothermal plant on Sao Miguel

M_{geo1} (MJ/Hz)	D_{geo1} (MW/Hz)
2.653	0.298

Table 9.20: Electromechanical parameters of the second geothermal plant on Sao Miguel

M_{geo2} (MJ/Hz)	D_{geo2} (MW/Hz)
2.331	0.262

Table 9.21: Electromechanical parameters of hydro 1 on Sao Miguel

M_{h1} (MJ/Hz)	D_{h1} (MW/Hz)
0.2038	0.0036

Table 9.22: Electromechanical parameters of hydro 2 on Sao Miguel

M_{h2} (MJ/Hz)	D_{h2} (MW/Hz)
0.162	0.0122

Table 9.23: Electromechanical parameters of hydro 3 on Sao Miguel

M_{h3} (MJ/Hz)	D_{h3} (MW/Hz)
0.1849	0.0033

Table 9.24: Electromechanical parameters of hydro 4 on Sao Miguel

M_{h4} (MJ/Hz)	D_{h4} (MW/Hz)
0.1424	0.0106

Table 9.25: Electromechanical parameters of hydro 5 on Sao Miguel

M_{h5} (MJ/Hz)	D_{h5} (MW/Hz)
0.1424	0.0106

Table 9.26: Electromechanical parameters of hydro 6 on Sao Miguel

M_{h6} (MJ/Hz)	D_{h6} (MW/Hz)
0.1424	0.0106

Table 9.27: Electromechanical parameters of hydro 7 on Sao Miguel

M_{h7} (MJ/Hz)	D_{h7} (MW/Hz)
0.0285	0.00051

Table 9.28: Electromechanical parameters of hydro 8 on Sao Miguel

M_{h8} (MJ/Hz)	D_{h8} (MW/Hz)
0.1216	0.0022

Table 9.29: Electromechanical parameters of hydro 9 on Sao Miguel

M_{h9} (MJ/Hz)	D_{h9} (MW/Hz)
0.1217	0.0022

Table 9.30: Electromechanical parameters of hydro 10 on Sao Miguel

M_{h10} (MJ/Hz)	D_{h10} (MW/Hz)
0.1217	0.0022

Table 9.31: Characteristics of the plants in the electric power system of Sao Miguel

Node number in the original system	Node number in the reduced system	Capacity (MW)	Type of plant
932	1	32.688	Diesel 1 (SLACK)
933	2	32.688	Diesel 2
934	3	32.688	Diesel 3
963	4	14.8	Geothermal 1
1049	5	13	Geothermal 2
1666	6	0.67	Hydro 1
1669	7	0.8	Hydro 2
1672	8	0.608	Hydro 3
1675	9	0.553	Hydro 4
1676	10	0.553	Hydro 5
1677	11	0.553	Hydro 6
1680	12	0.094	Hydro 7
1683	13	0.4	Hydro 8
1686	14	0.4	Hydro 9
1687	15	0.4	Hydro 10

Bibliography

[1] A. Narayanan and M. G. Morgan, *Sustaining Critical Social Services During Extended Regional Power Blackouts*, Risk Analysis, 32(7), 2012. 1

[2] B. Alderfer, M. Eldridge and T.J. Starrs, *Making connections: Case studies of interconnection barriers and their impacts on distributed power projects*, National Renewable Energy Laboratory, NRELSR200-28053, July 2000. 71

[3] C. Wang and M. H. Nehrir, *Analytical Approaches for Optimal Placement of Distributed Generation Sources in Power Systems*, IEEE Trans. on Power Syst. 19(4), Nov. 2004. 3

[4] C.L.T. Borges and D.M. Falcao, *Impact of distributed generation allocation and sizing on reliability, losses and voltage profile*, In Proc. Power Tech IEEE, 2, p. 5, Bologna, June. 2003. 3

[5] D. G. Feingold and R. S. Varga, et al, *Block Diagonally Dominant Matrices and Generalizations of the Gerschgorin Circle Theorem*, Pacific J. Math. 12(4) pp. 1241-1250, 1962. 24, 58

[6] D. L Hau Aik, and G. Andersson, *Use of Participation Factors in Model Voltage Stability Analysis of Multi-infeed HVDC Systems*, IEEE Trans. on Power Delivery. Vol. 13, No. 1, pp. 203-211, Jan 1998. 47, 55

[7] D. Siljak, *Large-Scale Dynamic Systems: Stability and Structure*, Dover Publications, Nov. 2007. 60

[8] EDA Report, *CARACTERIZAÇÃO DAS REDES DE TRANSPORTE E DISTRIBUIÇÃO DE ENERGIA ELÉCTRICA DA REGIÃO AUTÓNOMA DOS AÇORES* , March 2009. vii, ix, xi, 13, 37, 39, 94, 95, 98

[9] Energy.gov, *Energy Department Announces Funding to Develop Plug-and-Play Solar Energy Systems for Homeowners*, http://energy.gov/articles/energy-department-announces-funding-develop-plug-and-play-solar-energy-systems-homeowners, 2012. 73

[10] F. Jurado and A. Cano, *Optimal placement of biomass fuelled gas turbines for reduced losses*, Energy Conversion and Management, 47(15-16), pp. 2673-2681, Sept. 2006. 3

[11] G. Celli, E. Ghiani, S. Mocci, and F. Pilo, *A multi-objective evolutionary algorithm for the sizing and sitting of distributed generation*, IEEE Trans. on Power System, 20(2), pp. 750- 757, May 2005. 3

[12] G. Pepermans, J. Driesen, D. Haeseldonckx, R. Belmans, and W. Dhaeseleer, *Distributed Generation: Denition, Benets and Issues*, Energy Policy, 33, pp. 787798, 2005.

[13] H. L. Willis, *Analytical Methods and Rules of Thumb for Modeling DG-Distribution Interaction*, in Proc. 2000 IEEE Power Engineering Society Summer Meeting, 3, pp. 1643-1644, Seattle, WA, July 2000. 3

[14] H. Sharma , S. Islam and T. Pryor, *Dynamic Modeling and Simulation of a Hybrid Wind Diesel Remote Area Power System*, Int. J. Renewable Energy Eng., 2, p.19, 2000. 27

[15] http://www.eia.doe.gov/electricity/

[16] http://en.wikipedia.org/wiki/Azores 93

[17] http://en.wikipedia.org/wiki/Flores_Island_(Azores) 10, 93

[18] http://en.wikipedia.org/wiki/Corvo_Island

[19] http://en.wikipedia.org/wiki/Graciosa

[20] http://en.wikipedia.org/wiki/Terceira_Island

[21] http://en.wikipedia.org/wiki/S%C3%A3o_Jorge_Island

[22] http://en.wikipedia.org/wiki/Pico_Island

[23] http://en.wikipedia.org/wiki/Faial_Island

[24] http://en.wikipedia.org/wiki/Santa_Maria_Island

[25] http://en.wikipedia.org/wiki/S%C3%A3o_Miguel_Island 95

[26] http://www.epa.gov/chp/state-policy/funds_fs.html 71

[27] http://www.njcleanenergy.com/commercial-industrial/programs/combined-heat-power/combined-heat-power 71

[28] IEEE Guide for Design, Operation, and Integration of Distributed Resources Island Systems with Electric Power Systems, IEEE Standard 1547.4. 79

[29] International Energy Agency, *Energy Technology Perspective: Data Visualization*, http://www.iea.org/etp/explore/, 2012.

[30] J. Cardell and M. Ilić, and Tabors, R. D. *Integrating Small Scale Distributed Generation into a Deregulated Market: Control Strategies and Price Feedback*, Laboratory for Electromagnetic and Electronic Systems, Massachusetts Institute of Technology, 1998. 3, 6, 57

[31] J. Cardell and M. Ilić, *Maintaining Stability with Distributed Generation in the Restructured Electric Power Industry*, Proceedings of the IEEE PES GM, Boulder, CO, June 2004. 3, 6, 28, 40, 103

[32] J. Machowski, J. W. Bialek, and J. R. Bumby, *Power System Dynamics and Stability*, 1997: Wiley. 25, 28

[33] J. O. Kim, S. W. Nam, S. K. Park, and C. Singh, *Dispersed Generation Planning Using Improved Hereford Ranch Algorithm*, Elect. Power System Res. 47(1), pp. 47-55, Oct. 1998. 3

[34] J. P. Lopes, N. Hatziargyriou, J. Mutale, P. Djapic, N. Jenkins, *Integrating distributed generation into electric power systems: A review of drivers, challenges, opportunities* Electric Power Systems Research 77, 11891203, 2007.

[35] J. Pierik et al *Electrical and Control Aspects of Offshore Wind Farms II (Erao II), Volume 2: Offshore Wind Farm Case Studies*, Technical Report of ECN&TUD, ECNC04051, Netherlands, 2004. 41

[36] J. Qiu and S.M. Shahidehpour, *A New Approach for Minimizing Power Losses and Improving Voltage Profile*, IEEE Transactions on Power Systems, 2(2), May 1987. 17

[37] J. V. Paatero, P. D. Lund, *Effects of large-scale photovoltaic power integration on electricity distribution networks*, Renewable Energy, 32(2), pp. 216-234, 2007. 3, 71

[38] J. W. Chapman, *Power System Control for Large Disturbance Stability: Security, Robustness and Transient Energy*, Doctor of Philosophy, Massachusetts Institute of Technology, 1996. 30

[39] K. Nara, Y. Hayashi, B. Deng, K. Ikeda, and T. Ashizawa, *Optimal Allocation of Dispersed Generators for Loss Minimization*, Electrical Engineering in Japan, 136(2), pp. 1-8, 2001. 3

[40] K. Siler-Evans, M. G. Morgan, I. L. Azevedo, *Distributed cogeneration for commercial buildings: Can we make the economics work?* Energy Policy, 42, pp. 580590, 2012. 1

[41] K. Purchala , L. Meeus , D. V. Dommelen and R. Belmans, *Usefulness of dc Power Flow for Active Power Flow Analysis*, Proc. IEEE Power Eng. Soc. Annu. Meeting 2005, pp.454 2005.

[42] M. A. Pai, D. P. S. Gupta, and K. R. Padiyar, *Small-signal Analysis of Power Systems*, Harrow, Alpha Science International, 2004.

[43] M. Angelo and P. Lopes, *Simultaneous Tuning of Power System Stabilizers Installed in DFIG-Based Wind Generation*, Power Tech Proceedings, Lausanne, Switzerland, July 2007. 3

[44] M. Ilić et al, *Preventing Future Blackouts by Means of Enhanced Electric Power Systems Control: From Complexity to Order*, Proceedings of the IEEE, 93(11), Oct. 2005. 26, 27, 40

[45] M. Ilić, *Toward Standards for Dynamics in Future Electric Energy Systems*, PSERC White Paper, http://www.pserc.wisc.edu/documents/publications/papers/fgwhitepapers/Ilic_PSERC_Future_Grid_White_Paper_Dynamics_June_2012.pdf, June 2012.

[46] M. Ilić and J. Zaborszky, *Dynamics and Control of Large Electric Power Systems*, John Wiley & Sons, 2000. 24, 28

[47] M. K. Donnelly, J. E. Dagle, D. J. Trudnowski, and G. J. Rogers, *Impacts of the Distributed Utility on Transmission System stability*, IEEE Trans. on Power Systems, 11(2), May 1996. 3

[48] M. H. Nazari and M. Ilić, *Technical Challenges in Modernizing Distribution Electric Power Systems with Large Number of Distributed Generators*, Proceedings of the IEEE PES PowerTech, Bucharest, Romania, June 2009.

[49] M. H. Nazari, *Electrical Networks of the Azores Archipelago*, Chapter 3, Engineering IT-Enabled Electricity Services, Springer 2012. 94, 97

[50] M. H. Nazari and M. Ilić, *Potential for Efficiency Improvement of Future Electric Energy Systems with Distributed Generation Units*, Proceedings of the IEEE General Meeting, Minneapolis, Minnesota, July 2010.

[51] M. H. Nazari and M. Ilić, *Small-Signal Stability of Electric Power Systems on the Azores Archipelago*, Chapter 17, Engineering IT-Enabled Electricity Services, Springer 2012. 27

[52] M. H. Nazari, M. Ilić and J. P. Lopes, *Small-Signal Stability and Decentralized Control Design for Electric Energy Systems with Large Penetration of Distributed Generators*, Control Engineering Practice, 20(9), pp. 823-831, 2012. 33

[53] M. Honarvar Nazari, M. Ilić and P. Lopes, *Dynamic Stability and Control Design of Future Electric Energy Systems with Large Penetration of Distributed Generators* IREP Symposium, Rio de Janeiro, Brazil, August 2010.

[54] M. Honarvar Nazari, M. Parniani, *Determining and Optimizing Power Loss Reduction in Distribution Feeders due to Distributed Generation*, Proc. of 2006 IEEE PSCE Conference, 2006. 3

[55] N. Hamsic et al, *Increasing Renewable Energy Penetration in Isolated Grids Using a Flywheel Energy Storage System*, POWERENG 2007, Setubal, Portugal, 2007. 37, 49

[56] N. Kopell and R. B. Washburn, *Chaotic Motions in the Two-Degree of Freedom Swing Equation*. IEEE Trans. on Circuits and Systems, 29(11), pp. 738-745.

[57] N. Hatziargyriou, G. Contaxis, M. Papadopoulos, B. Papadias, E. Nogaret, G. Kariniotakis, J. A. P. Lopes, M. Matos, J. Halliday, G. Dutton, P. Dokopoulos, A. Bakirtzis, A. Androutsos, J. Stefanakis and A, Gigantidou, *Control of Isolated Power Systems with Increased Wind Power Generation*, Med. Power, Lefkosia, Cyprus, Nov 16-18, 1998.

[58] N. S. Rau and Y. H. Wan, *Optimum Location of Resources in Distributed Planning*, IEEE Trans. Power System, 9, pp. 2014-2020, Nov. 1994. 3

[59] N. Straub, and P. Behr, *Energy Regulatory Chief Says New Coal, Nuclear Plants May Be Unnecessary*, Energy & Environment, April 22, 2009.

[60] P. Brown, *Clean Energy Standard: Design Elements, State Baseline Compliance and Policy Considerations*, Congressional Research Service, March 2011.

[61] P. Kundur, *Power System Stability and Control*, 1994: McGraw-Hill. 24

[62] P. Kundur , J. Paserba , V. Ajjarapu , G. Andersson , A. Bose , C. Canizares , N. Hatziargyriou , D. Hill , A. Stankovic , C. Taylor , T. Van Cutsem and V. Vittal *Definition and classification of power system stability*, IEEE Trans. Power System, 19, 2004. 37

[63] R. Cossent, T. Gmez, P. Fras, *Towards a future with large penetration of distributed generation: Is the current regulation of electricity distribution ready? Regulatory recommendations under a European perspective*, Energy Policy, 37(3), 1145-1155, 2009.

[64] R. Davis, *Acting on Performance-Based Regulation*, The Electricity Journal, Volume 13, Issue 4, pp. 13-23, May 2000. 84

[65] R. H. Lasseter, *Microgrids and distributed generation*, Journal of Energy Engineering, ASCE, 133, pp 144149, 2007. 73

[66] R. T. Guttromson, *Modeling Distributed Energy Resource Dynamics on the Transmission System*, IEEE Trans. on Power Systems, 17(4), Nov. 2002. 3, 6

[67] S. K. Hung, and K. A. Oye, *Managing Uncertainty: Foresight and Flexibility in Cryptography and Voice over IP Policy*, Department of political Science, Massachusetts Institute of Technology, 2009. 84

[68] T. S. Basso, and R. DeBlasio, *IEEE 1547 series of standards: interconnection issues*, IEEE Transactions on Power Electronics, 19(5), 2004. xi, 72, 74, 76, 80, 81

[69] US Energy Information Administration, *Annual Energy Review: Electricity Overview, 1949-2010*, Oct. 2011. ix, 9, 71, 81, 82

[70] W. El-Khattam, Y.G. Hegazy, and M.M.A. Salama, *An integrated distributed generation optimization model for distribution system planning*, IEEE Trans. on Power System, 20(2), pp. 1158- 1165, May 2005. 3

[71] W. H. Kersting, *Radial Distribution Test Feeders*, IEEE Trans. on Power System, 6, pp. 975 -985, 1991. 2, 13

[72] W. Katzenstein and J. Apt, *Incorporating Wind into a Natural-gas Turbine Baseload Power System Increases NOx and CO2 Emissions from the Gas Turbines*, Future Energy Systems Conf., Carnegie Mellon University, March 2008. 45

[73] X. Liu *Structural Modeling and Hierarchical Control of Large-Scale Electric Power Systems*, Doctor of Philosophy, Massachusetts Institute of Technology, April 1994. 27, 28, 40, 42, 57